Experimental investigation of the impact in the heat transfer coefficient and pressure drop during boiling flow instabilities

Mikkel Sørum

MASTER THESIS

for

Student Mikkel Sørrum

Spring 2014

Experimental investigation of the impact in the heat transfer coefficient and pressure drop during phase flow instabilities

Eksperimentell undersøkelse av to-fase ustabiliteters innvirkning på trykkfallet og varmeovergangstallet

Background and objective

Density Wave Oscillation (DWO) is one of the main types of two-phase flow dynamic oscillations frequently encountered in industrial thermal-hydraulic systems. The self-sustained DWO may cause many undesired problems such as mechanical and thermal fatigue of components by mechanical vibration and thermal waves. To avoid or control density-wave oscillations is critical for two-phase systems, but unfortunately, there is not a perfect criterion to predict the stability of two-phase systems, neither a period correlation to calculate DWO period.

In this work an experimental work will be performed for studying the stability of the two phase flow system. The main purpose will be to investigate the impact of the instability (in particular DWO) in the heat transfer and pressure drop.

The following tasks are to be considered:

1 Literature review on DWO
2 Preparation of the experiment, data acquisition, error analysis, and data processing
3 Perform an experimental investigation on effects of DWO on heat transfer and pressure drop

-- ” --

Within 14 days of receiving the written text on the master thesis, the candidate shall submit a research plan for his project to the department.

When the thesis is evaluated, emphasis is put on processing of the results, and that they are presented in tabular and/or graphic form in a clear manner, and that they are analyzed carefully.

text, the candidate should make an effort to produce a well-structured and easily readable report. In order to ease the evaluation of the thesis, it is important that the cross-references are correct. In the making of the report, strong emphasis should be placed on both a thorough discussion of the results and an orderly presentation.

The candidate is requested to initiate and keep close contact with his/her academic supervisor(s) throughout the working period. The candidate must follow the rules and regulations of NTNU as well as passive directions given by the Department of Energy and Process Engineering.
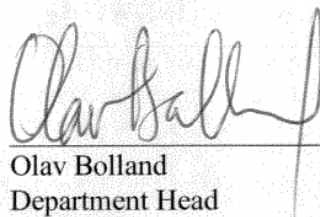
Risk assessment of the candidate's work shall be carried out according to the department's procedures. The risk assessment must be documented and included as part of the final report. Events related to the candidate's work adversely affecting the health, safety or security, must be documented and included as part of the final report. If the documentation on risk assessment represents a large number of pages, the full version is to be submitted electronically to the supervisor and an excerpt is included in the report.
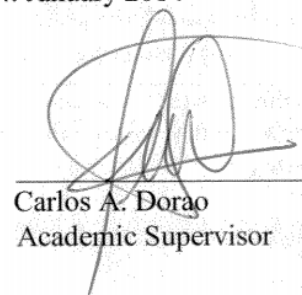
Pursuant to "Regulations concerning the supplementary provisions to the technology study program/Master of Science" at NTNU §20, the Department reserves the permission to utilize all the results and data for teaching and research purposes as well as in future publications.

The final report is to be submitted digitally in DAIM. An executive summary of the thesis including title, student's name, supervisor's name, year, department name, and NTNU's logo and name, shall be submitted to the department as a separate pdf file. Based on an agreement with the supervisor, the final report and other material and documents may be given to the supervisor in digital format.

☒ Work to be done in lab (Water power lab, Fluids engineering lab, Thermal engineering lab)
☐ Field work

Department of Energy and Process Engineering, 14. January 2014

Olav Bolland
Department Head

Carlos A. Dorao
Academic Supervisor

Research Advisor:
Ezequiel Manavela Chiapero

Preface

This Master thesis is original and independent work of the author, M. Sørum. It is written for the fulfilment of a degree in Mechanical Engineering at the Norwegian University of Science and Technology (NTNU), Department of Energy and Process Engineering (EPT).

The purpose of this study is to perform an experimental investigation of the effects of two-phase flow instabilities, in particular Density Wave Oscillations, in the pressure drop and boiling heat transfer characteristics of a horizontal in-tube boiling system. The work was conducted in the Two-Phase Flow Instability rig located in the NTNU Thermal laboratory.

Thanks are expressed to the thesis supervisor Carlos A. Dorao. Thanks are also given previous contributors to the experimental facility, in particular E. Manavela Chiapero and L. C. Ruspini for designing, and the laboratory staff for constructing, the facility. Their effort forms the fundament of the present work.

Abstract

High heat transfer rates at reasonably low temperature differences can be obtained by utilizing a boiling fluid. The use of boiling heat transfer is often limited by onset of a heat transfer crisis named the Critical Heat Flux (CHF). The CHF is accompanied by an inordinate increase in temperature with the most severe consequence being related to the physical burnout of the heated surface. Two-phase boiling flows in channels are sometimes prone to flow instabilities. Density Wave Oscillations (DWO) is the most common type of thermo-hydraulic instability. DWO are fluid waves of alternating higher and lower densities propagating across the system. It is characterized by large cyclic fluctuations in flow rate and pressure and has a period of about twice the heated channel transit time. The literature survey condenses previous results and identifies different approaches for obtaining them in experimental studies. The purpose of this study is to perform an experimental investigation on the effect of flow instabilities on the heat transfer coefficient and pressure drop characteristics of a 5 mm uniformly heated horizontal boiling in-tube system utilizing R134a as the working fluid.

The experiments confirmed that the system stability is improved by opening the inlet restriction valve and omitting exit orifice. The influence of the pump system characteristics on DWO was also explored. Establishing an unconditional stable system configuration allowed for generation of reference data. DWO was found to occur when vapor quality becomes sufficiently high in a system operating with inlet and exit restrictions and some degree of inlet subcooling. Mimicking DWO by superimposing flow oscillations by cycling the pump drive was also a viable solution. It was found that the overall heat transfer decreased proportionally to the flow amplitude. Shifting the period of oscillation from its natural frequency to lower frequencies reduces the heat transfer.

The saturated boiling heat transfer coefficient was highly dependent on heat flux, and almost independent of flow rate, indicating that nucleate boiling was the dominant heat transfer mechanism. Comparisons were made to saturated boiling correlations. Heat transfer scales generally well with pressure drop, except a sudden reduction when DWO commences. The local heat transfer coefficient in the test section outlet increased with heat flux until it suddenly dropped due to an abrupt increase in wall temperature, distinguished as the normal CHF. The onset of DWO was found to trigger premature CHF at heat fluxed of about 90% the normal CHF.

Sammendrag

Ved å benytte koking oppnås god varmeoverføring selv ved relativt små temperaturforskjeller mellom væsken og det som skal kjøles. Denne typen bruk av koking begrenses av et fenomen kalt den kritiske varmefluksen (CHF). Den kritiske varmefluksen er akkompagnert av en overdreven temperaturøkning av den oppvarmede flaten. Denne overopphetingen kan i verste fall kan medføre en fysisk utbrenning grunnet tørrkoking nært overflaten. Oppvarmede rør hvor koking skjer er i tillegg utsatt for ustabiliteter i damp-væske strømmen. Den vanligste typen er omtalt som Density Wave Oscillations (DWO). DWO er bølger med vekslende tetthet som forplanter seg gjennom det oppvarmede røret. De kjennetegnes ved relativt store svingninger i massestrøm og trykk, dessuten er perioden omtrent det dobbelte av blandingens oppholdstid i røret. I en kartlegging av litteraturen sammenfattes resultater fra tidligere arbeid samt at ulike eksperimentelle fremgangsmåter gjenkjennes. Hensikten med denne oppgaven er å undersøke eksperimentelt hvordan strømningsustabiliteter påvirker varmeoverføringstallet og trykkfallet ved koking av kjølemediet R134a i et jevnt oppvarmet 5 mm horisontalt rør.

Det ble bekreftet at systemstabiliteten bedres ved å åpne rørets innløpsventil samt å unnlate en begrensing i utløpet. Pumpesystemets beskaffenhet er også med på å påvirke DWO oppførselen. Disse tiltakene ble benyttet til å gjøre strømningen helt stabil, hvilket utgjorde en referansetilstand. DWO begynte i enhver situasjon hvor det var tilstrekkelig mye damp i rørets utløp gitt tilstedeværelsen av en opp- og nedstrøms ventil samt en noe underkjølt væske i innløpet. DWO kunne kunstig etterlignes ved å variere hastigheten på pumpen. Varmeoverføringen fra røret ble redusert proporsjonalt med en økning i utslaget på svingningene i væskestrømmen. Med pumpen kunne også perioden på DWO forskyves. Det viste seg at tregere svingninger førte til ytterligere forringing i varmeoverføringen.

Varmeoverføringen ved koking var høyst avhengig av den tilførte varmen, imidlertid var den nesten uavhengig av massestrømmen, hvilket tyder på at boble-koking er den viktigste mekanismen. Dette stemte overens med kjente korrelasjoner. Varmeoverføring og trykkfall henger tett sammen, utenom en brå reduksjon i trykkfallet idet DWO starter. Det lokale varmeoverføringstallet nært utløpet øker ved økende oppvarming inntil det plutselig faller grunnet en brå økning i veggtemperatur, hvilket kjennetegner den normale CHF. Dersom DWO begynte utløste dette en for tidlig CHF ved omtrent 90 % av oppvarmingen til den normale CHF

Table of Contents

List of tables

List of figures

Nomenclature

Abbreviations and acronyms

BWR   Boiling Water Reactor

CHF   Critical Heat Flux

DWO   Density Wave Oscillations

FDI   Flow Distribution Instability

HTC   Heat Transfer Coefficient

LNG   Liquefied Natural Gas

ONB   Onset of Nucleate Boiling

TAO   Thermal Acoustic Oscillations

ThO   Thermal Oscillations

Variables and Parameters

Symbol	Description	Unit
A_c	Cross sectional area	m^2
C_p	Specific constant pressure heat capacity	$\frac{J}{kgK}$
d	Diameter	m
G	Mass flux	$\frac{\mathrm{kg}}{\mathrm{m}^2\mathrm{s}}$
h	Enthalpy	$\frac{\mathrm{kJ}}{\mathrm{kg}}$
h	Heat transfer coefficient	$\frac{W}{m^2K}$
k	Conductivity	$\frac{W}{m\,K}$
K	Flow coefficient(valve)	-

L	Heated length	m
p	Pressure	Pa
t	time	s
T	Temperature	K
x	Vapor quality	-
ρ	Density	$\frac{kg}{m^3}$
μ	Dynamic viscosity	$Pa \cdot s = \frac{kg}{m\,s}$
σ	Surface tension	$\frac{N}{m}$
ΔT_{sub}	Inlet subcooling (temperature below the saturation)	$\Delta T_{sub} = T^{sat}(p_i) - T_{f,i}$ [K]

Non-dimensional numbers

Bo	Boiling number	$Bo = \dfrac{q''}{G\,h_{fg}}$
Nu	Nusselt number	$Nu = \dfrac{h\,d}{k_f}$
Pr	Prandtl number	$Pr = \dfrac{C_p\,\mu}{k_f}$
Re_D	Reynolds number	$Re_d = \dfrac{Gd}{\mu}$
We	Weber number	$We = \dfrac{G^2 D}{\rho}$
N_{pch}	Phase change number	
N_{sub}	Subcooling number	

Subscripts

b	Bulk

g	Gas
l	Liquid
f	Fluid
fg	Liquid to gas phase transition
i	Inlet
e	Exit
s	Surface (as in heated surface)
1p	Single-phase
2p	Two-phase
tp	Two-Phase
w	wall

Superscripts

sat	Saturated condition

1 Introduction

1.1 Background

The use of energy is deeply woven into the fabric of the modern society. Energy is demanded for farming, production of goods, services, transportation and in our households. Worldwide population growth, even more energy intensive activities, but still limited resources call for increased energy efficiency. Heat transfer is a vital part of almost any energy converting system. Enhancing heat transfer is thus crucial in order to reduce thermodynamical losses in such systems. Heat exchangers designed to utilize a boiling fluid has been a subject of considerable interest. In particular, in situations in which very high heat fluxes are desired, the use of subcooled local surface boiling has appeared to be quite attractive. This is due to the very large heat transfer coefficients obtained in a boiling situation over that expected with purely forced-convection heat transfer [1]. Boiling heat transfer is also essential in steam generators, boiling water reactors, refrigeration evaporators and distillation column re-boilers.

The use of boiling heat transfer is often limited by the onset of a boiling crisis [2] which involves departure from nucleate boiling to a condition named the critical heat flux (CHF). The most severe problem in the CHF is directly related to the physical burnout of the heated surface materials due to the inefficient heat transfer through the vapor blanket formed across the surface resulting from the replacement of liquid by vapor adjacent to the heated surface. Consequently, the occurrence of CHF is accompanied by an inordinate sudden increase in the surface temperature for a surface-heat-flux-controlled system. Or an abrupt decrease in the heat transfer rate of a surface-temperature-controlled system.

Density wave oscillations are the most common type of thermo-hydraulic instability encountered in the industry [3]. It is also the most studied type of two-phase flow instability, usually concerning vertical systems, motivated by the field of nuclear safety. Determination of a stable envelope has been important since evaluation of the instability threshold values is necessary to determine safe operating conditions [4]. Thermally induced oscillations of the flow rate and

system pressure are undesirable as they can cause mechanical vibrations, thermal fatigue, and even a CHF boiling crisis.

1.2 Motivation

The problem of obtaining high heat transfer rates at reasonable temperature differences can be addressed by utilizing a boiling fluid. However, issues with instabilities are occasionally encountered in two-phase systems [5]. It is commonly quoted that flow instabilities in extreme circumstances can disturb the heat transfer, provoking the occurrence of a boiling crisis, or premature dryout.

An application relying on boiling heat transfer is typically designed with a safety factor based on the normal critical heat flux, but new problems arise if flow instabilities trigger a premature critical heat flux situation. Further research is needed to address this.

In modeling of two-phase boiling flow instabilities the heat transfer to the fluid necessarily has to be accounted for. The current models commonly rely on heat transfer correlations obtained from experiments with stable flows. Prediction of the heat transfer is in this aspect highly uncertain.

The bulk of the work done on flow instabilities so far does mainly consider system stability. Experiments have been performed to find threshold values and to determine boundaries of safe operation. Theoretical studies have been focusing on stability in linearized models. Less work has been done in exploration of the actual consequences of operating a boiling system with DWO.

In the study of any physical phenomena, it is necessary to sort out the governing principles from the less important effects before any progress in analysis can be made. Although the present study does not claim to have completed this, it is sincerely hoped that the work described here will be of assistance to others who are struggling with the numerous issues involved in boiling flow instabilities.

1.3 Research objectives

The main objective of the thesis is to perform an experimental study on the effect of flow instabilities on the pressure drop and heat transfer characteristics of a two-phase boiling system. Focus will be on how the inception, period and amplitude of density wave oscillations may influence heat exchanger performance. A goal is to explore the possibilities of premature

triggering of the critical heat flux by the onset of density wave oscillations. Experiments will be performed with varied power, mass flux, system pressure, degree of inlet subcooling, and flow restrictions to map the effects of different system conditions and configurations.

1.4 Scope of Work

Experiments will be performed to investigate the effect of Density Wave Oscilations on the pressure drop and heat transfer characteristics in a horizontal single tube boiling channel using R134a as working fluid. DWO, artificial flow instabilities induced by variable pump drive, and a stable reference case will be examined. Flow restrictions will be modified to accommodate this. A parameters analysis will be performed with varied heat flux, mass flux and two levels of inlet subcooling and system pressure. These levels will be chosen so that generation of DWO and exploration of the CHF is feasible within the operational limitations of the rig which is, 4-12bar, with less than 1500 W of power, not voiding the test section temperature limits. The test section consists of 2035 mm stainless steel tube of circular cross-section with 5 mm inner diameter.

1.5 Outline

The chapters are intended to be read in chronological order. First, the concept of flow instabilities introduced. An exhaustive literature review makes a survey of the current knowledge within the most relevant research fields, namely DWO, CHF and boiling heat transfer coefficient. A variety of experimental apparatuses are described in the literature, this is why the next chapter is dedicated to provide a throughout description of the current experimental facility. This includes information on instruments and uncertainties. Chapter 4 describes the experimental program and scientific methods. Data reduction and details in computation of heat transfer coefficients are important topics. Before the main investigation started, experiments had to be set up and verified. A chapter is dedicated to the rather extensive pre-work. The mainly objective results chapter is separated from the discussion of main results. Discussion is done to give interpretation of results emphasizing the practical significance and evaluate the results in view of relevant literature. The aim of the conclusion is to synthesize rather than summarize. Some further direction will finally be given.

2 Literature survey

The study of two-phase flow instabilities was pioneered by Ledinegg (1938). Development of high density industrial boilers and boiling water reactors gave more attention to flow instability phenomena in boiling systems, but it was not until the late 1960's that main mechanisms were widely recognized and understood. A brief introduction to flow instabilities will be given. The literature survey will then provide an overview of previous experimental studies describing two-phase flow instabilities, critical heat flux, and heat transfer, in boiling fluid. In view of this thesis, every reviewed article represents a piece in the ongoing two-phase boiling flow instability puzzle.

2.1 Fundamentals of boiling two-phase flow instabilities

The objective of this section is to describe the main mechanisms of instabilities occurring in two-phase flow systems. This work does mostly consider macroscopic instabilities involving the entire two-phase flow system. Microscopic phenomena occurring locally in the gas-liquid interface, for instance bubble collapse, are not treated. Even though this thesis focuses on DWO, an overview of other instability phenomena in two-phase flow is given since they are frequently encountered in literature concerning DWO, and might also be encountered in the experimental program. DWO are thoroughly treated, the others more briefly. The work on classifications of flow instabilities was pioneered by Stenning and Veziroğlu [6].

2.1.1 Density Wave Oscillations (DWO)

Density wave oscillations (DWO) are fluid waves of alternately higher and lower densities traveling across the system. DWO is characterized by quite large flow rate amplitude oscillation and possibly occurrence of reversed flow, and its distinctive period to transit time ratio.

2.1.1.1 DWO classification

Fukuda & Kobori [7] (1979) presented a classification of density instabilities according to phenomena involved in their occurrence. Five categories were presented encompassing three main types of density wave instabilities based on the mechanism that provoke them. These are density wave instabilities caused by gravity, friction and momentum [8].

Type I: Density wave instabilities due to gravity are experimentally reported at low quality conditions in long upward riser sections. Feedback between head, flow and void fraction can lead to cyclic flow behavior, particularly in natural convection loops.

4

Type II: Density wave instabilities due to friction are the most common density wave instability encountered in the literature. Notice that the DWO abbreviation when used later in this report generally refers to DWO Type II. The governing mechanism is described in the next section.

Type III: Density wave instability due to momentum has received very little attention. This phenomenon is caused by interactions between the inertia and momentum pressure drop.

2.1.1.2 DWO mechanism

Density Wave Oscillations are due to multiple feedbacks between the flow rate, vapor generation and pressure drop [9].
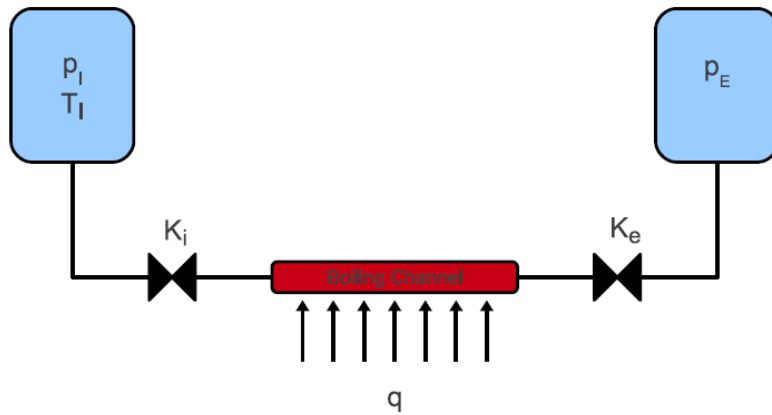
Figure 2.1 DWO mechanism [10]

The mechanism of DWO [11] [10] can be explained by considering a system similar to the one shown in Figure 2.1. The pressure of the inlet and exit reservoirs are kept constant at all times. Two flow restrictions are placed at the inlet and the exit of the test section, and as a simplification, it is assumed that the system pressure drop is concentrated over the two restrictions. Vapor generation in the heated test section is assumed to be constant. A density wave oscillation is triggered by a perturbation of a system boundary condition. Suppose that, at t_0, the exit restriction pressure drop ΔP_e undergoes an infinitesimal drop from its initial steady-state value. Since the total system pressure drop has to be constant, a signal travels upstream with the speed of sound, yielding a rise in inlet pressure drop ΔP_i. Larger ΔP_i implies a lower channel inlet pressure. The result is an infinitesimal increase in the inlet velocity since u_i is proportional to $\sqrt{\Delta P_i}$. In short, the inlet velocity u_i evolves to keep system pressure drop ($\Delta P_i + \Delta P_e$) constant. A higher inlet velocity causes a wave of higher density fluid to enter the test section at t_0. All this

5

happens at the fluids' speed of sound, which is regarded as instantaneous. After time t, which is the time taken by the high density wave to propagate through the channel; denser fluid reaches the exit restriction and causes an increase in ΔP_e. This is followed by an instantaneous decrease in ΔP_i, decreased inlet velocity, and hence a longer residence time thus the fluid attains greater enthalpy, greater vapor quality and less density, when it reaches the exit restriction. Greater enthalpy denotes higher void fraction, vapor quality, and lower mixture density. As the low density wave reaches the exit restriction, the pressure drop once again decreases, and the cycle is completed. It takes one high and one low to make a cycle, so it is evident that the DWO period can be concluded to be approximately equal to twice the boiling channel residence time. This is regarded as the classical DWO description.

The density wave type oscillations are fluid waves of alternately higher and lower densities traveling across the system. Density wave oscillations can also be viewed as instabilities where temperature or enthalpy perturbations cause density or void fraction perturbations, which travel at the kinematic-wave velocity of the mixture [9].This causes fluid waves of alternately higher and lower density to travel across the heated channel. Pressure and density, temperature and enthalpy, and void fraction, are inherently linked through phase equilibrium, but pressure is the quantity that one typically measure, so the description above could be more convenient.

2.1.2 Pressure wave oscillations (PDO)

Pressure wave oscillations (PDO) [11] are caused by dynamic interactions between the channel and compressible volume. The condition necessary is that the operation conditions are in a negative slope region of the pressure drop vs. flow rate characteristics [12]. PDO also rely on a sufficient amount of compressible volume, represented by a surge tank, placed upstream of the heated section acting as energy storage element. However, very long boiling channels may suffer from PDO due to the compressibility inherent in the boiling channel itself [1]. This is a controversial conclusion not well supported in literature and DWO was not well defined at that time. DWO are often seen on the falling portion of the PDO curve. PDO are characterized by being a very low frequency process.

2.1.3 Thermal oscillations (ThO)

Thermal Oscillations (ThO) [11] are caused by interaction between the heat transfer coefficient and flow dynamics. Thermal Oscillations are related to dynamic instabilities in the liquid film in

6

the fluid-solid interface next to the tube wall. The phenomenon is associated with large fluctuations in the heated wall temperature due to transition between transition boiling and film boiling [3], i.e. movement of nucleate boiling and dryout boundaries. Thermal oscillations are highly undesirable as they may lead to failure of equipment caused by the continuous cycling of wall temperatures.

2.1.4 Other dynamic instabilities (TAO, FDI)

Thermo-Acoustic Oscillations (TAO) is oscillations with 5-30Hz [13] or higher frequency caused by resonance of pressure waves. The main mechanism triggering this oscillation is acoustic resonance in the two-phase media. Notice that the two phase speed of sound usually is much slower than, not in between, the liquid and gas speed of sound

Flow distribution instability (FDI) [14] refers to unsymmetrical flow rate distribution in parallel tube systems.

2.2 Stability of two-phase boiling systems

Triggering two phase instabilities such as DWO can have detrimental effects on a boiling system. A stability map is a useful tool for the designer searching to avoid DWO. The stability threshold of DWO can be predicted by a two-dimensional stability map based on non-dimensional groups. These groups are, the phase change number N_{pch} and the subcooling number N_{sub}, introduced by Ishii and Zuber [15].

The phase change number [8] is based on thermal equilibrium theory and calculated from channel inlet properties. In a thermal equilibrium model, it is assumed that no significant vapor generation starts until the liquid temperature reaches its saturation temperature. N_{pch} scales the amount of phase change due to heat addition (q) relative to the mass flow rate ($\dot{m} = G \cdot A_c$) and heat of evaporation (h_{fg}), which allows for interchangeable comparison in phase change between different systems.

$$N_{pch} = \frac{q}{G\,A_c\,h_{fg}} \frac{\rho_{fg}}{\rho_g}$$

The subcooling number [10] gives a dimensionless scale for single phase residence time. Subcooling is represented by the difference in the mixing enthalpy (h_i) at the inlet of the heated channel and the liquid saturation enthalpy (h_l)

$$N_{sub} = \frac{h_l - h_i}{h_{fg}} \frac{\rho_{fg}}{\rho_g}$$

Both N_{pch} and N_{sub} accounts for the system pressure by a relative difference in phase density correction. This ratio ($\frac{\rho_l - \rho_g}{\rho_g}$) will become lower as the pressure approaches the critical pressure of the fluid in consideration. Ishii and Zubber proposed a dimensionless stability map with the two above mentioned scaling parameters.
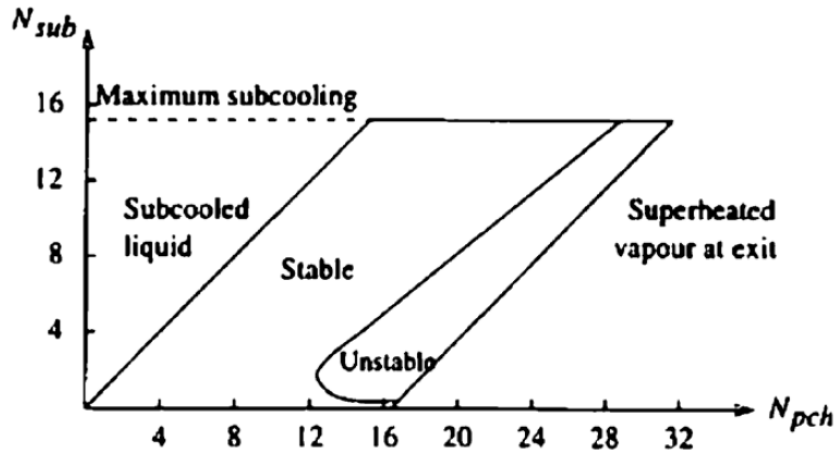
Stability map of Ishii and Zuber [Aldridge and Fowler, 1996]

Figure 2.2 Ishii and Zuber stability map

Boiling system operation condition is situated to the right of the subcooled line, indicating an exit quality less than zero. The upper corner, to the left of the subcooled liquid line, indicates in fact a single phase system. In the stable region, boiling of the bulk flow does occur but not to such extent that instabilities is initiated. The curved line between stable and unstable region projects the threshold value, or the lower limit at which self-sustained oscillations can be sustained, also referred to as marginal stable. A system operating in the unstable region will be subject to growing instabilities when experiencing a perturbation. The unstable region stretches far into the superheated vapor at exit region.

2.3 Experimental studies overview

The following section is intended to provide an overview of previous experimental investigation where DWO is reported and described in detail, mainly focusing on horizontal macro channel configurations in accordance to the scope of this work. Even though DWO is the main subject of interest, other flow instabilities are usually encountered in experiments, so a literature survey

8

cannot be written without briefly mention them. Similarities and differences in procedure, apparatus and results are outlined rather than attempting to give a summary of each experimental study. Major findings related to the oscillations characteristics in DWO are outlined. The second part will be more specific in the coverage of previous investigations on the critical heat flux. The third part puts attention toward pressure loss and heat transfer characteristics in boiling systems. Due to the limited amount of research on the later topics, micro channel and vertical systems is also included.

Several experimental investigations have been conducted to investigate two phase flow instabilities. Various systems has been designed and built to generate PDO, DWO and ThO, and to investigate the effect of flow restrictions, pressure, flow rate, heat flux, inlet temperature on different characteristics among them stability. The literature on two-phase flow instabilities in boiling systems can roughly be subdivided into three categories dealing with vertical forced, vertical natural and horizontal flow. Most of the former research has been concentrated on vertical systems with either single or parallel arrangement [16]. This is due to its similarities with boiling water reactors and evaporators typically found in thermal (coal fired) power plants. Less attention has been given towards horizontal boiling systems, even though they often are encountered in systems commonly found in the industry [3] such as shell and tube heat exchangers, distillation column reboilers, and air condition evaporators. A benefit of doing horizontal experiments is that the effect of gravity can be disregarded in flow direction.

2.4   Experimental studies on DWO in horizontal macro-channels

DWO is by far the most studied kind of two-phase flow instability [8]. Experimental investigations of two-phase flow instabilities in horizontal boiling systems where DWO is reported are summarized in Table 2.1. It is evident from the range in system parameters that two phase flow instabilities phenomena can occur under a very wide range of system conditions. This should be kept in mind when results from different studies are compared to each other. The difference in geometry spans from L/D=25 to L/D=10 000. It is seen that most of the experimental studies utilized water or Freon (R11, R113) as working fluid. A refrigerant is often found suitable as a working fluid due to its relatively low boiling point and low latent heat of vaporization. This minimizes the heat flux needed in the test section. Some more recent studies have utilized hydro-fluorocarbons (R22, R134a). These are more environmentally acceptable

alternatives to traditional refrigerants while still being less flammable than common hydrocarbons like propane.

Experiments in vertical boiling flows are performed with both natural and forced circulation [11]. In horizontal systems is, however, the only viable option induced flow circulation. Three different flow circulation approaches are identified among the existing experimental studies on two-phase instabilities in horizontal systems. One approach is simply having a pump feeding fluid through the loop [17]. Flow rate at the test section inlet is fully dictated by the volumetric displacement of the pump and is often supposed to be constant. Another option is to pump liquid through a large bypass channel parallel to the test section imposing a constant pressure drop condition [4]. This configuration intends to resemble the conditions in a single tube placed in a tube bundle. Flow rate can either be controlled by changing pump speed or by adjusting a bypass valve. Third approach uses a fundamentally different concept. Flow is imposed between two reservoirs at different pressure levels, typically a nitrogen pressurized supply tank in conjunction with an atmospheric receiver tank. This is essentially an open loop with constant inlet and exit pressure. Several experiments, or more precisely those intended for studying PWO, utilizes a surge tank to incorporate a compressible volume upstream of the heated section. The surge tank can often be disconnected to allow for measurement of steady state characteristics. One should also be aware the fact that the parameters kept constant in experiments may not be the same in the variety of studies (e.g. constant inlet or outlet pressure).

A table of experimental studies in horizontal boiling macro channels is found on the subsequent page. The experimental studies on two-phase flow instabilities covered in this part are exclusively for tube boiling in macro channels. Although, research on micro-channel flow in general, and two phase micro channel flow in particular, are becoming very important in many fields such as micro-electromechanical systems, space industry and biomedical applications [11].

10

Table 2.1 List of experiments on two-phase flow boiling instabilities in horizontal macro-channels

Reference [8]	Chan nels	Fluid	D_h [mm]	L [m] Length	P_{in} [bar] Inlet p	ΔT_{sub} [C]	Q [W] Q" [W/m²]	Configuration (t/τ)
H. Andoh (1965) [17]	1	Water	4.58	3	7.9	90	(<2400W) 3.85-55.8kW/m²	Forced, pump (**t/τ ~0.5-1.1**, tau reported)
J.S. Maulbetsch & P. Griffith (1965) [1]	1	Water	1.19-6.35	<1.5 l/d~25-250	1-6	50-120	<18 000W	Pump, bypass controlled. Greatest heat flux in the shortest tubes (**See Andoh**)
A. H. Stenning and T.N Veziroglu (1965) [18]	1	R-11	3.75	0.95	3-10	14	< 5000W (350-700)	Pressurized reservoir (**Categorization in paper**) Surge tank
K. Akagawa & T. Sakaguchi (1971) [14]	1, 3	R-113	4	40 (!) l/d=10 000	1-41	80	1197W (2.4kW/m²)	Forced, pump. Hor. coiled test sect. (**t/τ~0.4-0.7**)
P. Saha et al. (1976) [4]	1	R-113	10	2.743	<16.5	0-110	<100 000W	Pump, large bypass channel parallel to the test section (**t/τ ~3.5-4** [19])
M. Ozawa et al. (1979) [12]	1	R-113	3.8	6	2.17	47.8	2000W (36kW/m²)	Diaphragm pump with speed, stroke and throttling control Surge tank. (**t/τ~0.9**)
H. Yuncu (1990) [20] [5]	1	R-11	5	0.8	7	20-40	300, 600W (<47kW/m²)	Open loop with const. inlet and exit pres. Surge tank. (**t/τ ~1**)
Y. Ding et al (1995) [3]	1	R-11	10.9	1.06	7.6	20-50	2500W 0-100kW/m²	Dp, Surge tank. (**t/τ~0.2-0.35**)
Ö Çomaklı et al. (2002) [16] M. Yılmaz et al. (2002) [21]	1	R-11	11.2 11.2	3.5 3.196	7.5 7.5	68-80	16 000W 16 000W	Dp, Surge tank. (**t/τ ~6-8** long periods not clear why)
S. Kakaç & L. Cao (2009) [22]	1	R-11	7.5	0.605	3-6	50-100	400-1000W (<8 kW/m²)	Dp, surge tank (**t/τ~0.5-0.85** calculation based on [11])
N. Liang et al. (2011) [23]	1	R-22	8	3	5-8	50	<3000W 5-17kW/m²	Resembles a refrigeration loop. Mass flow controlled by compressor speed and EEV. (**t/τ ~2**)
NTNU Facility [8] [24] [25]	1	R-134a	5	2.035	4-12	0-50	<2000W (<62,5kW/m²)	Pump (variable speed drive), bypass valve (**t/τ ~1.5-2**)

The table indicates typical sizes and ranges of variables, and may be subject to error reflecting the challenges associated with investigating various sources in the literature. Experimental data is often expressed in various forms, at different positions, and with various units of measure.

Legend: Dp= Constant pressure difference configuration approach, open loop with inlet and exit reservoirs at constant pressure.

(numbers in parenthesis) are calculated values.

Effort has been made to calculate the boiling channel residence time in former experimental studies. A formula for calculating the channel residence time was given by Colombo et al. [26]

$$\tau = \tau_{1p} + \tau_{2p} = \frac{A_c L}{q} \left[\rho_{in} \Delta h_{in} + \rho_{lg}\, h_{lg}\, ln\left(1 + \frac{\rho_l}{\rho_{lg}} x_e\right) \right]$$

It is important to stress the fact that the transit time τ only is a calculated value and should therefore be perceived as guidance. DWO is commonly identified by having an oscillation period in order of one to twice the residence time of a fluid particle in the heated section. Calculation was based on the conditions given in the different papers. The period to transit time ratio t/τ should due to the numerous uncertainties only be considered rough estimate. But, it provides an indication whether the instabilities can be classified DWO-type or not. Indeed of discerning usefulness as naming of different instabilities was not fully established yet in the time of the earliest papers, possibly making room for some confusion.

2.4.1 Experimental configurations and results

Experimental studies on DWO horizontal macro channels are chronologically reviewed with emphasize on system configuration and significant findings.

The purpose of the study of H. Andoh [17] (1964) was to observe the region of density wave instability, and examine the causes of oscillation, in a long uniformly heated horizontal pipe with boiling water. It is recognized that heat transfer is an essential part of the two-phase instability mechanism, since flow oscillations occur for various flow regimes when there is boiling, but do not occur for various flow regimes of air-water mixtures with no boiling. The configuration was forced-convection and the inlet flow remained constant even though oscillations of exit flow rate occurred. It was a tendency for flow oscillations to increase with increased subcooling. Frequency of oscillations, the inverse of the period, was obtained by counting pressure trace. The period was found to be in a rather wide range from about 1 to 7 seconds. However, a definite trend of the periods with power input, flow rate and subcooling could not be found. The general tendency was that increased flow rate reduced the oscillating period. The period of oscillation was found to be approximately equal to the transit time in the test section. It was suggested that compressibility in the steam voids had significant effect on the oscillation period. An analytic expression for the test section natural frequency was proposed in order to investigate how oscillations in experiments deviate from this value. A burnout eventually occurred in conjunction

12

with a complete absence of water as the heat input was raised. At higher heat inputs, flow the test section became quite as a result of flow oscillations and periodic buckling occurred because of thermal expansion.
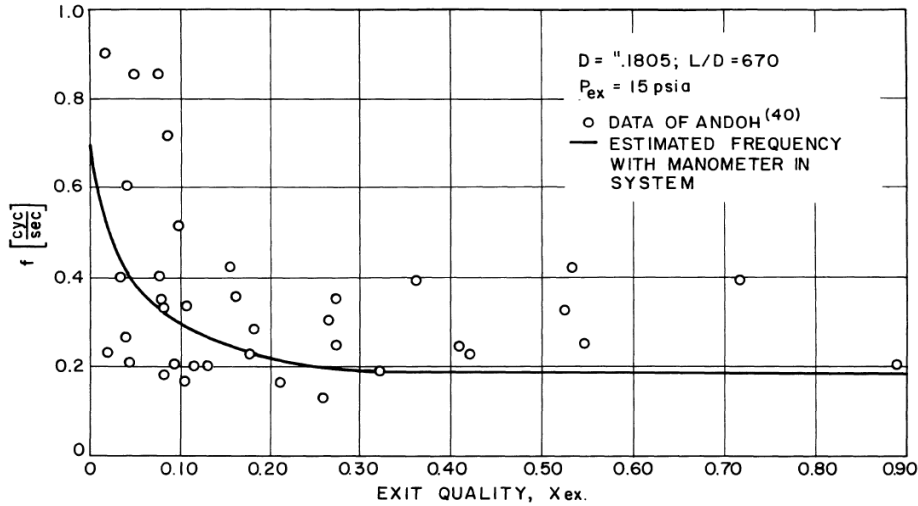
FIGURE 59: FREQUENCY MEASUREMENTS OF OSCILLATORY INSTABILITY

Figure 2.3 Oscillation frequency – exit vapor quality, Maulbetsch and Griffith (1965) [1]

Maulbetsch and Griffith [1] plotted the data of Andoh one year later. The only conclusion that could be drawn was that oscillation frequency is dependent on more factors than the exit quality alone.

The effect of an upstream compressible volume as energy storage element on system compression volume oscillations (PWO) stability was investigated by Maulbetsch and Griffith [1] (1965). They found that for certain geometries such as very short test sections operating at high heat fluxes, the required amount of compressibility for unstable behavior was surprisingly small. These instabilities could always be eliminated by sufficient throttling between the compressible volume and the test section. Except long test sections (L/D > 150) where the compressibility inherent in the heated section itself, due to vapor generation, could be sufficient to initiate instabilities. External throttling did not have any value in this case. The PDO instability criterion was primarily intended for use with subcooled conditions or very low vapor quality. In high quality situations, PWO was likely to be precluded by DWO. Hence, even a design which satisfies the stability requirements for PWO cannot be termed unconditionally stable. A DWO criterion is also needed.

A salient report by Stenning and Veziroğlu [18] (1965) describes an experimental program identifying three distinct types of oscillatory behavior. Those are classified as density wave-, pressure drop- and thermal oscillations. Freon-11 was pressurized by means of nitrogen in a container at the upstream side of the test section and a constant pressure regulation valve to maintain flow into the test section. Superheated, or a mixture saturated vapor and liquid, Freon leaving the test section was led into a recovery system. A surge tank was installed to isolate the heated section from the long column of liquid in the upstream tubing, whose inertia tended to damp out the density wave oscillations if connected directly to the heated section. The surge tank was omitted from the apparatus during film boiling experiments.

In experiments with nucleate boiling; PDO were observed in flows where the slope of the pressure drop versus flow curve was negative. DWO were observed at higher exit qualities, in regions where the pressure drop increased with increasing flow, and where the ratio of inlet liquid density to mixed mean density leaving the heated section was of the order of 40 or greater. Burst of higher frequency DWO were in some cased observed in the low frequency PDO. Experiments with film boiling were stable on reduction in flow rate until DWO appeared. DWO would only persist at lower flow rates, just as in the other experiments. DWO was observed at density ratios (test section inlet to outlet) of 40 or more with nucleate boiling in the first 2/3 of the heated section length and film boiling in the remaining 1/3.

The period of DWO was found to be in the order of the mean residence time of a particle in the test section. DWO could be eliminated by providing sufficient orificing at the inlet of the evaporator, provided that no cavitation occurred in this inlet orifice.

Thermal oscillations were detected by large fluctuations (128-202°C) in temperatures measured in thermocouples close to the test section exit. It was reported that when ThO occurred, it was always just after the onset of DWO with nucleate boiling and ThO were always replaced by fully developed DWO with film boiling upon further reduction in flow rate. ThO was not obtained after replacing a badly fouled heater tube by a new tube, suggesting that surface conditions may have a strong influence on ThO.

Akagawa et al. [14] (1971) performed a systematic analysis of flow distribution instability phenomena in parallel long-evaporator tube system. Circulation of R-113 in the loop was forced by a diaphragm pump. The pressure ranged from atmospheric to supercritical, in order to

14

simulate phenomena in steam generators. It was found that for "thermal oscillatory instabilities" (i.e. DWO Type-II) to occur is it necessary with a relative low system pressure and the fluid in the downstream portion of the tube has to be superheated, or of very high quality. Large variations in temperature of the tube close to the test section exit at low flow rate was indicated to be because of deficiency of liquid and/or the superheating of the fluid. It is concluded that the instabilities occurs due to variation of heat transfer coefficient on the inner surface and that of the heat capacity of the tube. In retrospect, it is hard to determine whether the "thermal oscillatory instabilities" was the DWO or the ThO mode. It is acknowledged that the DWO period is in order of several tenths of seconds due to the immoderate length (40m) of the heated section, so the observed instability might be a hotchpotch of the two.
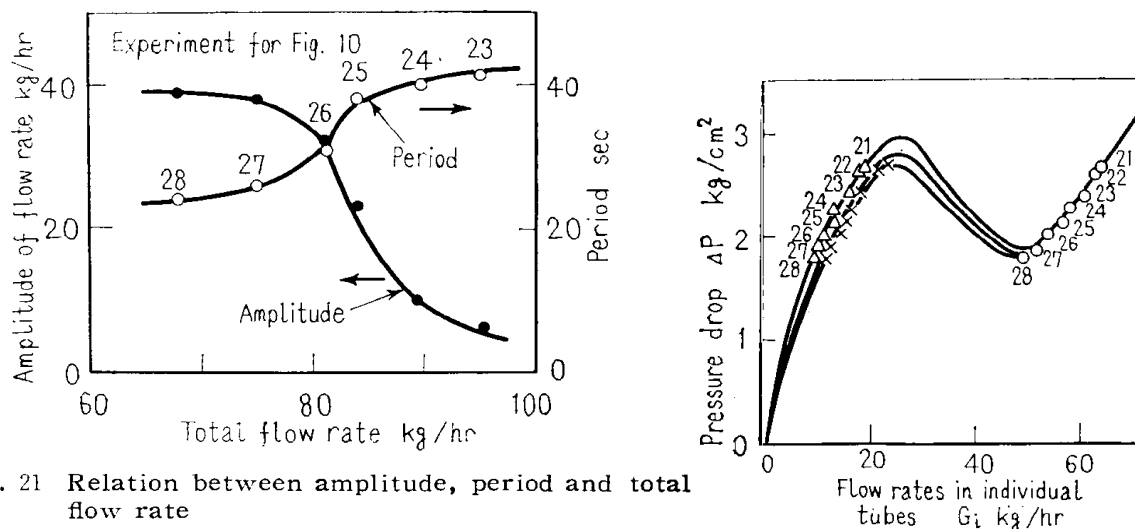
Fig. 21   Relation between amplitude, period and total flow rate

Figure 2.4 Oscillation amplitude and period – flow rate, Akagawa et al. (1971) [14]

Figure 2.5 Test section pressure drop- flow rate, Akagawa et al. (1971) [14]

Amplitude and period related to flow rate in a 3-channel experiment with constant heat flux, subcooling and exit pressure (6 bara). There is a relative large pressure loss associated with the 40 m test section (L/d=10 000, coiled tube) which causes the inlet pressure to change on variation in flow rate. It is also questionable whether the whole test section is active to the DWO phenomena due to its excessive length. One can imagine that the excess length and pressure drop led to an inactive single phase region.

P. Saha et al. [4] (1976) accomplished an experimental study on the onset of DWO in a uniformly heated boiling channel using R-113 as the operating fluid. Focus was to determine the effects of

system pressure, inlet subcooling, flow restrictions and inlet velocity. A slightly different approach on forcing the boiling flow was chosen. A constant pressure drop is imposed across the heated channel by using a large parallel bypass channel. This configuration is supposed to imitate the behavior of one tube in an array of several tubes, similar to what is found in a heat exchanger tube bundle. Flow rate was controlled by adjusting the test section bypass valve. Unlike some other studies, only one mode of sustained well defied oscillations of significant amplitude could be detected in the experimental program by Saha et al., namely the DWO-mode. The frequency of oscillation was determined from the inlet flow trace. One major finding was observation of a significant time lag between system pressure drop and the inlet flow during DWO.

Period and frequency of oscillations in experimental data, set II as reported by Saha et al., was compared to the average channel transit time calculated from N_{sub} and N_{pch}. Rizwan-Uddin [19] (1994) found that the ratio of oscillation period to average channel transit time was about 3,5-4. A number significantly larger than the typical one-to-two times the transit time reported in many other experimental studies. The paper of Rizwan-Uddin stresses that the classical description of the DWO mechanism (section 2.1.1.2) needs to be supplemented. This conclusion has been subject to both support [10] and controversy.
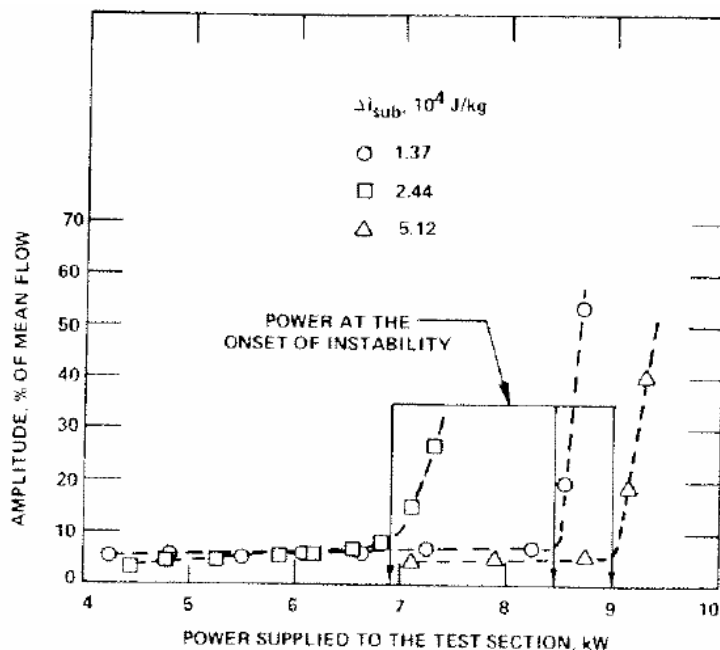
Fig. 3   Determination of the point of inception of flow instability (set No. IV)

Figure 2.6 Normalized flow rate amplitude– test section power input, Saha et al. [4] (1976)

16

As inlet subcooling was increased the onset of instability, or the power corresponding to where the amplitude of oscillation starts to increase rapidly, dropped until a certain subcooling, but started to grow thereafter. DWO Amplitude of oscillation increases with increasing test section power.
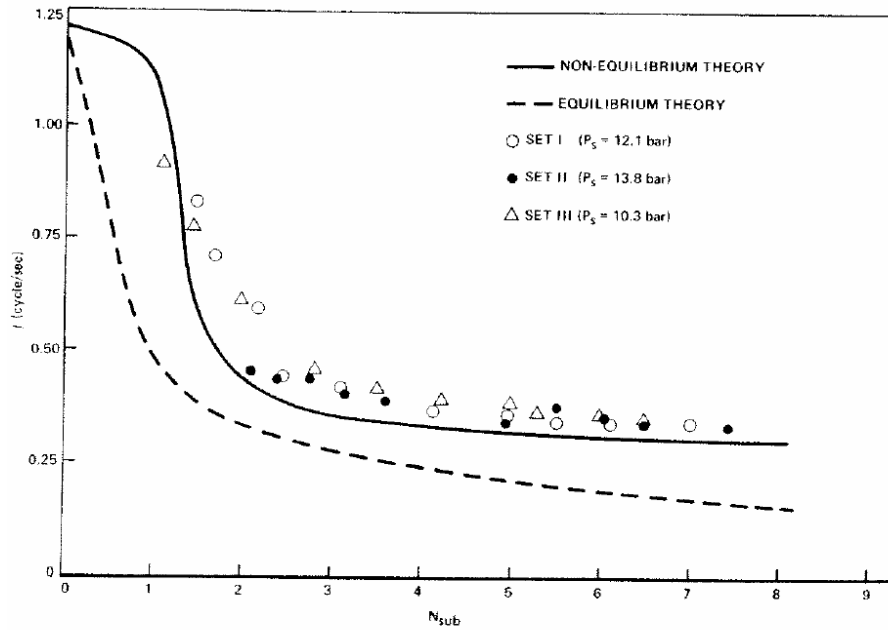
Fig. 6 Comparison of experimental data on the frequency of oscillation with various theoretical predictions

Figure 2.7 Oscillation frequency – Subcooling number, compared to equilibrium and non-equilibrium theory. Saha et al. [4] 1976

The period of oscillation was found to be in the order of the transit time of the kinematic wave (i.e. on the order of length divided by velocity). Oscillation period increased monotonically with increased inlet subcooling, completely in agreement with both equilibrium and non-equilibrium theory discussed in the same work. No appreciable fluctuation of wall temperature could be observed at either of the two thermocouples mounted near the exit of the test section. This ascertains that DWO not necessarily trigger large amplitude wall temperature oscillations (ThO) in the two phase region.

Ozawa et al. [12] (1979) observed high amplitude DWO in parts of the PDO cycle. The experimental apparatus used was a forced flow boiling loop with R-113. The flow rate was controlled by adjusting the diaphragm pump speed, pump stroke and opening of two valves. A surge tank was incorporated to study the behavior of PDO.

17
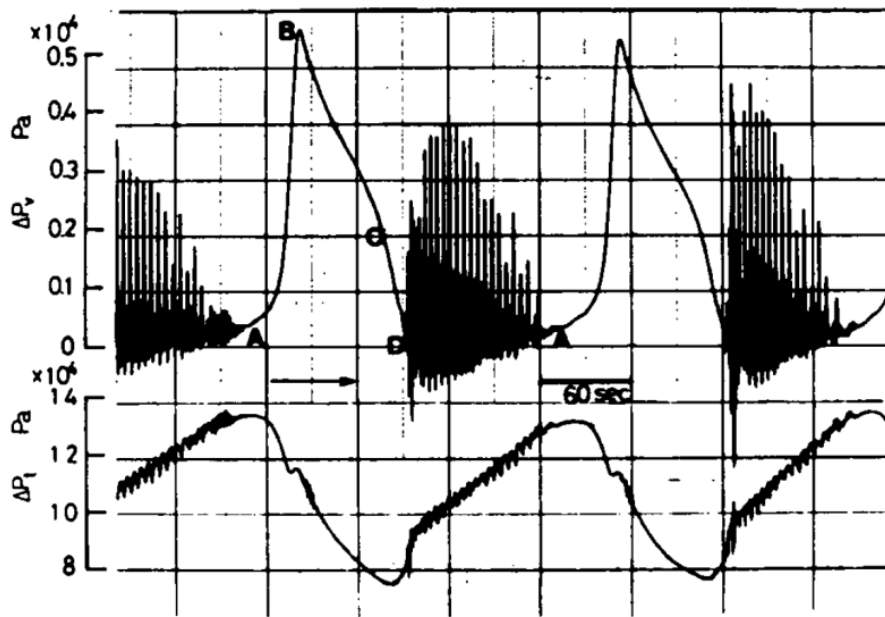
$P = 2.17 \times 10^5$ Pa $\quad q = 3.59 \times 10^4$ W/m
$\Delta T_{sub} = 47.8$ K $\quad G = 60.5$ kg/h $\quad V_S = 3.6 \times 10^{-3}$ m^3

Figure 2.8 Pressure trace – time, DWO superimposed on PDO. Ozawa et al. [12] (1979)

At a state where the pressure drop oscillation (PDO) has a minimum value, the flow begins to oscillate with high frequency (DWO) until damped, and the PDO cycle repeats. A Burn-out was also reported to occur during the DWO sequence. The occurrence of DWO and/or burn-out was entirely dependent upon the experimental range, and not essential features of PDO.

Ding et al. [3] (1995) conducted an experimental investigation of two phase flow instabilities (PDO, DWO and ThO) where steady state internal characteristics was obtained under different system parameters, such as system pressure, heat input and inlet temperature. The dependence of amplitude and period on system parameters is investigated and discussed in detail. DWO amplitude of inlet pressure oscillations did not change significantly with flow rate at same heat input but decreased as the heat input increased. DWO oscillation period decreased: as flow rate decreased, as heat input increased, as the subcooling increased. See the figures on the next page. Ding et al. did not consider the effect of system pressure; fluid that was discharged from the exit restriction went through a condenser, and was later collected in the recovery tank which was maintained at constant pressure.

18
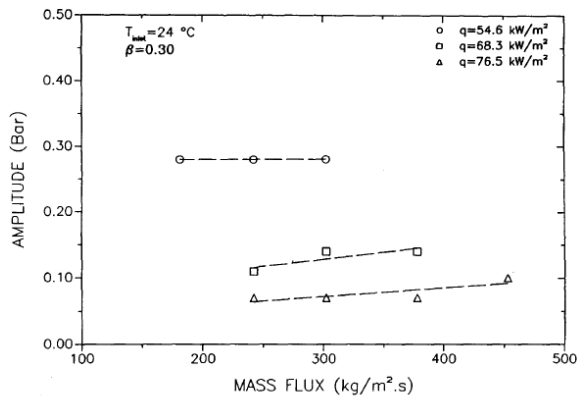
Figure 11. Effects of mass flux on the amplitudes of density wave type oscillations. T_{inlet} = 24°C, β = 0.30.
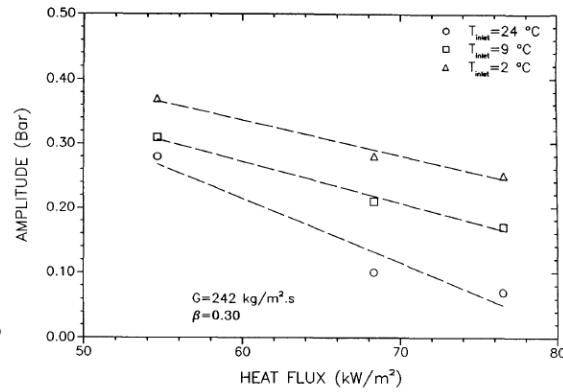
Figure 13. Effects of heat input on the amplitudes of density wave type oscillations. G = 242 kg/(m² s), β = 0.30.
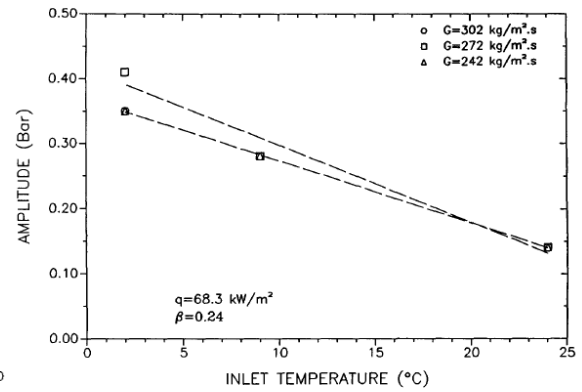
Figure 15. Effects of inlet temperature on the amplitudes of density wave type oscillations. q = 68.3 kW/m², β = 0.24.
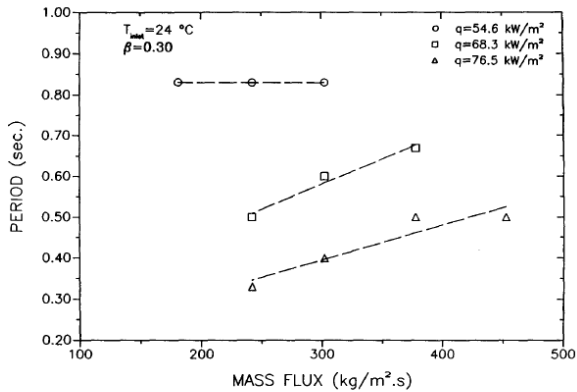
Figure 12. Effects of mass flux on the periods of density wave type oscillations. T_{inlet} = 24°C, β = 0.30.
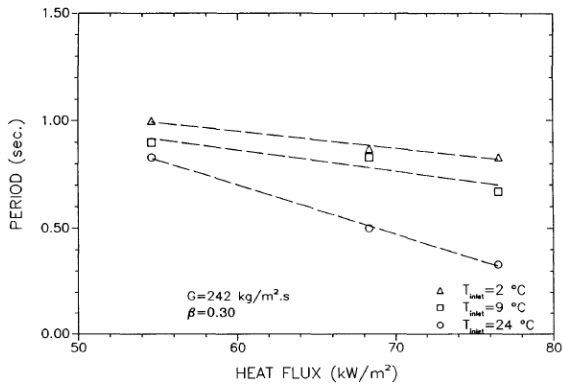
Figure 14. Effects of heat input on the periods of density wave type oscillations. G = 242 kg/(m² s), β = 0.30.
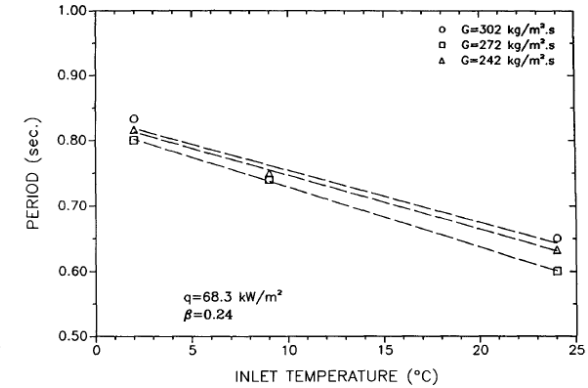
Figure 16. Effects of inlet temperature on the periods of density wave type oscillations. q = 68.3 kW/m², β = 0.24.

Figure 2.9 Amplitude and period – Mass flux, at 3 levels of heat input. Ding et al. [3] (1995)

Figure 2.10 Amplitude and period – Heat flux, at 3 inlet temperatures. Ding et al. [3] (1995)

Figure 2.11 Amplitude and period – Inlet temperature, at 3 different flow rates. Ding et al. [3] (1995)

19

All experiments by Ding et al. were conducted with a constant pressure in the Refrigrant-11 main supply tank. Flow rate was adjusted using a valve controlling the pressure drop over the test section. Pure pressure drop oscillations did never occur alone in the experiments; they were always accompanied with other higher order oscillations. DWO was found superimposed on the falling portion of the PDO curve. ThO was in this study regarded an independent phenomenon rather than an accompaniment of PDO. The main reason for wall temperature variations was indicated to be due random motion of the liquid-vapor transition point.

DWO period was related to the test section residence time. The study concludes that period of DWO is governed by the balance between heat input, which accelerates the vapor particles, and flow rate, which dominates the liquid particle speed. It was observed in test section exit sigh glass that the bottom was covered with a layer of liquid, whose thickness varied with mass flux. The bottom wall temperature remained almost constant during DWO, while the top wall temperature fluctuated to some degree. Indicating that vapor was shifted to the upper part of the tube, flow stratification may to some degree have influenced the results.

Kakaç and Cao [22](2009) experienced that density wave oscillations was superimposed on the pressure drop oscillations. The experimental apparatus featured both an upflow and a horizontal boiling channel. The working fluid Freon 11 was supplied from a half filled pressurized liquid container. A surge tank was present during all experiments as PWO had the main focus. The experiments confirmed that a drift flux based numerical model adopted in the theoretical study predicted PDO quite well, in contrast to DWO, which could not be predicted because the model did not take the propagation of continuity waves that generates DWO explicitly into account. Period and transit time (calculated with both equilibrium and non-equilibrium) was only reported for the PWO mode. Thermal oscillations accompanied the pressure drop oscillations.

Liang et al. [23] (2011) uses an experimental configuration based on an R-22 vapor-compression refrigeration cycle. The paper is concerned with an experimental investigation of two-phase flow instabilities in a horizontal straight tube evaporator. Heat flux in refrigeration systems is often much less than the case of evaporators tube in water systems; and moreover, the working condition in a refrigeration system is also different from that in a water system, such as throttling device and the quality at the inlet and exit. Three types of dynamic instabilities including DWO, PDO and ThO was found. DWO took place in the single tube evaporator thorough the whole

range of mass velocities (150-1500kg/m²s). DWO was by the authors regarded as the least critical form of instability in refrigeration cycles since it has the smallest amplitude and shortest period among the three types. The period of DWO was found to be proportional to the transit time of a fluid particle traveling through the evaporator. Liang et al. concludes that DWO takes place when the heat flux is high enough for a given mass velocity.

Çomaklı et al. [16] (2002) performed experiments at constant heat input, system pressure and exit restriction. The working fluid was pressurized with nitrogen in the main tank. A surge tank placed upstream of the test section provides a compressible volume acting as a capacitance. It was found that the stability boundary moved to lower mass flow rates with decreasing inlet temperature (increased subcooling). Both period and amplitude of DWO decreased with decreasing mass flow rate and increases with decreasing inlet temperature. Wall temperature is reported to be much higher at the top of the tube than at the bottom indicating that the top of the tube was in a dry-out condition.
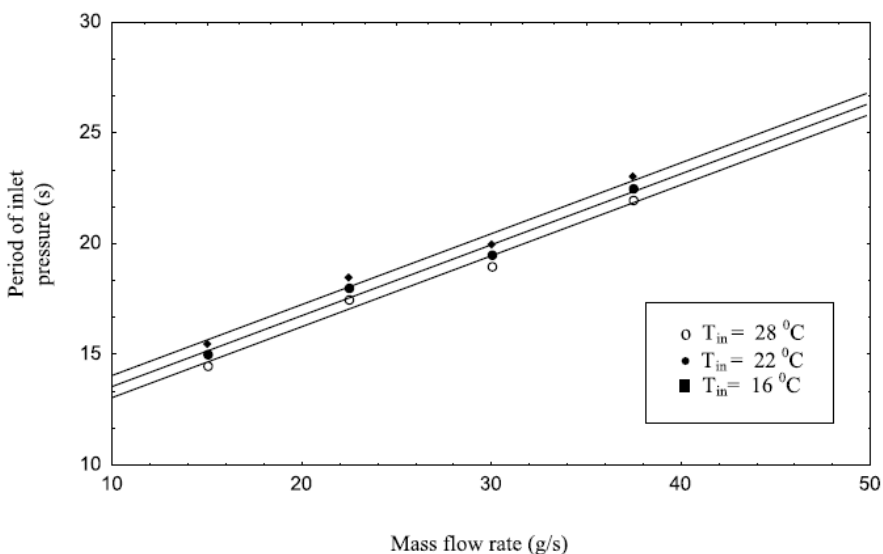
Effect of inlet temperature and mass flow rate on the period of density wave type oscillations.

Figure 2.12 Period of oscillation – Mass flow rate, at 3 inlet temperatures. Çomaklı et al. [16] (2002)

The period of oscillations appears to be rather independent of inlet subcooling. This corresponds well with observations of Colombo [26] (2011) which wisely points out that the period to transit time ratio will as a matter of fact increase with increasing inlet temperature even though the period remains the same.
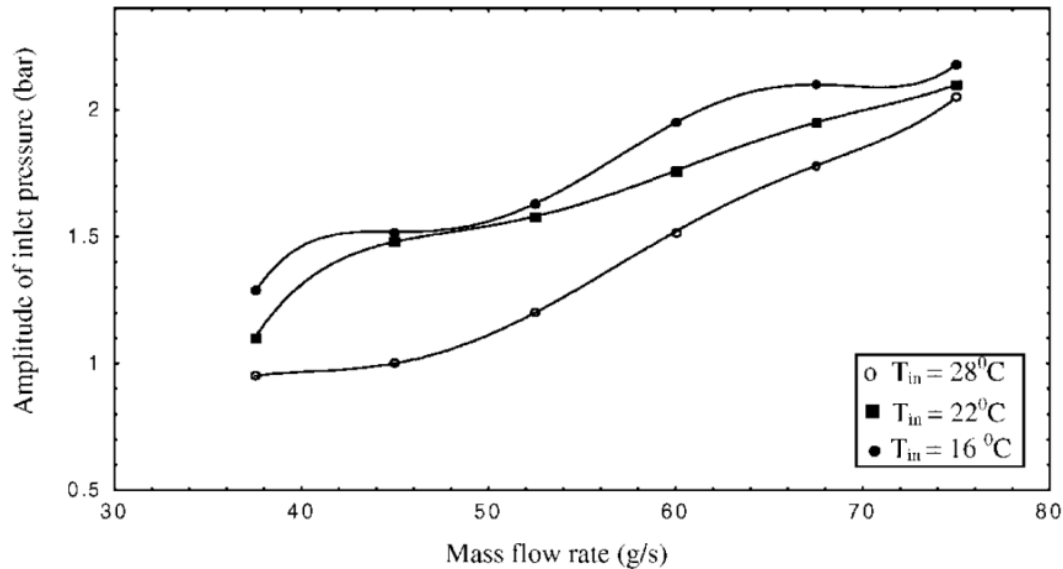
Figure 2.13 Amplitude of inlet pressure – Mass flow rate, at 3 inlet temperatures. Yılmaz et al. [21] (2002)

The study of Çomaklı et al. was followed up by Yılmaz et al. [21] (2002). In this study, the effect of inlet subcooling on two-phase flow instabilities in a horizontal in-tube system with augmented surfaces. Five different inlet temperatures and five different configurations of the heat transfer surface were used. Experiments were carried out at constant pressure, heat input and exit restriction. All three modes of flow instabilities (PDO, DWO and ThO) were observed in all combinations of subcooling and surfaces. Increasing the inlet subcooling moved the stability boundaries to lower mass flow rates both the smooth tube and all four enhanced tube configurations, thus increasing system stability. Both DWO period and amplitude of oscillation increased with increased degree of subcooling and with increasing mass flow rate for all five heater tube configurations. However, DWO period is longer and amplitude is stronger for tube with enhanced surfaces than those of the bare tube. The system was found to be more stable at higher inlet subcooling but the penalty was more violent oscillations.

In recent studies, like the one of Liang et al. [23](2011), main focus on is still on determination instability boundaries. It is also evident that systematic work changing only one parameter at the time will be appreciated in further work.

2.4.2 Summarizing literature on DWO in horizontal macro-channels

Upon reviewing the literature, one can notice that most studies have explored vertical systems for the understanding of boiling flow instabilities. This part has focused on experiments in horizontal

22

in-tube boiling systems. Consequently, only a fraction of the literature available has been reviewed.

Early experiments were performed to establishing stability criteria and flow maps. Focus was mainly on avoidance by determining safe operation boundaries of steam generation though definition of threshold values of system parameters such as flow rate, pressure, inlet temperature and exit quality. Later studies shifted its focus towards mechanisms governing DWO. Systematical studies on how period and amplitude is affected by system parameters have been conducted for different fluids and system configurations. DWO is often reported in coexistence with other instabilities, such as ThO, or superimposed on the falling portion of the PDO curve. Most experiments are conducted with refrigerants as working fluid due to its low critical pressure, low boiling point, and low latent heat of vaporization. Experiments have been performed in both single and multiple channel configurations. A driver for research on multi tube systems is the fact that instabilities becomes very difficult to detect in presence of parallel channels, since the total mass flow rate in the system remains constant while the instability is locally triggered among some of the channels. [26]

An issue in some former studies on DWO in horizontal systems is void fraction distribution caused by a flow stratification tendency. Ding et al. [3] observed that the bottom wall was covered completely by a layer of flowing liquid. Çomaklı et al. [16] experienced higher temperatures at the upper part of the test section. There are doubts about whether the liquid filled bottom part of the channel participates in the density (void fraction) oscillations. Void fraction distribution effects will also be the case in real applications at diminished flow rates. A sight glass featuring high speed visualization is regarded as crucial in order to know the flow regime.

2.5 Experiments on the effect of flow instabilities in the critical heat flux

Almost every article mentions the possible adverse effects of DWO. Those are, vibrations and mechanical fatigue, thermal cycling of material, and dry out, but the effects are seldom quantified. It is known that flow oscillations may induce premature CHF situations at the heat flux levels much lower than that for a stable condition [27]. A generic quote is that CHF is detected by excessive temperatures some small distance upstream from the test section exit. Or, that a drastic decrease in the pressure drop is followed by a rapid increase in the wall temperature.

The occurrence of critical heat flux (CHF) limits the high cooling capacity of boiling systems. It can ultimately lead to the burn-out and destruction of heated surfaces. [28] Therefore is the prediction of CHF with accuracy of importance for design and safety analysis, in particular of the nuclear power industry where CHF can deteriorate fuel rod integrity [29]. Many correlations have been developed under stable flow conditions, but boiling channels is generally known to be subject to various flow instabilities. Unsteady states might in particular occur during transit operation or accident conditions, such as a loss of coolant accident in a nuclear reactor. Under flow instability conditions, the CHF may be overestimated by correlations based on steady flow conditions.

A few experimental studies dealing with the effect of boiling flow instabilities on the critical heat flux in macro-channel systems are treated in the table below.

Table 2.2 Experimental studies on the CHF in macro channel oscillatory flows

Reference	Fluid	D_h [mm]	L_{heated} [mm]	P [bar]	ΔT_{sub} [°]	Q / Q" [W]	G [kg/m^{2}s]
Chang et al. (1996) [28]	Water	1-10.8	12-860	1-40	X_{in}=0.1	0-4.0 MW/m^2	1300 - 27000
Umekawa et al. (1996) [30]	Water	3.0 4.0 5.8	900	3-4 (exit)	T_{in}=80°C	Dg/g_0 = 0.18-5.53	100 – 700
Kim et al. (1997) [27]	Water	5.0 6.6 9.8	600 500 600	1.2 (exit)	T_{in}=20°C	< 200 kW	40- 400

Chang et al. [28] (1996) performed theoretical and experimental work where CHF correlation of water based on the Ledinegg instability (static) was derived.

Umekawa et al. [30] (1996) conducted a numerical and experimental study on the CHF under oscillatory flow conditions in a forced boiling channel system. Three different test sections were used in order to investigate the effect of tube wall heat capacity. A mechanical oscillator composed of a cylinder and piston assembly was able to superimpose a predetermined flow oscillation on steady flow. The oscillation periods were determined so as to simulate DWO in a steam generator. The CHF value was defined as the heat flux when the outer tube wall temperature exceeded predefined values specific to the tube thickness. Results from simulations

24

were used to link fluctuations in wall temperature and heat transfer to the exit quality and velocity cycle.
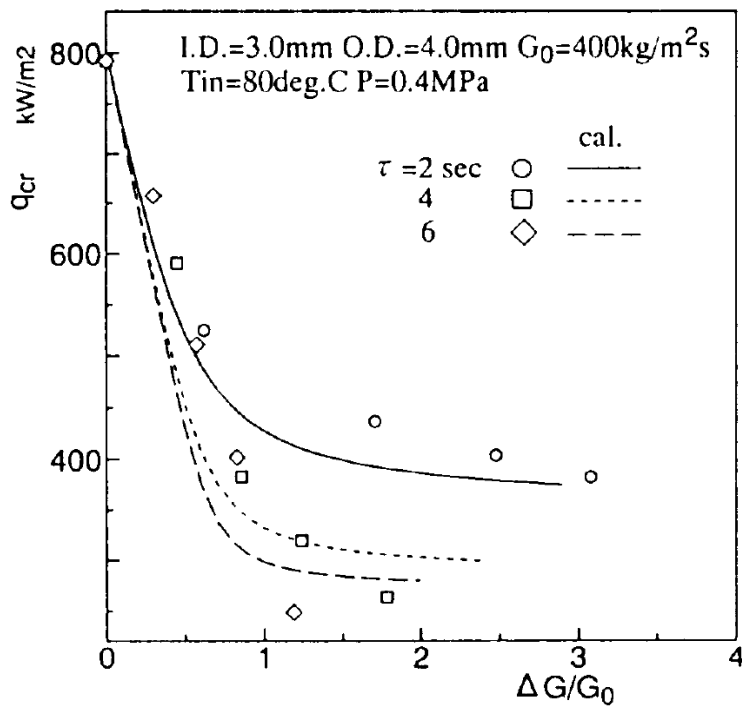
Figure 2.14 CHF – $\Delta G/G_0$, CHF under the oscillatory flow condition. Umekawa et al. [30] (1996)

Experimental results of the CHF under oscillatory flow conditions are shown together with the simulated in Figure 2.14. CHF decreases when increasing the normalized amplitude of oscillation ($\Delta G/G_0$), and has a saturation tendency toward a certain level uniquely determined by the oscillation period. Simulation results showed that an increasing the amplitude cases the dryout period to increase, causing larger temperature raise during the dryout. Therefore, increasing the amplitude results in a decrease of the CHF. The dryout period was limited to half of the oscillation period, explaining why CHF stabilizes on a low value dependent on the oscillation period.
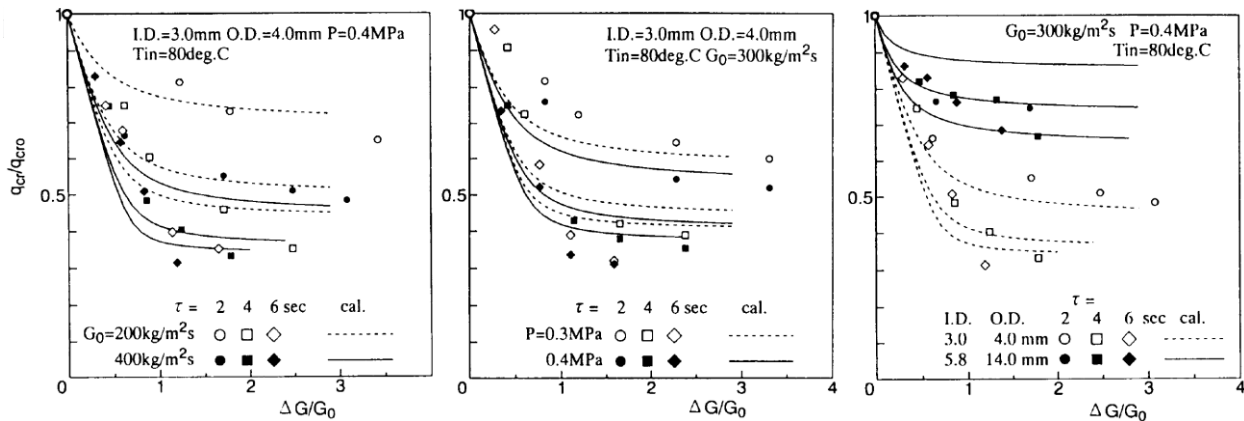
Figure 2.15 Critical Heat Flux Ratio – Normalized flow oscillation amplitude. Umekawa et al. [30] (1996)

Umekawa et al. did also investigate the influence of mass flux, system pressure and the tube wall heat capacity on the CHF. In Figure 2.15 are the CHF ratio normalized by CHF under steady flow condition. Larger heat flux is required to trigger a dryout at higher mass flux. Same goes on for the pressure, as a higher pressure means a larger relative subcooling as the inlet temperature was constant. The large heat capacity tube shows less heat transfer degradation than the thin walled. More thermal mass translates into a much less dynamic wall temperature, giving less feedback from the wall to the flow. It is concluded that the heat flux distribution and its dynamics have to be taken into account when evaluating the CHF for tubes with large heat capacity.

Kim et al. [27] (1997) investigated the effect of flow oscillations on the CHF for water flow in three vertical round tubes. An experimental study was conducted to investigate the difference between stable and oscillation flow in forced and natural convection.

Flow oscillation CHF correlation factors were developed for both natural and forced circulation. The data on oscillatory flows indicates that the CHF generally decreases as the amplitude or period of flow oscillations increases. It was also found that the CHF can be much lower for natural circulation all though oscillations in the inlet have similar characteristics.

Figure 2.16 shows the effect of averaged mass flux (left), period (right), and $\Delta G/G_{avr}$ on the critical heat flux. The developed correction factors indicates that mass flux, period and amplitude are important variables in prediction of the CHF for forced convection boiling flows.

26

(a) P=400kPa, τ=4sec, T_i=80°C, D=3mm, L_h=0.9m

(a) P=400kPa, G_{avg}=300kg/m^{2}s, T_i=80°C, D=3mm, L_h=0.9m

(b) P=400kPa, τ=6sec, T_i=80°C, D=3mm, L_h=0.9m

(b) P=400kPa, G_{avg}=400kg/m^{2}s, T_i=80°C, D=3mm, L_h=0.9m
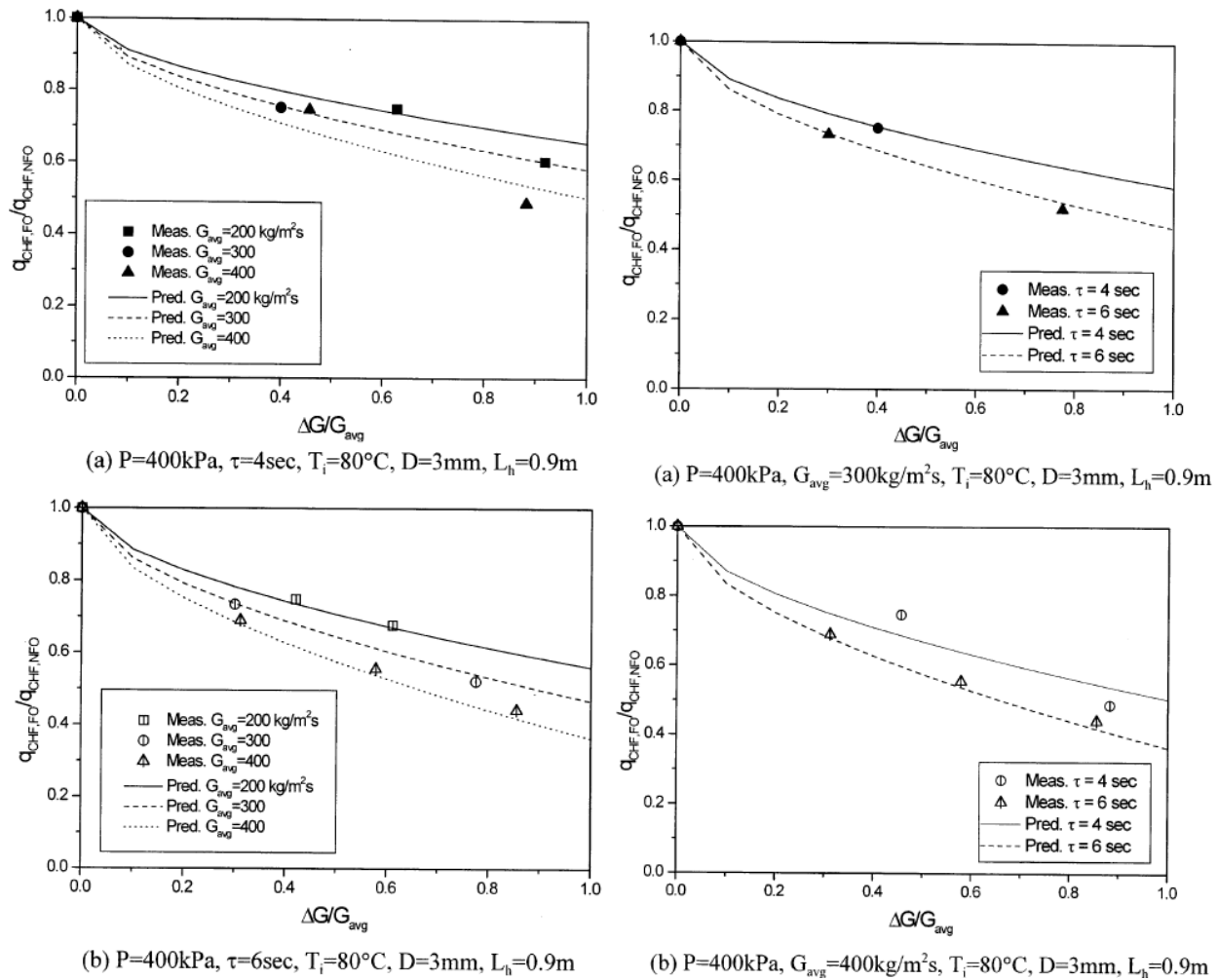
Figure 2.16 Critical Heat Flux Ratio – Normalized flow oscillations. Kim et al. [27] (1997)

2.6 Experiments on Pressure loss and Heat Transfer Characteristics

The next section will focus experiments dealing with heat transfer coefficients in boiling flows. The selected articles focus on the effect of different flow conditions; most important are heat flux, flow rate, and pressure, which all are highly relevant to the experimental program of this thesis. Several studies do also consider the cross-sectional dimensions of the heated channel. Heat transfer augmentation by heater surface configuration [31] is not considered either. In a comparative study on flow boiling heat transfer coefficients, Fang et al. [32] commented that five out of the six best correlations fitting their data best had a simple non-additive form.

Table 2.3 Experimental studies on heat transfer and pressure drop in boiling refrigerants

Reference	Fluid	D_h [mm]	L_{heated} [mm]	P [bar]	ΔT_{sub}	Q" [kW/m²]	G [kg/m²s]
Lazarek and Black 1982 [33]	R-113	3.1 12.6 circular tubes	123 246 Upw./down.	1.3-4.1	33K X_{in}=-0.2	14-380 kW/m²	125-750
Tran et al. 1996 [34]	R12 / R113	2.40 Circ/Rectang:	900 Horizontal	5.1-8.2	X_{in}~80%	3.6-129 kW/m2	44-832
Saitoh et al. 2007 [35]	R134a	0.51 1.12 2.0 3.1 Circular tubes	550 935 1400 3235 horizontal	4.9 30 37	X_{in} 0-0.2	5-39	100-450
Saisorn et al. 2010 [36]	R134a	1.75 minitube	600	8, 10, 13		1-83	200-1000
Copetti et al. 2011 [37]	R134a	2.6 Smooth tube	horizontal	4.43 6.08		10-100	240-930
Agostini and Bontemps 2005 [38]	R134a	2.01mm x 11 parallel rectangular	695 vertical	4.05 6.08	1-17K	6-31.6	90-295
Kew and Cornwell 1997 [39]	R141b	1.39-3.69 single tube	500	~1		9.7-90	212-1480

Lazarek and Black [33] 1982 measured the local heat transfer coefficient, pressure drop and critical heat flux for saturated boiling R-113 in vertical up-flow and down-flow round tubes. The onset of CHF was determined by occurrence of a dry wall condition that sustained long enough to cause a measurable excursion in wall temperature. A simple flow boiling heat transfer correlation was proposed based on 738 data points covering the entire range of qualities up to CHF.

$$Nu = 30 \, Re^{0.875} Bo^{0.714}$$

This correlation was modified by Kew-Cornwell (1997) [39] to allow for compensation for an observed increase in the heat transfer coefficient with vapor quality observed in larger tubes.

$$Nu = 30 \, Re^{0.875} Bo^{0.714} (1 - x)^{-0.143}$$
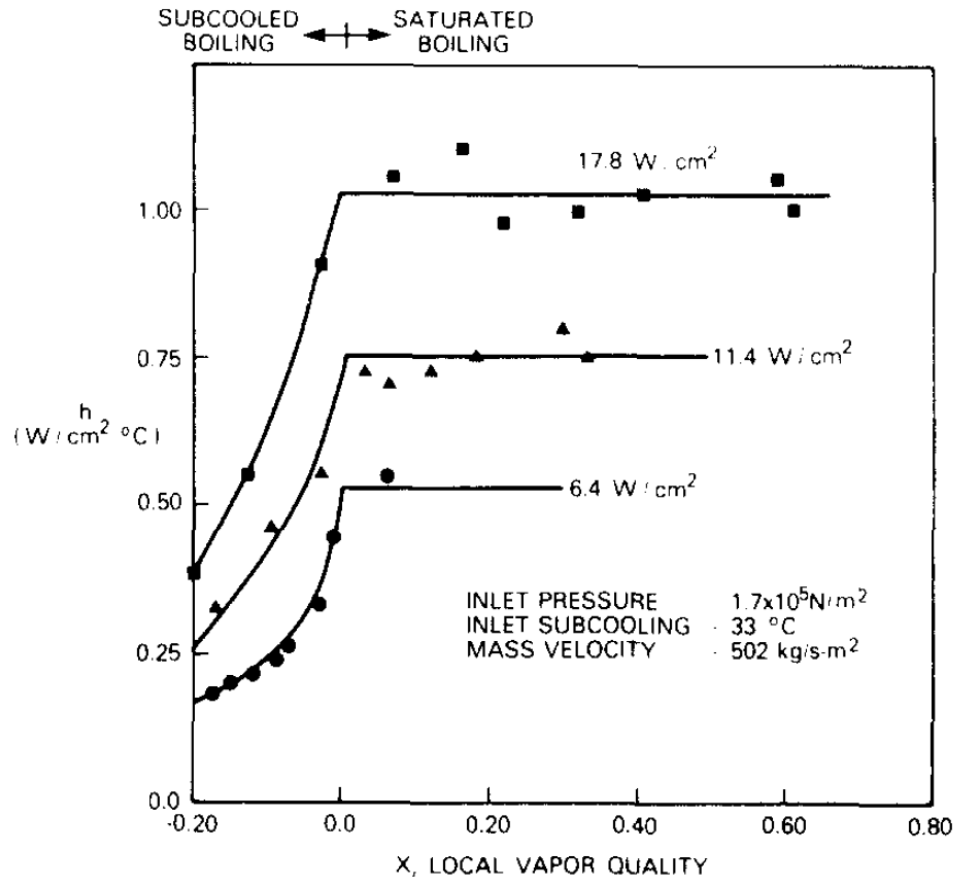
Figure 2.17 Local HTC – vapor quality. At 3 heat fluxes, Lazarek and Black 1982 [33]

Local heat transfer coefficient as function of local vapor quality. The local heat transfer coefficient increased rapidly during subcooled boiling. Beyond this point was the saturated boiling heat transfer coefficient independent of quality. Boiling heat transfer was strongly dependent on heat flux.

Tran et al. [34] (1996) determined the heat transfer coefficient experimentally over a wide range of vapor qualities up to x=0.94. Boiling flow experiments were performed in circular and rectangular small channels using R12 and R113 as working fluids.
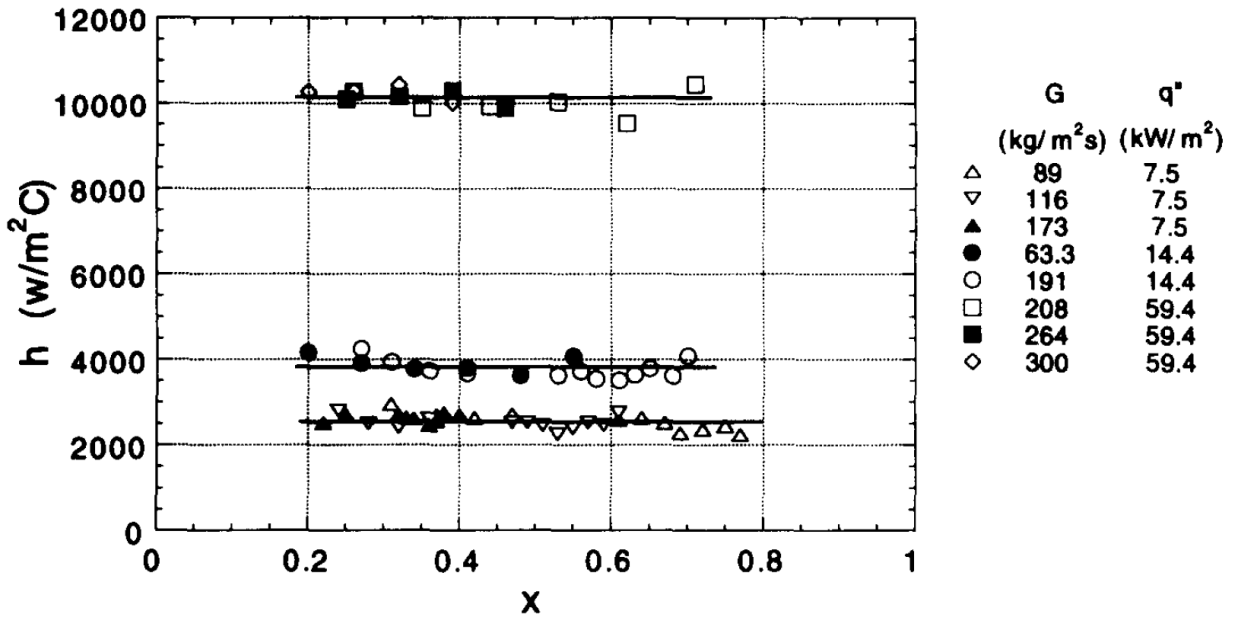
Figure 3. Circular-tube (R-12) local heat transfer coefficients for various combinations of mass flux at three constant values of heat flux and $\Delta T_{sat} > 2.75°C$; $p_{sat} \approx 825$ kPa.

Figure 2.18 Local HTC – vapor quality, experiments with several mass fluxes groups according to the three heat flux levels. Tran et al [34]

The figure shows local heat transfer coefficient is presented as quality along the length of the test section. The local heat transfer coefficient is independent of quality at $x > 0.2$. Nucleate boiling appeared to be dominant in this region. The result in Figure 2.18 indicates mass flux independence, while the dependence on heat flux is strong. Saturation pressure had also measurable effect, increasing heat transfer as pressure increases. All these results agree with the previous mentioned investigation of Lazarek and Black [33]. The heat transfer data was correlated as follows (within a 15% error band):

$$h = 8.4 * 10^{-5} (Bo^2 We_l)^{0.3} \left(\frac{\rho_l}{\rho_v}\right)^{-0.4} \quad [W/m^2C]$$

Saitoh et al. [35] (2007) performed an experimental investigation on local heat transfer coefficient and pressure drop in horizontal tubes with inner diameter of 0.51, 1.12, 2.0 and 3.1 mm. The working fluid was R134a. A Chen-type correlation for R134a in horizontal tubes taking into account the effect of diameter was proposed.

30

Two phase saturated flow boiling heat transfer coefficient, [W/m²K], consists of a convective contribution (Dittus-Boelters' equation for liquid flow in a tube) and nucleate boiling contribution.

$$h_{tp} = F\, h_l + S\, h_{pool}$$

X Lockhart-Martinelli parameter:

$$X = \left(\frac{1-x}{x}\right)^{0.9} \left(\frac{\rho_g}{\rho_l}\right)^{0.9} \left(\frac{\mu_l}{\mu}\right)^{0.1}$$

Some other quantities are needed, weber for vapor, two phase correction for Reynolds and bubble departure diameter of nucleate boiling

$$We_g = \frac{G^2 d}{\sigma\, \rho_g} \qquad Re_{tp} = Re_l F^{1.25} \qquad d_b = 0.51 \left(\frac{2\sigma}{g(\rho_l - \rho_g)}\right)^{0.5}$$

S is the suppression factor.

$$S = \frac{1}{1 + 0.4\left(Re_{tp}\, 10^{-4}\right)^{1.4}}$$

F is the enhancement factor.

$$F = 1 + \frac{\left(\frac{1}{X}\right)^{1.05}}{1 + We_g^{-0.4}}$$

Finally a pool boiling correlation for organic refrigerants:

$$h_{pool} = 270 \frac{k_l}{d_b} \left(\frac{q d_b}{k_l T_l}\right)^{0.745} \left(\frac{\rho_g}{\rho_l}\right)^{0.581} Pr_l^{0.533}$$
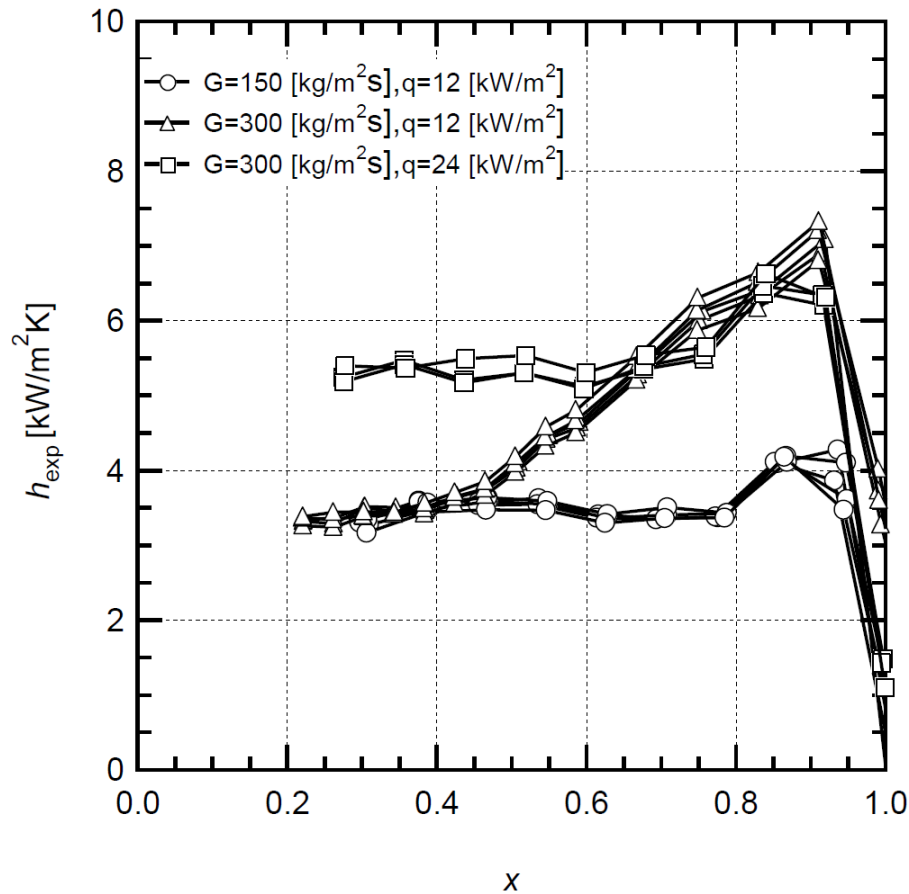
Figure 2.19 Local HTC – vapor quality, at two different heat and mass flux levels in a 3.1mm ID tube. Saitoh et al. conference paper 2007 [35]

Figure 2.19 extracted from the paper shows the effect of heat flux and flow rate on boiling heat transfer in the larges (3.1 mm) tube. The experimental heat transfer coefficient increased with increasing heat flux, but was not significantly affected by the flow rate. It was indicated that the nucleate boiling mechanism was dominant in the low quality region, while forced convective evaporation became more dominant in the high quality region. Increasing the pressure increased the local heat transfer coefficient. This effect was most accented in the low quality region.

Dry-out occurred at much lower qualities in the small tubes. Three flow patterns were observed, namely annular flow, plug flow and slug flow. Neither bubbly nor stratified flows were observed. Flow oscillations occurred in the largest (3.1 mm) tube with 1.62 and 3.24 m heated length. Once flow oscillations occurred the heat transfer decreased significantly for a wide range of vapor qualities. Oscillations in flow were apparently coincided with oscillations in the outer surface temperature. Oscillations were observed at low inlet qualities with period ranging from 0.8 – 4

32

seconds. By its period and information from the paper of Ding et al. the authors suggest that they likely were encountering DWO.

Saisorn et al. 2010 [36] experimentally investigated boiling heat transfer of R134a in a circular mini-channel. Emphasis was on flow visualization and obtaining heat transfer data. Five different flow patterns were detected, including slug flow, throat-annular flow, churn flow, annular flow and annular-rivulet flow. In accordance with several other studies; the heat transfer coefficient was found to increase with increasing heat flux, while being mostly independent of mass flow rate and vapor quality.
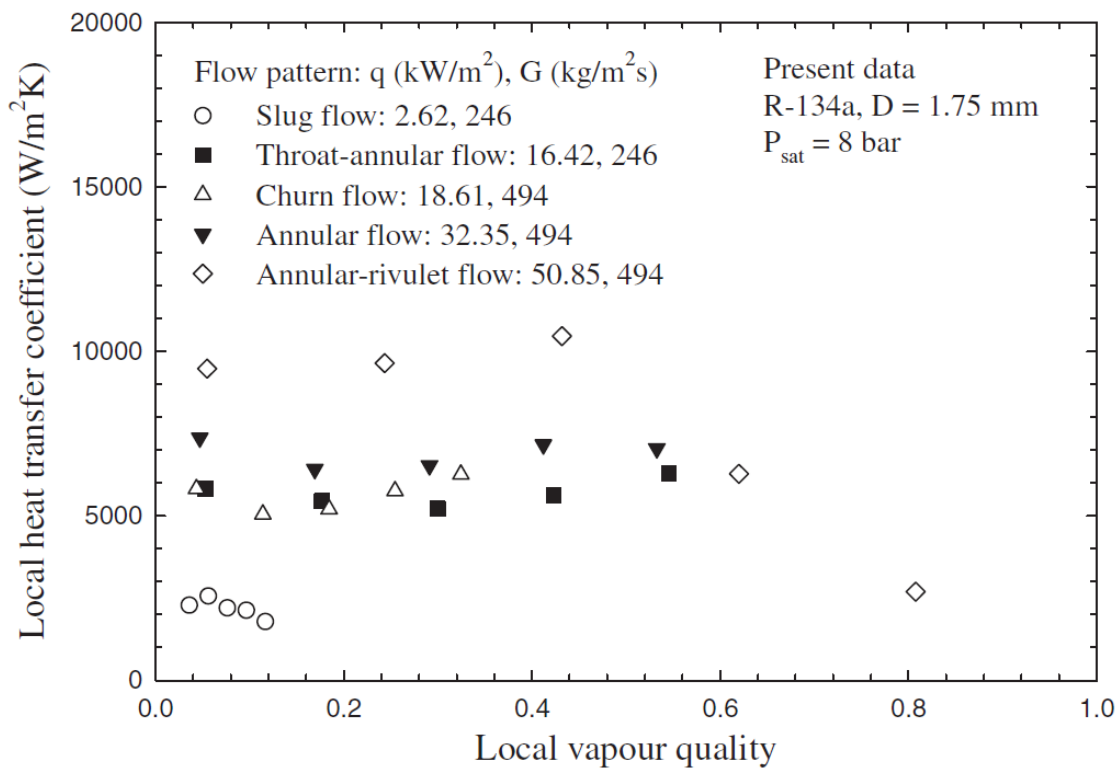
Figure 2.20 Local heat transfer coefficient – vapor quality, data for various flow patterns. Saisorn et al. 2010 [36]

Figure 2.20 is the result of taking heat transfer measurements and simultaneously recording flow patterns. A local dry-out was observed at the highest qualities. Flow patterns have significant effect on heat transfer. Slug flow appears to have the lowest performance in comparison to other flow regimes. The chance of encountering slug flow during boiling at high heat fluxes seems to be less in macro-geometries.

2.7 Experiments on Pressure loss and Heat Transfer Characteristics (including flow instabilities)

To find relevant literature focusing on heat transfer characteristics, the search has to be broadened to include studies dealing with unsteady flows and boiling instabilities in mini- and micro-channels. In these small geometries, however, phenomena are often related to the confined effects on bubble behavior in micro ducts. The predominance of surface tension forces significantly reduces the slip between vapor and liquid velocity thus changing flow characteristics. This, and the occurrence of very large velocity and temperature gradients near the walls of the heated channels, is features distinctive for micro-channels. It implies that the bubble nucleation, bubble growth and bubble detachment mechanism commonly associated with subcooled boiling in large channels do not apply to micro-channels [40]. The effects of gravity on flow in micro-geometries can usually be disregarded moving the orientation of the boiling channel out of concern.

Table 2.4 Experimental studies on heat transfer characteristics in unstable boiling systems

Reference	Fluid	D_h [mm]	L_{heated} [mm]	Pressure [bar]	ΔT_{sub} [°C]	Q / Q"	Configuration [kg/m²s]
J. E. Kennedy et al. (2000) [40]	Water	1.168 /1.448	160	3.44 – 10.44		0-4.0 MW/m²	800-4500
Brutin and Tadrist (2006) [41]	n-Pentane	0.889	200			15-125 kW/m²	
Fan (2013) [42]	FC-72	0.889	130	<0.517 0.1045	25-45	<1kW 6-170kW/m²	<3000 160-870

Kennedy et al. [40] (2000) studied convective boiling in mini-tubes of 1.17 and 1.45 mm diameter using deionized and degassed water. Numerous experiments were performed for the two test sections at a specified heat flux. The focus was on the nucleate boiling and unsteady flow threshold which were obtained experimentally by analyzing pressure losses curves as function of inlet mass flow rate for several heat fluxes. From these observations the heat flux when flow boiling becomes unsteady was deduced to by the authors to be 90% of the heat flux necessary for a full fluid vaporization. It was concluded that the onset of significant void generally occurs at a slightly higher mass flux, or lower heat flux, than the onset of flow instability. As a result,

correlations for the onset of significant void can provide a conservative estimate for safe determination of the range of operational parameters.

Brutin and Tadrist [43] (2006) performed an experimental study on destabilization mechanisms and scaling laws of convective boiling. The loop was composed of an 889 μm hydraulic diameter mini-channel coupled to a hydraulic jack type injection device providing a constant mass flow rate. A buffer tank completely filled with liquid was placed upstream of the test section to reduce mass flow rate fluctuations [41]. A fast recording camera was used to observe the flow patterns. Slug formation did always occur in the first half of the mini-channel. Experiments were conducted at several heat fluxes for variable mass flow rates. Scaling laws was developed from non-dimensional analysis on the experimental results.
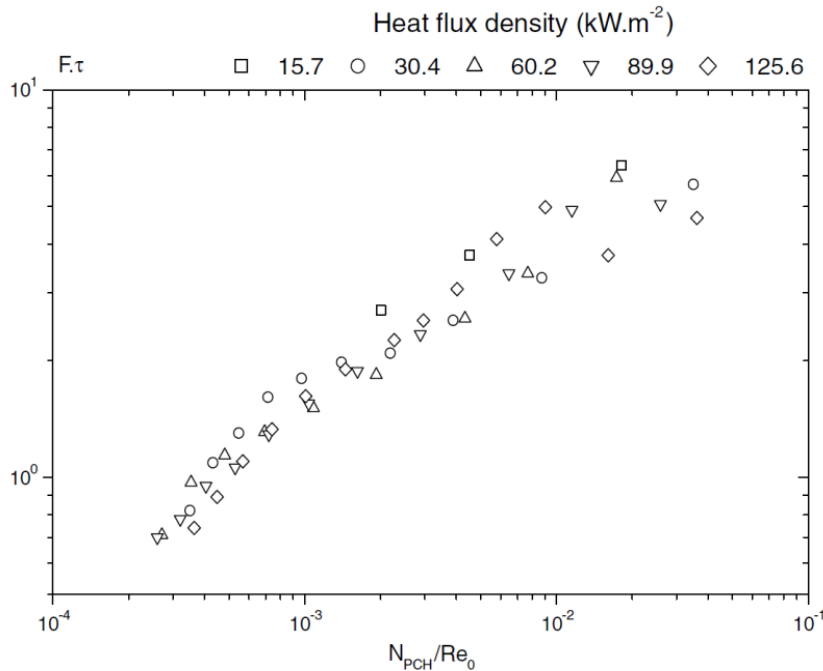
Figure 2.21 Normalized DWO frequency – N_{pch}/Re_{in}. Brutin and Tadrist [43] (2006)

The fundamental frequency Figure 2.21 of oscillation, obtained from a fast Fourier transformation of the pressure drop, was analyzed using a non-dimensional approach. A unique curve was found potting the frequency over the so called convective time $\tau_{conv.} = \frac{L}{U_{in}} = \frac{L_{hs}}{U_{sp}}$ as a function of $\frac{N_{pch}}{Re_{in}}$.
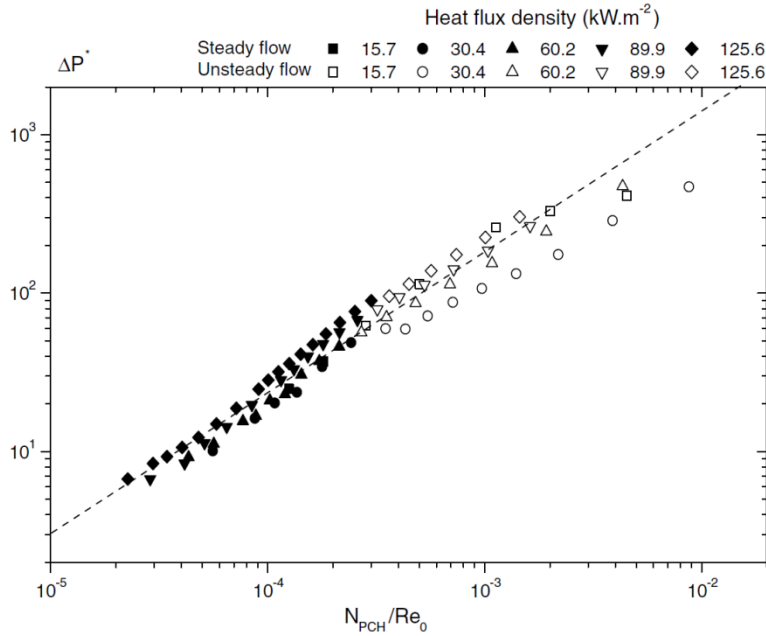
Figure 2.22 Normalized Pressure Loss– N_{pch}/Re_{in}. Stable/Unstable flow. Brutin and Tadrist [44] (2006)

Figure 2.22 of Brutin and Tadrist [44] presents the total test section pressure loss for points with an exit vapor quality between 0 and 1, experiments dominated by liquid or superheated vapor was excluded. Plotting $\Delta P^* = \dfrac{\Delta P}{\frac{1}{2}\rho_{in}U_{in}^2}$ against $\dfrac{N_{pch}}{Re_{in}}$ was done to create a pressure loss scaling law.
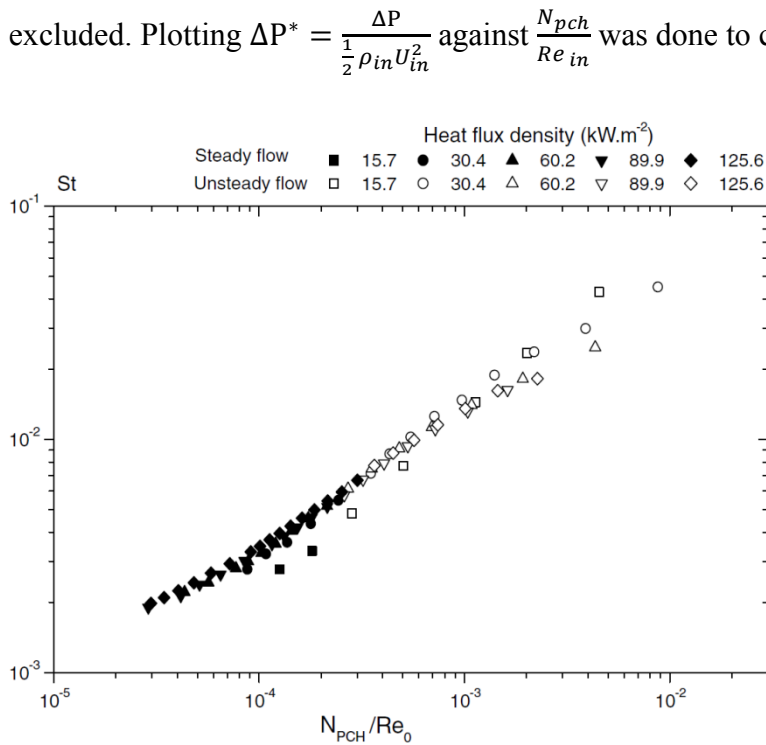
Figure 2.23 Heat transfer (St) – N_{pch}/Re_{in} . Transition from stable to unstable flow. Brutin and Tadrist [43] (2006)

36

The overall heat transfer coefficient was calculated using the average temperature difference between surface and fluid, and the total heat flux transferred to the fluid. This was rendered the only option since local heat flux and temperature redistributes inside the aluminum rod. The deduced heat transfer coefficient was restricted to the experiments with presence of mainly a two-phase zone in the channel. This two-phase flow contribution to heat transfer was represented by the Stanton number. Dark points in Figure 2.23 represent steady flow, whereas the white are for unstable flow. Heat transfer relative to transport was quoted by the non-dimensional Stanton number.

$$St = \frac{\bar{h}}{\rho_{in} C\, P_{in} U_{in}}$$

The Doctoral thesis of Fan [42] (2013) covers work done in an experimental investigation on boiling flow heat transfer and flow instability in a horizontal micro-tube with an inlet orifice. The Dielectric FC72 was chosen as the working fluid. Several instabilities were encountered, such as Ledinegg, DWO and PDO, either individually or in combinations. A great amount of data was collected on flow instabilities in micro-channels: stability, frequency, and the effect of various system parameters included.
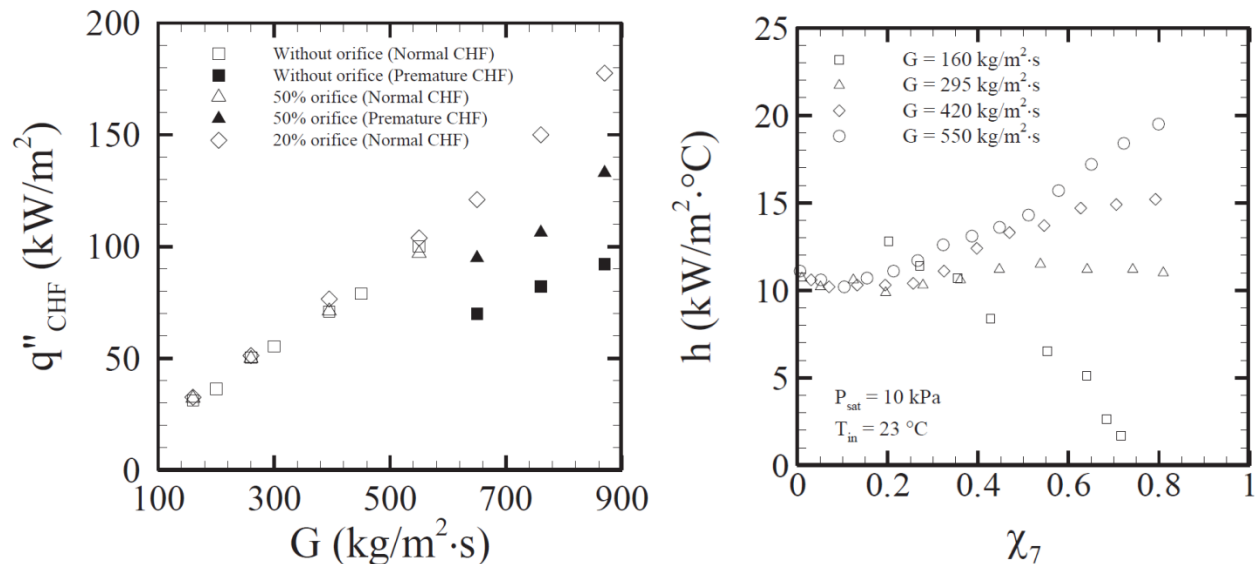
Figure 2.24 Normal & Premature CHF – Mass flow rate. Different inlet orifices. Fan [42] & [45]

Figure 2.25 HTC – Vapor quality. Different flow rates. Fan [42] & [45]

The two previous figures show the CHF at different mass fluxes in micro-tubes with various inlet orifice configurations at constant pressure and inlet temperature. The white normal CHF points are stable, while the author reports that the black premature CHF points usually were accompanied with flow oscillations. Adding an orifice could not increase the normal CHF in a micro-tube. However, adding a small orifice can avoid or delay the premature CHF since it helps improve flow stability [45].

The heat transfer coefficient evaluated against vapor quality in Figure 2.25 was subject to two trends. At low flow rate, heat transfer decreased as vapor quality increased because nucleate boiling was predominant. At higher flow rates was forced boiling the dominant heat transfer mechanism, and the heat transfer coefficient increased with saturation pressure.

Fan [46] observed that the frequency of oscillation increases with increasing heat flux, while the amplitude remains constant.

2.7.1 Previous work at the NTNU Two-Phase flow instability facility

Details of the experimental apparatus of the following experimental studies are described later in this thesis since the same facility was used.

Manavela Chiapero et al. [47] (2014) investigated the characteristic pressure drop steady-state curve for horizontal boiling flow through a heated pipe. Pressure drop was evaluated as a function of mass flux and the outlet quality to find the conditions necessary for a negative slope. In this region, the pressure drop gets higher as the mass flux decreases giving the characteristic pressure drop curve an N-shaped behavior. This behavior may have significant impact on the stability of the system. Experiments were conducted to provide a systematic analysis of the effect of different parameters in the steady-state behavior of the system. These parameters were inlet pressure, inlet temperature (degree of subcooling), and heat flux and heat distribution. The results were used to validate the numerical analysis performed by Manavela Chiapero et al. [48] The heat flux in this study was likely too low for the DWO phenomenon to commence.

Another recent study by Manavela Chiapero et al. [49] (2014); presents experiments with different conditions chosen in order to characterize the heat transfer coefficient and the fictional pressure drop for refrigerant R134a. The available literature is very limited on high saturation temperatures (>25°C) Different heat flux and flow rate conditions for vapor qualities were

ranging from subcooled liquid to overheated vapor. The pressure drop was directly measured using the pressure transducer. The local heat transfer coefficient was calculated by the inner wall temperature derived from the outside thermocouples, the internal in-flow thermocouple and the supplied power.
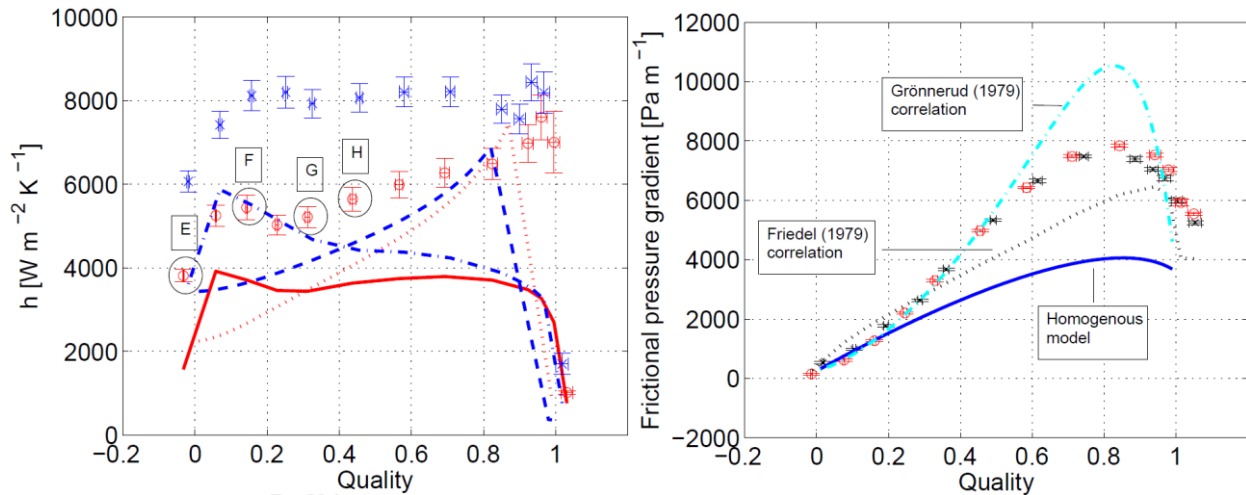
Figure 2.26 Heat transfer coefficient – Vapor quality. Manavela Chiapero et al. [49]

Figure 2.27 Adiabatic frictional pressure drop – Vapor quality. Manavela Chiapero et al. [49]

The lines do all represent different correlations. The points with error band are experimental results, were red corresponds to G=300 kg/m²s T_{sat}=32.7 °C $q"$=_10.5_ kW/m² and blue/black corresponds to G=298 kg/m²s T_{sat}=34.3 °C $q"$=20 kW/m².

Mass flux was reported to increase heat flux mainly in the high quality region, while the low quality region is less sensitive to mass flux. Heat flux had large impact on heat transfer in the low quality region, but did not have significant impact on the dryout quality. Flow patterns were captured with a high speed camera for comparison with flow maps.

3 Experimental facility

This chapter presents several aspects of the experimental facility used in the present research. The goal of this chapter is to provide a detailed description of the apparatus in its current setup and instrumentation. Uncertainties relative to measurements are reported. Key specifications for further reference are summarized in the end of this chapter. Purpose of the experimental program is to explore and gather data on the influence of inception, amplitude and period of the DWO-mode on the pressure drop and heat transfer characteristics of the system.

A great amount of work has been done by the academic staff designing and technical staff constructing the facility. The chapter to come is primarily a summary of effort made prior to the work on this thesis. In the first step of construction of the rig, a planned high pressure reservoir is omitted. The rig has a vast amount of features, such as a multi-tube arrangement, that not will be covered in this thesis. All experiments were performed in a single heated channel with uniform heat flux and flow circulation induced by a pump. A schematic diagram of the loop is presented in Figure 3.1.

3.1 Description of apparatus

3.1.1 Background

The experimental facility features a horizontal evaporator test section. The experimental facility has been designed and built to generate and investigate both static and dynamic two-phase flow instabilities. This resembles a tube in a heat exchanger or once-through evaporator. The idea, when fluid and overall range of conditions were selected, was to mimic the behavior of two-phase hydrocarbon flow heat exchangers (cold boxes) used in natural gas liquefaction processes [8]. These heat exchangers, typical spiral-wound with boiling and condensation of mixed refrigerants used in the LNG industry, are in fact susceptible to two-phase flow instabilities. Horizontal once-thorough evaporators are also found in vapor-compression cycles known from air condition, heat pumps and refrigeration system.

Nuclear reactors, on the other hand, are not within the prime scope. Boiling water reactors (BWR) are of vertical orientation. The only horizontal oriented nuclear reactor is the Canadian invented CANDU-type which is a pressurized heavy water reactor not featuring boiling phase transition in the primary loop under normal operational conditions.

3.1.2 Thermo-hydraulic system

The experimental facility is an R134a closed loop consisting of a main tank, a pump, pre-conditioner, a heated test section with in and outlet restrictions, and a condenser. The loop is schematically represented in the Figure 3.1.
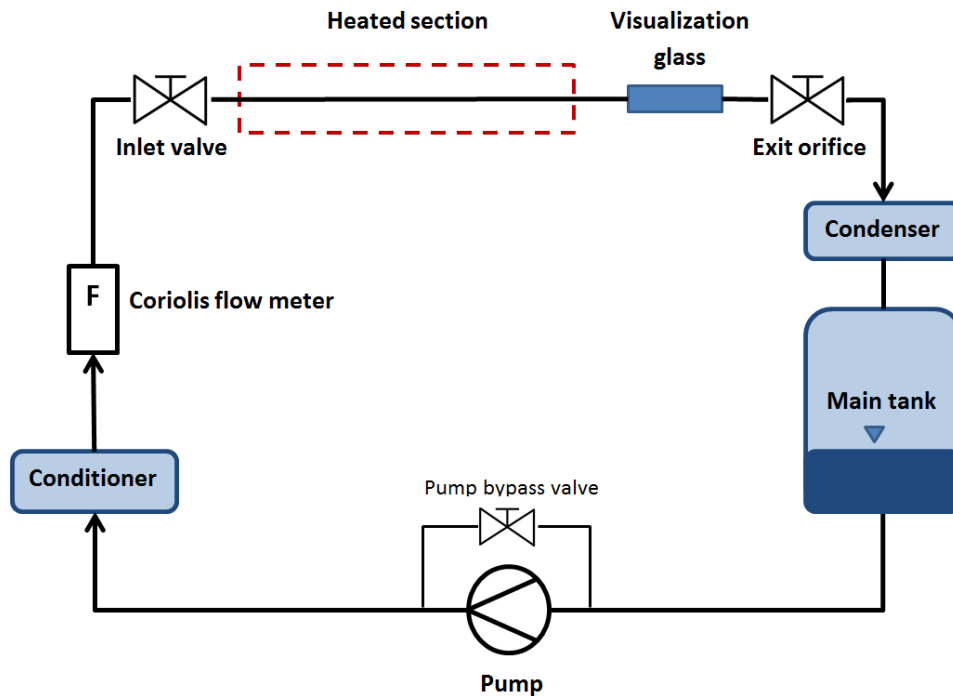
Figure 3.1 Simplified schematic flow diagram of the current experimental configuration

3.1.3 Fluid

R134a was chosen as the working fluid due to its characteristics similar to those of hydrocarbons in natural gas. When the rig was first designed [8], propane was used as a reference substance, and a working fluid was chosen accordingly. Advantages of using a refrigerant is that boiling can be accomplished at reasonable temperature and pressure levels. The latent heat of vaporization is relatively low, about one tenth compared to water, effectively reducing the heat input required. R134a is also more environmental friendly than traditional CFC refrigerants. This, and the non-flammable characteristics of R134a, greatly reduce complexity and improve safety of the rig.

3.1.4 Pump

A gear pump (GB-MICROPUMP) with magnetic drive coupling circulates the fluid through the loop. Liquid refrigerant is supplied to the pump form the bottom of the main tank. Checking the

main tank liquid level is done by looking into two sight glasses in the vessel. Speed of the pump is adjusted by changing the DC-voltage of the motor drive. It is specified within the software interface and dictates the flow rate in the loop.

A bypass valve parallel to the pump allows for a very wide range of experimental flow rates. Having the bypass partly open allows some fluid to be recirculated though the pump. Experiments with relative low flow rate can be executed with a higher pump drive speed. This is convenient as it gives better resolution in flow rate since the pump drive speed is adjusted in increments. Allowing fluid to bypass the pumps is standard procedure on startup. It then serves as a safety precaution in case of blockage of the flow path by an erroneous valve configuration. Moreover, the open pump bypass valve helps destabilizing the flow system favoring the DWO-mode [8].

The experimental configuration in this study with bypassed pump falls between the traditional setup with pump forcing liquid directly to the test section inlet of Andoh [17] among others, and the large bypass of Saha et al. [4] The implication of the pump bypass valve configuration is more thoroughly treated in the pre-work chapter.

3.1.5 Pre-conditioner

The temperature of R134a entering the test section controlled by a plate-and-fin heat exchanger (B8THx14 SWEP). Heat is exchanged to the water-glycol mixture subsequently cooled by an Applied Thermal Control (ATC) K9 chiller. Temperature of the chiller is set in the software interface. The pre-conditioner is necessary to ensure that R134a entering the test section has the correct degree of subcooling. Subcooling refers to the difference in temperature between the liquid saturation temperature and its actual temperature. A small sight glass is fitted upstream of the test section so it can be verified that only pure liquid is entering.

3.1.6 Heated test section

The test section is a 2035 mm long, horizontal circular tube made of stainless steel, with 5 and 8 mm inside and outside diameter respectively. The test section is electrically heated by applying a rectified sine wave (Joule heating) between six individual electrodes dividing heating into 5 equally long segments. Because of the constant wall thickness of the tube, the heat generation is essentially uniform within each segment. Heating within each of the five different segments can

be individually controlled in order to achieve a non-uniform heating profile. Although the heat source is usually not uniform in real systems such as fired evaporators, re-boilers, and nuclear reactors, the present experimental study only consider uniform heat profile with equal power in all five segments. This harmonizes with previous work in the literature reviewed. The test section is insulated to reduce heat loss to the surroundings. The heat loss will never exceed 8 % and is indeed accounted for when calculating the actual heat transfer to the fluid [8].
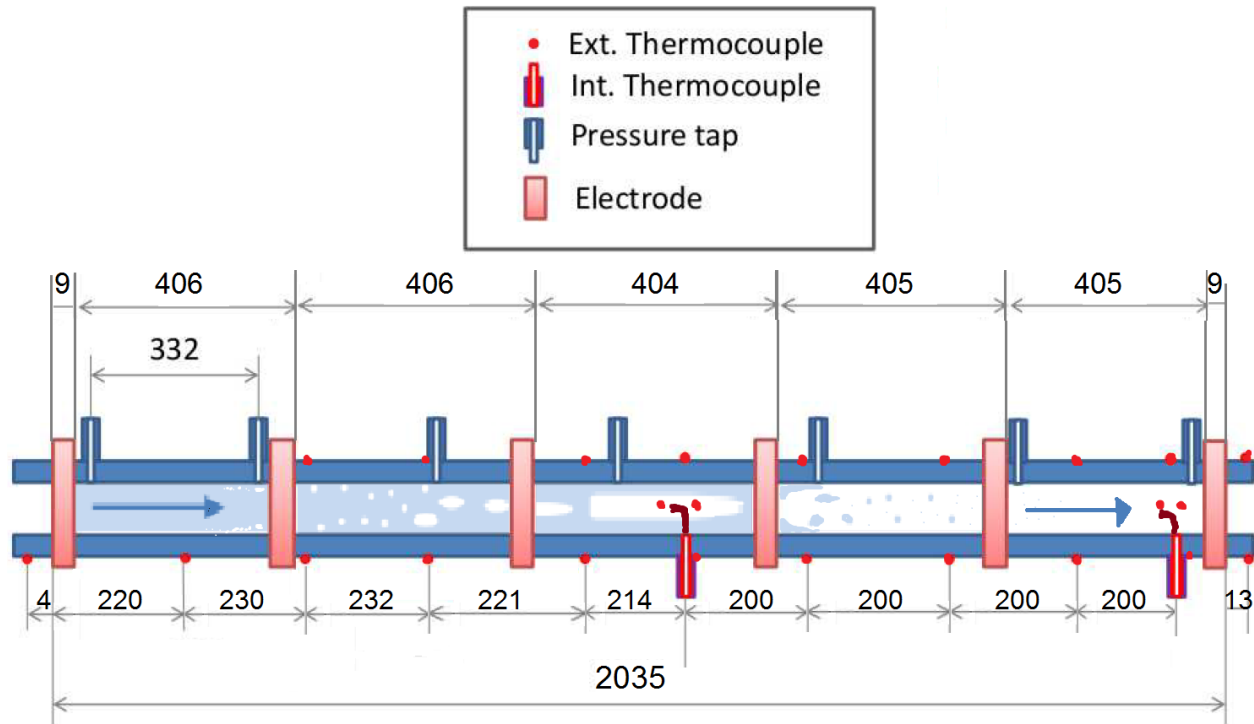
Figure 3.2 Sketch of the test section – not to scale, adopted from Ugueto [25]

The test section is the part of the system where boiling and the related two phase oscillations occur under well controlled conditions. Monitoring the test section is therefore crucial. The test section is equipped with 7 pressure taps for differential pressure drop measurements, a number of external (wall temperature) thermocouples, and 2 internal thermocouples to study heat transfer to the fluid. The pressure taps are connected to two pressure transducers by a network of valves which allows for a custom point of measurement. An additional third pressure differential transducer measures the overall test section pressure drop. Ten thermocouples are distributed along the outside bottom wall of the test section while there are seven on top. Position 6 and 10 boasts the greatest amount of measuring points with thermocouples on top, bottom, both sides of the wall plus an in-flow internal thermocouple.

43
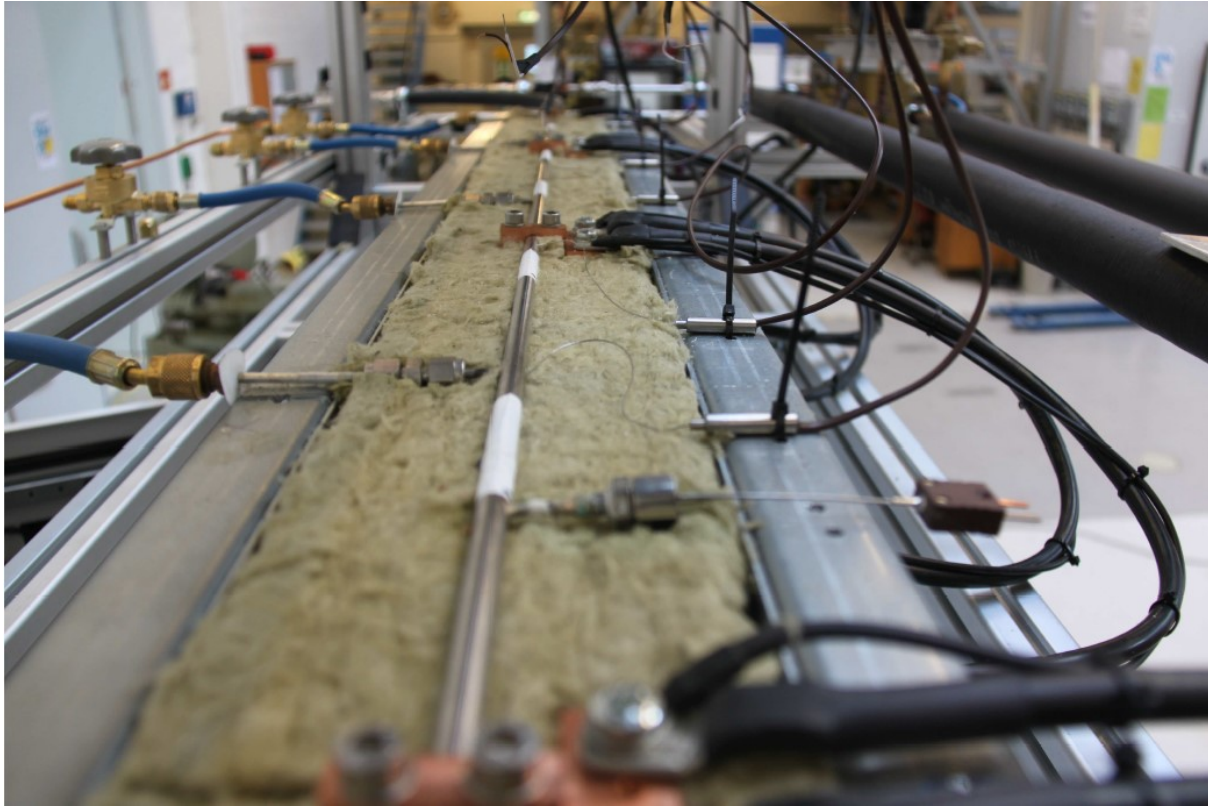
Figure 3.3 View of the horizontal test section, Ruspini [8]

A picture of the test section with view from its exit can be seen in Figure 3.3. Pressure taps are connected from the left hand side and internal and external thermocouples from right. Electric power is applied through the copper blocks. The test section is mounted between two sheets of insulating material to minimize heat loss to the surroundings.

3.1.7 Flow restrictions

The test section is equipped with an inlet throttling valve and an exit orifice.

A manually operated valve provides a local pressure drop at the inlet of the heated section. An inlet resistance coefficient $K_i \approx 2.63$ was kept as the default setting, unless experiments were performed without flow restrictions which mean that the valve was fully open.

The outlet pressure drop can be arranged in two ways, either distributed or local pressure drop. Distributed outlet pressure drop can be studied by routing the flow through a 1 m pipe with dimensions similar to the test section. Local pressure drop is imposed by an orifice plate. The two legs are connected in parallel. Experiments in this study will be performed with the later

44

arrangement, local pressure drop with exit resistance coefficient $K_e \approx 2.70$, unless both legs were opened to practically omit exit flow restriction.

The flow resistance coefficients were found from single phase (liquid) calibration of the flow loop, and calculated according to:

$$K = \frac{\Delta P}{\frac{1}{2}\, \rho u^2} = \frac{2\Delta P \rho}{G^2}$$

3.1.8 Condenser

Working fluid leaving the heated section is condensed back to liquid form in the tubes of a shell and tube heat exchanger (CFC-12-Alfa Laval). Heat is exchanged to the water-glycol shell side fluid. The secondary coolant circuit is thermally controlled by an ATC K6 Chiller, in which the reference temperature can be adjusted inside the software interface. Condenser temperature governs the loop pressure.

3.2 High speed flow visualization

A borosilicate sight glass mounted at the test section exit allows photographic analysis of the flow. High speed flow visualization is performed with a Photron- FastCam SA3 high speed camera. The OXFORD infrared laser previously used is replaced by a LED arrangement. The light source now consists of a single white LED which can be driven at 1600mA with a light diffuser placed in front of it. A polarizer was fitted between the camera lens and the visualization glass. This camera setup permitted video capture at 1000 FPS (frames per second) with shutter times in the area from 1/20.000 − 1/40.000 seconds. Sight glass and camera are shown in the picture bellow.
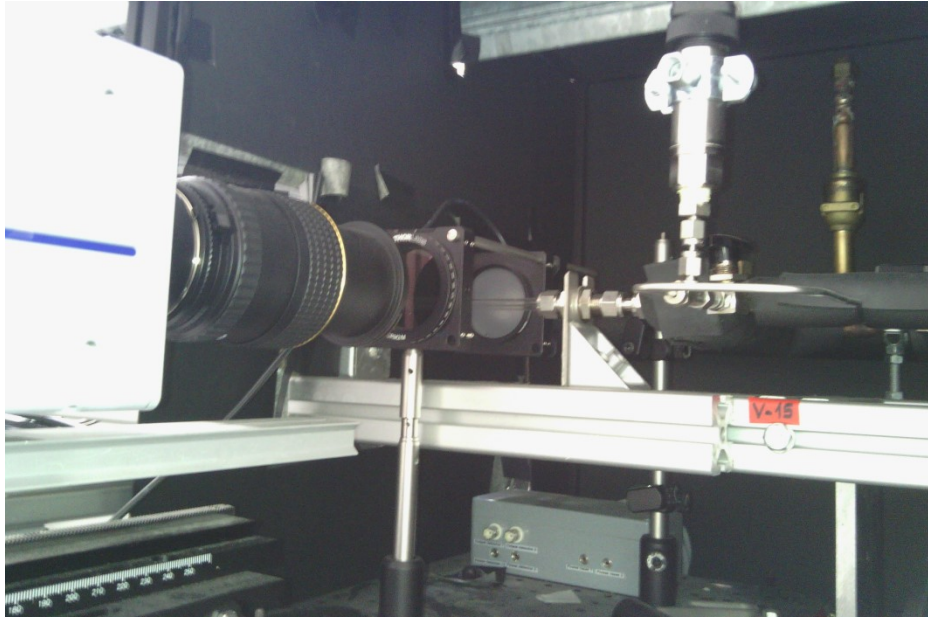
Figure 3.4 Test section outlet, visualization glass and high speed camera arrangement.

R134a being a clear and colorless substance, and the fact that the visualization area is not micro nor huge, makes this rig a good starting point for decent quality flow visualization.

3.3 Associated instrumentation

The next section will describe the measurements and the accuracy or calibration of different instruments present in the facility. The experimental facility has great amount of features and instrumentation, only the most relevant to this study will be presented here.

3.3.1 Mass flow rate

The oscillation flow trace is measured at the test section inlet where the flow is liquid single phase. The reason for doing this is that it is generally hard to do accurate measurements of two-phase flow which would be encountered at the test section exit. Other experimental studies where the outlet oscillatory behavior is recorded usually reports the pressure trace.

The flow rate (G2) is recorded by a Coriolis flow meter (Bronkhorst Cori-Tech R134A 3L/min) placed upstream of the test section. Another flow meter (G1) of same kind is placed even further upstream closer to the pre-conditioner. An accuracy of 0.2 % of the reading is given by the supplier. The volumetric flow rate reading of the liquid refrigerant R134a is converted into the mass flux using densities from NIST REFPROP properties database.

3.3.2 Pressure

The absolute pressure was recorded between the inlet restriction and the heated section. This pressure is regarded as the system pressure. The overall accuracy for the GE-UNIK 5000 Premium pressure sensor is 0.04% of full scale where full scale is 16 bars. This translates to about 0.14% (or ±0.01bar) in the relevant experimental pressure range.

The two phase pressure drop across the test section was directly measured with a differential pressure transducer. Currently, three DP cells are connected to the test section, and the desired pressure taps for measurement is chosen by changing a number of valves. The test section inlet restriction and the exit (orifice plate or outlet section) are also equipped with DP cells. The inlet DP-cell is actually as a matter of convenience measuring the pressure difference over both the inlet restriction valve and the "G2" flow meter. All differential pressure transmitters are of the Endress+Hauser brand and Deltabar S type with high (±0.075 %) reference accuracy.

3.3.3 Temperature

The fluid temperature was recorded at the inlet of the heated section. All thermocouples used in the facility are standard K-Type of 0.5 mm diameter. The thermocouple accuracy after in-house calibration was found to be 0.1 K. The absolute pressure in the test section inlet was used to determine the saturation temperature T^{sat} of the fluid based on the equilibrium thermodynamical properties calculated with NIST REFPROP. The inlet subcooling is defined as the difference between the calculated saturation temperature and the measured actual temperature.

3.3.4 Heat flux

The power supply is constructed in-house. A voltage potential from a controller-rectifier circuit is applied over 6 electrodes evenly distribute along the heated section. Though smooth direct current (DC) would have been the ideal, the use of capacitors in the power supply has been omitted to reduce load on the transformers, resulting in a rectified sine wave. Due to the massive ripple in the signal, a digital oscilloscope was used to obtain the actual shape of the voltage and current signal to each of the heated sections. Data is acquired at every 0.1 second (10Hz) while the mains frequency is 50Hz rendering the first unusable to sample the later. Thus, averaged DC-equivalent values derived by numerical integration of the actual signal shape must be used as correction factors to the voltage and current measured by the acquisition card.

Errors in the heat input are also associated with the voltage and current measurements. Calibration has shown < 10% accuracy. Accuracy of the power measure chain was taken assuming a power of 200 W giving a final accuracy of ±20W [8].

The fact that the heated section is thermally well insulated forces almost all volumetric heat generated in the pipe wall to flow to the fluid. However, the effects of thermal losses are taken into account when determining the heat transfer to the fluid [8]. Calibration was done using the test section inlet and the two internal thermocouples in conjunction with energy conservation. It is remarked that the heat losses in experimental cases never are higher than 8 %.

3.3.5 Measurements and accuracy of measurements

The heat transfer coefficient and vapor qualities were calculated from the mass flow, heat flux, pressure and different temperatures recorded. A detailed description is given in the methods chapter.

Details regarding associated instrumentation and its uncertainties are summarized in the two tables to come.

Table 3.1 Accuracy of the facility instrumentation [8]

Name	Instrument	Localization	Range	Measurement accuracy	Max. statistical error
G1,G2	Coriolis Flow Meter	Test section entrance	0–3 l/min	0.01 l/min	<0.01 l/min
DP1	DP-transducer	Test section	0–1 bar	0.075 kPa	0.1 kPa
DP2	DP-transducer	Orifice plate	0–1 bar	0.075 kPa	0.5 kPa
DP3	DP-transducer	Inlet restriction	0–1 bar	0.075 kPa	0.2 kPa
DP4	DP-transducer	Test section distributed ΔP	0-30 mBar		
DP5	DP-transducer		0-50 mBar		
P1-5	Abs. pressure	Whole loop	1–16 bar	10 kPa	1 kPa
T1-20	Thermocouple K-type std.	Whole loop (10+8+4) @Wall 1Inlet 2Internal 5Various	-50 – 100 °C	0.1 °C	0.2 °C
Q1-5	Power Supply	Test section	0–2500 W (5 zones)	20W	20W

3.3.6 Uncertainties

Table 3.2 Uncertainties of the main operational parameters [25]

Parameter	Symbol	Error
Mass flux	G	±10 kg/m²s
Inlet pressure	P_i	±10 kPa
Inlet temperature	T_i	±0.2 °C
Heat flux (all 5 zones)	q″	±<40 W

3.3.7 Software Interface

The National Instruments LabVIEW software (short for Laboratory Virtual Instrument Engineering Workbench) is used to control and monitor the experimental facility. The software interface is used to set pump speed, control heaters and the two chillers (K6 and K9). It is also used for monitoring as it shows all measurements provided by the heaters, flow meters, absolute and differential pressure transducers, and thermocouples in a schematic flow diagram. Moreover, the software provides a very useful on-line visualization of the inlet flow trace. Logging of experiments is performed with the LabVIEW data acquisition tool. The logging feature allows for online monitoring of the experimental condition in Matlab.
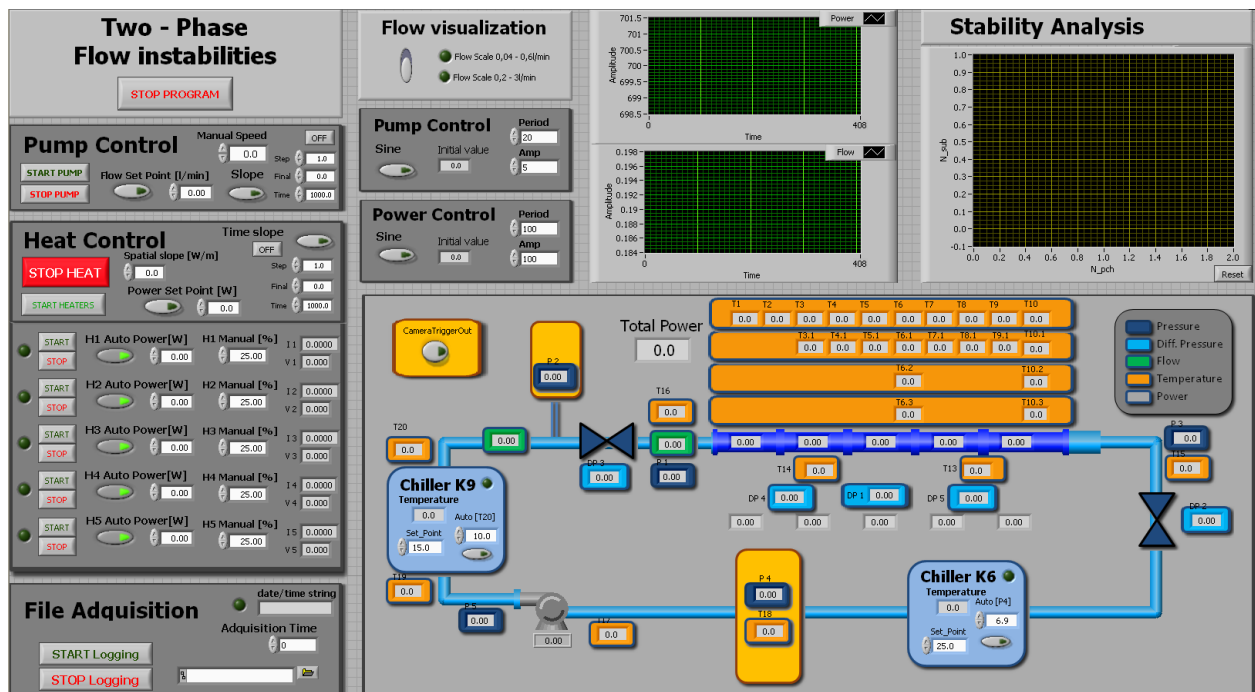
Figure 3.5 Software interface - main system overview in LabVIEW

The picture above shows the main window of the LabVIEW software interface.

3.4 Main specification overview

Table 3.3 Key specifications of the two-phase flow instability facility

Fluid	R134a
System pressure	P = 4 – 12 bar
Mass flow rate	G = 5 – 2000 kg/m^{2}s
Inlet temperature (Subcooling)	T_{in}=-20 – 40°C (ΔT_{sub}=0 - 50°C)
Max power input	Q = 1500W
Other limitation, test section exit temperature	T_e< 110°C (glue used to fix thermocouples) T_e > 0°C (icing on sight-glass)
Horizontal test section	
Length	L_{HS} = 2.035m (L_{total}≈6m)
Diameter	d_h = 5mm (d_{piping}=12.4mm)
Inlet flow restriction coefficient	K_i≈2.63 (default in present study, if not open)
Exit flow restriction coefficient	K_e≈2.70 (default in present study, if not open)

3.5 Risk assessment and safety

A complete risk assessment report was created by L.C. Ruspini and E. Langørgen [50] in order the get an operation authorization at the Thermal Laboratory at NTNU. The facility is built after best laboratory practice.

An experimental apparatus cannot be described without recognizing some of the main hazards. The loop contains a pressurized fluid, also when not in operation. As a general precaution, safety glasses where always used when physically working on the rig. The room has as sizable volume so local frostbites is the primary risk in case of leakage. Experiments was controlled and monitored from a computer station next to the facility. Repetitive strain injuries (RSI) might actually be a risk involved in this kind of laboratory work. None of the mentioned issues, or other incidents, was ever encountered during the experimental program.

3.6 Closing words on the configuration

A key difference in the configuration of this study, compared to other experimental facilities described in literature, is the partly bypassed pump. A consequence of operating the facility with partly open pump bypass is that fluid is allowed to be recirculated thorough the pump. This is favorable in case of a system blockage by avoiding uncontrolled pressure build up, but not critical since the pump has a magnetic drive couple. Another expected implication is flow rate oscillations in the inlet of the test section. Ruspini [8] states that the pump bypass valve was open, in order to destabilize the DWO mode, since no compressible volume was used for the

50

study. The effect of a compressible volume, the surge tank, on the DWO stability limit for this rig was investigated by Ruspini (see fig. 11.12 [8]).

Theoretically, the pump bypass allows for variable, even transit reversed flow, in the test section inlet. In contrast to a closed bypass, or alternatively a (over)pressure relief valve, where the pump forces a steady flow of liquid to the heated section inlet, thus disallowing any significant inlet flow rate oscillations [17]. An advantage of making allowance for oscillations in the test section inlet is that the fluid is a liquid at this point, oscillations can then easily and accurate be measured in the inlet flow, which is obviously not the case for the two-phase test section exit. This partly bypassed pump configuration should not be confused with the configuration in the experiments of Saha et al. [4] whereas the test section was parallel to a large bypass channel causing a constant test section pressure drop. Although an option in the facility, this feature was not explored in the present work.

4 Methods

This chapter describes and explains the scientific methodology deployed. The aim of this chapter is to provide objective information on the experimental procedures and map out the methods utilized. That is a throughout description on how to collect the necessary experimental data and the analytic procedures that will be used to draw conclusions based on this data. The intention is to bridge the previous chapter describing the experimental facility to experimental results and finally a conclusion.

4.1 Execution of experiments

The task is to determine how the occurrence of flow instabilities, in particular DWO, influences the heat transfer characteristics of a horizontal in-tube boiling system. First, a reliable way to trigger and sustain flow instabilities in a boiling system is needed, and preferably having a stable condition as reference. An appropriate way of conducting experiments to capture the effect of flow instability onset has to be developed. Secondly, the necessary experimental data has to be collected and the effect of changing some variables, for instance; flow rate, inlet temperature and pressure should be examined. Third, analytical procedures such as data reduction and computation of heat transfer coefficients are required to draw conclusions based on this information.

4.1.1 General steps in operating the facility

- Inlet restriction, outlet configuration and the pump bypass valve are configured.
- The pump is started.
- K6 and K9 chillers are set to values corresponding to the desired system pressure inlet subcooling.
- Heat applied in and ascending order while system circulation is assured.
- Pump drive, condenser chiller (K6) and conditioner chiller (K9) requires iterative tuning in order to achieve an accurate flow rate, pressure and subcooling according to the planned experiment. Adjusting one variable usually affects several parameters making this process quite complex.
- Tuning of operating condition is manually carried out by the operator.

- A considerable run-in time at the given conditions is needed to allow the system to settle at a true steady state. This can typically take an hour for each set of conditions.

- Repeated logging of a number of experiments was done while maintaining the desired conditions

All experiments (500 seconds each) are repeated several times until it is ensured that the measured value represented the steady state nature of the system.

4.1.2 Density Wave Oscillations

DWO is expected to occur in a system with; test section inlet and outlet restriction, some degree of inlet subcooling, and heat input sufficiently high, yielding an outlet vapor quality of about one. When exploring DWO close to its stable boundary, or in absent of a self-imposed onset, oscillations must be triggered in order to start. There are several ways to triggering DWO:

- Perturbing the flow by decreasing pump speed for a short while

- Increase heat to a level where DWO commences; reduce heat back to the desired value.

- Similarly, DWO can be triggered by modifying (stop/start) one (the last) heating section.

Afterwards, some time is needed to see if the oscillations persist. The basic strategy is to perform sequences of experiments at steady state system conditions allowing enough time to observe the steady-state unstable behavior of the system. An unstable condition, or DWO, is easily recognized by its self-sustained periodic oscillations in flow rate and pressure. The different ways to generate DWO are totally equivalent and the chosen way is just a matter of convenience since DWO is regarded as a fundamental phenomenon [51].

4.1.3 Mimicking Density Wave Oscillations

The concept of mimicking DWO [30] is yet to be explored in the pre-work. The idea is to impose flow instabilities externally by oscillating either the pump or the heat input. In this way a DWO equivalent situation can be created in an otherwise stable system, though it has to be verified how well this imitation resembles the true DWO phenomenon. Having external controlled flow instabilities poses some interesting opportunities in modifying characteristics such as period and amplitude of oscillation.

4.1.4 Stable system configuration

Excluding the flow restrictions is believed to obstruct the feedback effects generating DWO. This is achieved by opening the inlet restriction valve and allowing flow to bypass the exit orifice through the adiabatic outlet section (1m pipe). Furthermore, the pump bypass can be closed to insure that the boiling system remains totally stable or non-oscillating. Such configuration is expected to be unconditional stable. Even though pressure, inlet subcooling, heat input and flow rate all are within the unstable region for a system with restrictions. Such configuration is hence intended to be used as a reference.

4.2 Experimental program

The main objective of this study is to investigate how flow instabilities, in particular DWO, influence the pressure drop and heat transfer performance of the system. The main system parameters to be varied are heat flux, mass flow rate, inlet pressure and inlet temperature (degree of subcooling). These parameters are known to change the characteristics of DWO such as the threshold limits, amplitude and period of oscillation.

What eventually became the experimental program is summarized below.

- Verification of instrument readings and measurement method.
  - Pressure drop verification
  - Heat transfer coefficient verification
- Pre-work focus on the implications of altering various system configurations. Measurements were done to learn how the main experiments could be carried out.
  - Effects of having a partially opened bypass-valve in parallel with the pump.
  - Effect of oscillation amplitude on heat transfer is examined
  - Effect of oscillation period on heat transfer is examined.
  - Mimicking flow instabilities by means of externally imposed flow oscillations:
    - Possible and feasible, or not?
    - The effect of DWO amplitude was isolated from period by this technique.
    - The effect of DWO period was isolated from amplitude by this technique.
- Flow rate controlled experiment (changing the inlet Reynolds number)
- Heat controlled experiment. Experimental matrix:
  - Three configurations

- With restrictions (features DWO)
- Without restrictions (unconditional stable) reference case
- Mimicked flow instabilities

○ Four cases

- Base case $\qquad$ G = 300kg/m^{2}s $\qquad$ P = 7bar $\qquad$ ΔT_{sub} = 10K
- High subcooling $\qquad\qquad\qquad\qquad\qquad\qquad\qquad$ ΔT_{sub} = 20K
- High Pressure $\qquad\qquad\qquad\qquad$ P = 10bar
- Low flow rate $\qquad$ G = 200kg/m^{2}s

4.3 Data acquisition and Logging

The fact that all experimental data is acquired and logged digitally, gives almost unlimited opportunities when it comes to data processing and plotting. "One experiment" is captured by logging in a 500 seconds time interval. Experiments are repeated at the given conditions until it is evident that it resembles the steady state nature of the system. Acquisition period (sampling interval) was set to 100 ms (i.e. 10 samples per second) during all experiments. This frequency should according to the Nyquist sampling theorem give sufficient resolution to accurately represent DWO, which has an oscillations period in order of a few second in the system.

Several MatLab scripts have been prepared to do monitoring and processing of experimental data. An essential tool was a post processing script utilizing the Fast Fourier Transform (FFT) to extract average DWO period and amplitude from each experimental run. For the purpose of this thesis, however, some more data processing tools have to be purpose made. This is described in the paragraphs to come.

4.4 Data reduction

The rig facilitates a two figured number of sensors in which data is logged continuously when experiments are running. It goes without saying that a significant effort has been spent in data reduction. That is to transform the bulk numerical information derived from in-experiment measurements into a corrected, ordered and simplified form. The prime goal is to convert experimental results into a suitable and convenient form that can be easily summarized in charts and tables. Among these key figures characterizing the system is the heat transfer coefficient. This step is preformed after data from one experiment lasting 500 seconds has been time averaged. Results that for different reasons are out of trend are left out, in particular if the reason

is due to a known error or disturbance. This could for instance be sudden change in temperature inside laboratory or simply that insufficient time was spent for the condition to settle.

4.5 Measuring a heat transfer coefficient

The heat transfer coefficient is the proportionality coefficient between the heat flux and the thermodynamic driving force for the heat flow (ΔT). The heat transfer coefficient for convective boiling flows is based on the wall surface temperature (T_s) and bulk fluid temperature (T_f).

$$h = \frac{q''}{T_s - T_f}$$

There are several ways to quote a heat transfer coefficients, one is the overall, or global, heat transfer coefficient. To give a wider perspective on boiling flow heat transfer, a local heat transfer coefficient will also be quoted on two locations were fluid temperatures could be attained directly from internal thermocouples.

It should be noticed that this thesis will name the global, or length averaged, heat transfer coefficient the overall heat transfer coefficient. This overall (global) heat transfer coefficient do only account for the heat transfer inner wall of the heated tube to the fluid.

4.6 Global heat transfer coefficient

Using an average of the difference between the surface and fluid temperatures along the length of the heated section and the total heat flux transferred to the fluid, the global heat transfer coefficient was calculated.

$$\bar{h} = \frac{\bar{q}''}{\bar{T}_{w,i} - \bar{T}_f}$$

Here, temperature index $T_{w,i}$ and T_f refers to the inner wall and bulk fluid temperature respectively. It cannot be measured directly and need some special care. A comprehensive description of the method is given in the next sections.

4.6.1 Calculating the test section wall temperature

Recapitulate that thermocouples are glued to the outside of the test section; however, definition of the heat transfer coefficient is based on the surface of heat transfer interface. Thus, the inner wall

56

temperature values have to be derived from the thermocouples placed on the test section outer wall surface [49]. With the assumption of no heat loss (i.e. perfect insulation see section 3.1.6) and negligible heat flow in axial direction, the steady state equation for heat conduction through the tube wall is given by

$$\frac{1}{r}\frac{d}{dr}\left(r\frac{dT}{dr}\right) + \frac{q'''}{k_w} = 0$$

Where r [m] is the length in radial direction, q''' [W/m3] is the volumetric heat generation, and k_w [W/m^{2}K] is the thermal conductivity of the tube wall. The boundary conditions are no heat flux, and a known temperature ($T_{w,o}$) at, the outer surface. Integrating and solving for the inner wall temperature yields

$$T_{w,i} = T_{w,o} + \frac{q'''}{4\,k_w}(R_o^2 - R_i^2) - \frac{q'''}{2\,k_W}R_0^2\,ln\left(\frac{R_o}{R_i}\right)$$

R_o and R_i denotes the outer and inner radius of the heated tube. The volumetric heat generation is assumed to be uniform and can be rewritten to the following form

$$q''' = \frac{P_{el}}{\pi\,(R_o^2 - R_i^2)\,\Delta z}$$

With P_{el} being the total applied electrical power and Δz [b] being the length of the heated section. Combining the last two equations gives the final expression for calculating the inner wall temperature.

$$T_{w,i} = T_{w,o} + \frac{P_{el}}{4\,\pi\,k_w\,\Delta z} - \frac{P_{el}}{2\,\pi\,k_W\,\Delta z}\frac{R_0^2}{(R_o^2 - R_i^2)}\,ln\left(\frac{R_o}{R_i}\right)$$

This result is implemented in the MatLab scripts calculating the heat transfer coefficient.

4.6.2 Calculating the fluid temperature

The fluid temperature was calculated form the inlet temperature, inlet pressure, and total heat flux supplied, using a steady-state thermodynamic equilibrium model. An approach as simple as possible was chosen rather than implementing features such as two phase distributed pressure drop, non-equilibrium thermodynamic models or using fancy numerical schemes.

A homogeneous flow model was chosen for its simplicity, assuming that the two-phase flow is well mixed. The slip ration, defined as the ratio between gas and liquid velocity, is then (by definition) assumed to be unity (non-slip condition). This is a fair assumption since the high Reynolds numbers of all experimental cases are associated with a great deal of turbulent mixing caused by Eddies diffusion. It also makes sense as the heat transfer coefficient is based on the bulk fluid temperature.

Any effects of non-equilibrium thermodynamic are disregarded, even though the time for phase transition to occur is limited.

Starting with the distance, velocity and time formula

$$z = v\,t$$

Changing it to incremental form and rewriting the velocity gives

$$\Delta z = v\,\Delta t = \frac{\dot{V}}{A_c}\Delta t = \frac{G}{\rho}\Delta t$$

Next to come is discretization in time and space. Notice that the upcoming time step is based on the current density

$$t_{n+1} - t_n \;=\; \frac{\rho(n)}{G}\,(z_{n+1} - z_n)$$

This gives the time a fluid particle spends in one of the infinite small control volumes, commonly referred to as grid cells. For the practical purpose of this thesis it was chosen to use a stationary grid with grid cells of equidistant spacing. Furthermore, the grid used was of an unstaggered type with both velocity and temperature (i.e. enthalpy) on the cell walls. See Figure 4.1

58
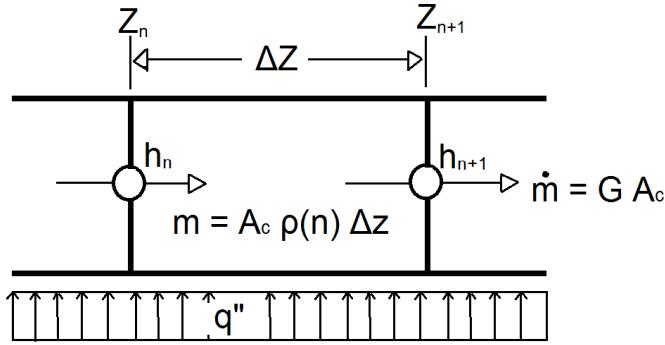
Figure 4.1 Grid cell

The energy balance contains the enthalpy $h(P,T)$ which will later be used to finally determine the temperature.

$$\dot{m}\,\Delta h = q$$

The mass entering a cell is equal to the mass exiting the same cell, guaranteeing mass conservation in this steady state model.

$$\dot{m} = \rho\,A_c\,v$$

Combining the two equations above contains the enthalpy change of the fluid inside a single cell.

$$(\rho\,V)\,\Delta h = q''\,A_s\,\Delta t$$

The test section is a tube with cylindrical geometry.

$$\rho\,\frac{\pi\,d^2\,dx}{4}\,\Delta h = q''\,(d\,\pi\,dx)\,\Delta t$$

Reorganizing, and discretizes

$$h_{n+1} - h_n = \frac{q''\,(t_{n+1} - t_n)\,4}{d}$$

Finally, the two discretized equations, time and state (enthalpy) equation were implemented in a Matlab script on the following form:

$$t_{n+1} = t_n + \frac{\rho(n)}{G}\,(z_{n+1} - z_n)$$

$$h_{n+1} = h_n + \frac{q'' \, (t_{n+1} - t_n) \, 4}{d}$$

The scheme is first order explicit in both time and thermodynamically state. Relative small steps were used to mitigate the adverse numerical effects, in particular numerical diffusion, such simple schemes tend to introduce. The heat flux is uniform and the diameter remains the same. The temperature at any incremental position can finally be found from the computed enthalpy and test section inlet pressure.

$$T_n = f(p, h_n)$$

The described scheme makes it possible to evaluate the fluid temperature at any position in the test section based on the geometry, a known inlet condition (temperature, pressure and mass flow rate) and the heat input. Other quantities, such as vapor quality and mean fluid particle residence time (transit time or tau) can also be acquired form this model.

This simple unambiguous, textbook like, approach for computing the fluid temperature was chosen by practical reasons. In the end, the heat transfer coefficient will always be a computed or derived value, since it cannot be measured directly.

In experimental setups where axial conduction is significant the overall heat transfer coefficient is rendered the only option [43]. This is not a particular issue in the current experimental configuration; a more elaborated study regarding the influence of axial condition in a heated pipe was performed by Manavela Chiapero et al. [52]

4.7 Local heat transfer coefficient.

Heat transfer performance will also be evaluated and quoted locally for two locations, namely the thermocouples at position 6 and 10 (See Figure 3.2). These two location features four external thermocouples placed on top, bottom and both side of the tube in addition to an internal thermocouple measuring the in-fluid temperature. The heat transfer coefficient can hence be calculated from the actual measured fluid temperature rather than the modelled. Measurements in these two particular points will therefore be given special attention. However, do notice that the internal thermocouples measure the temperature at one distinctive location within the flow cross-section, which might be different from the average bulk fluid temperature at that location. Also, the thermocouple may be subject to radiant heat transfer from the tube wall, in particular if

60

undergoing a burnout situation where the tube walls are unusual hot while the refrigerant is solely in its vapor form.

In view of the measurement of a local heat transfer coefficient, the choice of using stainless steel as tube material has its advantages as the heat conductivity is less than for metals such as copper and aluminum minimizing the axial redistribution of heat within the tube.

Thermocouple position 10: Close to the test section exit ($z = 1917$mm) but still within the heated zone. This is the point of highest vapor quality or sometimes even superheated vapor, highest velocity, and the location in the tube most prone to dry out. Dry out of the heat transfer surface will most likely result in poor heat transfer and excessive wall temperatures.

Thermocouple position 6: For all practical system conditions involving experiments within or in proximity of the DWO region in the current experimental setup, are the thermocouples at position 6 ($z = 1117$mm) situated in the evaporation region (bulk fluid vaporization). To elaborate this a bit further, if the bulk fluid was not yet at its boiling point when being past the mid of the heated channel, it is doubtful that it ever will reach a sufficiently high vapor quality prior to exiting the tube for DWO to even occur. On the other hand, if the bulk fluid was already superheated at about the mid-way down the tube, wall temperatures in excess of the highest allowable 110°C would certainly be experienced at the outlet of the heated section, assumed that the test section is supplied a flat heat profile (i.e. uniform heat flux).

5 Pre-work and calibration

The aim of this chapter is to review and address all issues that need to be considered when in order to tackle the main goal, mapping out the effect of flow instabilities on boiling flow heat transfer, pressure drop and critical heat flux.

The starting point is to perform validation of the measurements with single phase liquid condition against well-known and tested correlations. The following activities to be carried out are characterization of valve positions and overall configuration of the rig. Characterization of Density Wave Oscillations in the present experimental facility are regarded as mandatory, since the behavior likely will be different in another flow loop, with other fluids, at different conditions, and in other geometries. The pre-work will therefore highly stress the implications in configuration of the flow loop, as it is required in order to obtain, and properly interpret, the final results. In this pre-work chapter, experiments and results are presented and discussed immediately after.

5.1 Single phase pressure drop validation

Single phase data on adiabatic frictional pressure drop is acquired for validation against the Colebrook correlation. Test section pressure drop was measured directly using one of the differential pressure transducer.
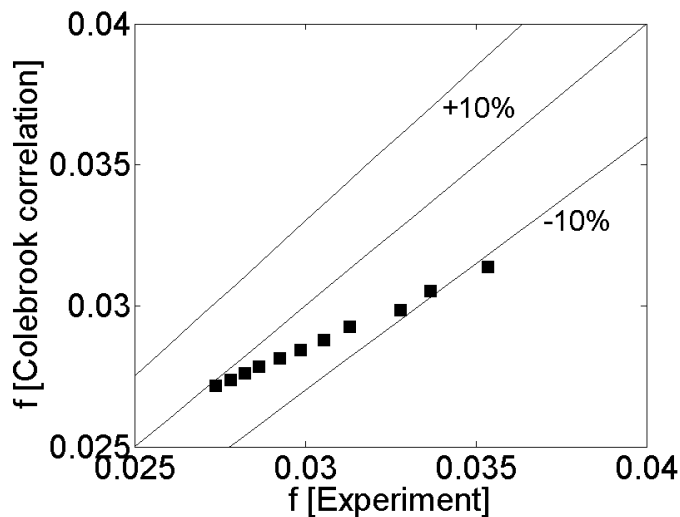
Figure 5.1 Single phase pressure drop validation

Almost all experimental data is inside the 10% confidence interval.

5.2 Single phase heat transfer coefficient validation

The local heat transfer coefficient was measured 1117 mm downstream in the heated section. It was computed from the difference between measured fluid temperature and inner wall. Inner wall temperature was deduced form the four thermocouples surrounding the outside of the heated section at this location.

The heat transfer coefficient measurement in single phase was validated against the Petukhov-Kirilov correlation. The procedure is based on Manavela Ciapero et al. [49]

$$Nu_d = \frac{h\,d}{k} = \frac{\frac{f}{8}Re_d Pr}{1.07 + 12.7\sqrt{\frac{f}{8}}\,(Pr^{\frac{2}{3}} - 1)}$$

The friction correlation f in the above formula was obtained from:

$$f = \frac{2D}{L}\frac{\Delta P}{\rho V^2} = (0.79\ln Re_d - 1.64)^{-2}$$
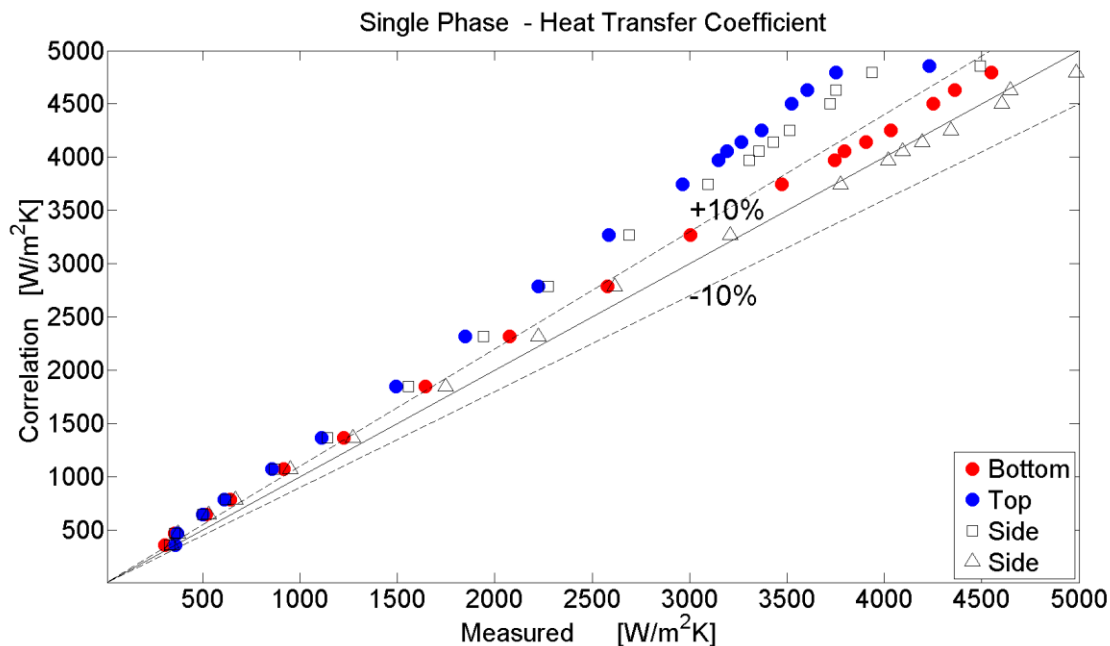
Figure 5.2 Single phase heat transfer coefficient validation (for four thermocouples)

One would immediately notice the significant dispersal in heat transfer coefficient among the four thermocouples placed around the test section. It is notable that the top side has somewhat

poorer heat transfer, immediately shifting the attention towards the possibilities of flow stratification, or occurrence of voids in the upper part of the liquid. The facility was not equipped with a high speed camera at the time of single phase verification so no hard evidence exists, but it is know that the bulk liquid had a vapor fraction well beyond zero (x < -0.2) at this position. The situation in the test section outlet has another trend, here; the highest temperature was generally recorded at one of the side thermocouples. It is necessary to dig a bit further into the experimental data to find a reason for the unsystematic dispersal in single phase local heat transfer coefficient.

Single phase experiments (Figure 5.2) were set with maximum achievable inlet subcooling (in practice ΔT_{sub}=32-42°C with inlet pressure in the P_i=6.3-8.3 bar range). Experiments were performed at various flow rates, with Reynolds ranging all the way from 2200 to 52400. Heat input was increased with flow rate in a fixed ratio, the upper condition was G = 3000kg/m^{2}s with Q = 1000W. This choice of flow rate to heat input is a trade of between two factors. High heat input can lead to occurrence of subcooled surface boiling, a heat transfer regime totally different from single phase forced convection where the heat transfer coefficient depended on heat flux. On the other hand, higher heat input means larger wall surface to fluid temperature difference, effectively giving both a larger numerator and denominator (see equation below), which allows for a more accurate prediction of the heat transfer coefficient.

$$h = \frac{q''}{T_s - T_f}$$

Analysis of the single phase verification data shows that $T_s - T_f$ is in between 3.5 and 8.4°C, where the later corresponds to the experiments with highest heat flux and flow rate. These are rather small numbers considered that the mutual difference among the thermocouples distributed around the outside of the test section is ≤ 0.4°C This error in temperature measurement is within expectation, but can still cause at least 10 % disperse in measured heat transfer coefficient among the four circumferential distributed thermocouples. There are also uncertainties in other quantities, such as the heat input, having equal impact on the four measurements.

To summarize, single phase verification (Figure 5.2 has shown that the measured local heat transfer coefficient is found to be within a 20% confidence interval. Measurement of the heat transfer is sensitive to inaccuracy in temperature, in particular in single phase forced convection

situations. Comprehended that most experiments in this study will involve boiling, thus much greater surface to fluid temperature difference, this single phase calibration result is regarded to be sound.

5.3 Characteristic curve of the pump subsystem (single phase)

The characteristic curve (pressure head – flow rate) of the pump subsystem is generated. Experiments were conducted by gradually opening the pump bypass valve in small steps. Flow rate and pressure drop was recorded for 60 seconds at each step. This procedure was repeated with three different pump drive speeds to cover a wider range of pressure drop and flow rate. Logging for rather short periods was allowed since single phase adiabatic experiments tend to have a much less complex nature than the DWO counterpart.

Liquid R134a enters the pump form the main tank by means of gravity (schematically diagram in Figure 3.1). Absolute pressure is recorded inside the tank and after the pump giving $\Delta P = P_{pump\ outlet} - P_{tank}$ It was corrected for the pressure differential observed when the system is at rest of 8.4864 kPa (equals ~ 0.7 m) caused by a combination of the liquid head in the tank supplying the pump and static error in the absolute pressure sensors. The inlet temperature conditioner was used to add a suitable amount of subcooling. This ensures single phase liquid flow through the flow meters and rest of the loop. The system pressure (main tank) was about 6.5 bars.
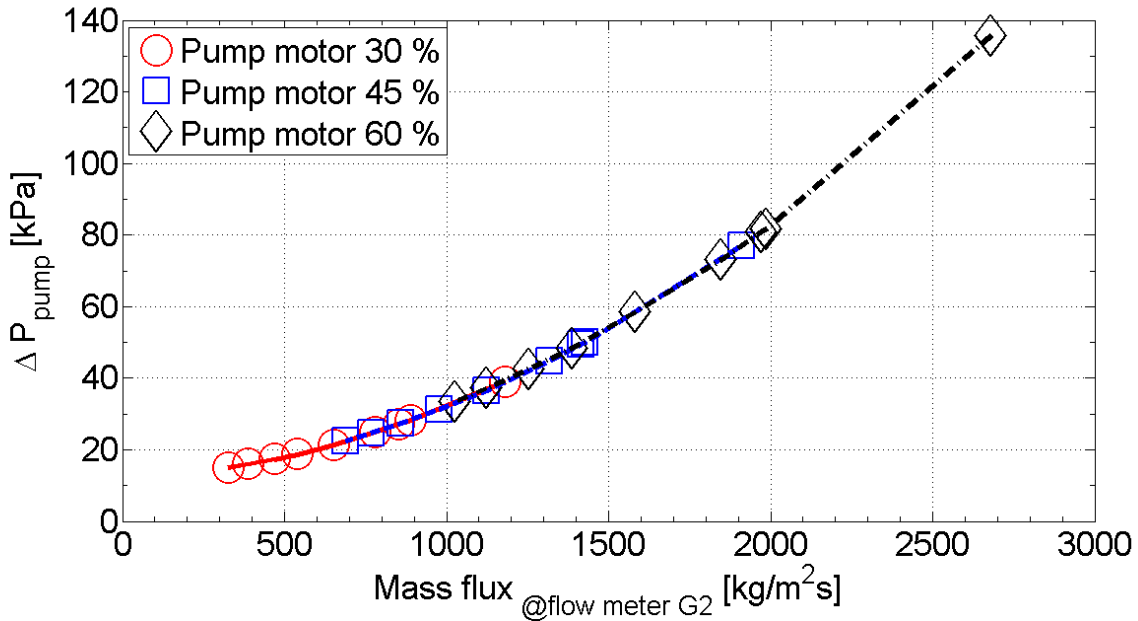
Figure 5.3 The characteristic curve of the pump upon modification of the bypass-valve for three pump motor (M) speeds.

The three curves are perfectly overlapping each other. This shows that the choice of, running with slow pump drive speed and closed pump bypass, or, running with high drive speed and open bypass, is a matter of convenience because both are equal for a given flow rate. Or, it is at least proven true for experiments with stable single phase flow. The three characteristic curves do also display how altering the pump bypass valve can broaden the practical achievable range of flow rates. Partly opening the bypass allows experiments with moderate to small flow rates to be performed even though the pump moves a larger volume by design.
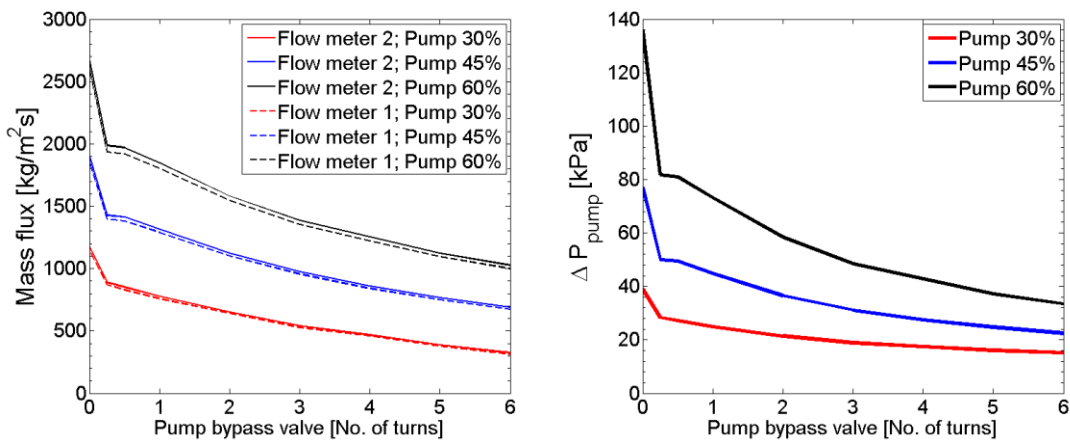
Figure 5.4 Mass flux & Pump pressure head – bypass valve configuration (3 pump drive settings)

The first plot in Figure 5.4 shows explicitly how flow rate responds to modification of the pump bypass valve. Acknowledge that the two flow meters show almost identical readings. The second plot shows pump pressure head versus pump bypass valve position. What might be perceived as a discontinuity in the left hand side of both plots are not a physical property of the system, it is due to the coarse quarter turn resolution when the pump bypass was adjusted during experiments.

The discussion regarding the external characteristics of the system might seem to be a bit overelaborated. Next to come is an exploration of the dynamic behavior of the pump subsystem when experiencing flow instabilities within the loop.

5.4 The influence of pump bypass valve in the characteristics of DWO

The pump by-pass valve has been modified to see how it influences the DWO-mode. A key difference in the configuration of the experimental facility in this study, compared to other apparatuses described in literature, is the partly bypassed pump. Ruspini [8] stated that the pump bypass valve was opened in order to destabilize the DWO mode, since no compressible volume was used for the study. Doing experiments to learn how external characteristics, or the pump with bypass subsystem, influences DWO behavior internally in the test section will be crucial to do well considered choices in the further innovation of the present experimental program.

The influence of partially bypassing the pump will be evaluated for both internal and external characteristics. Where internal refers to the test section including inlet and outlet restrictions, while the external part of the system is rest of the flow loop.

5.4.1 Hypothesis

A closed pump bypass valve means that the test section is hydraulically in direct connection with the gear pump. This enables the pump to force a steady flow of liquid to the test section inlet, thus disallowing any significant oscillations in inlet flow rate. If oscillations persist with closed bypass, however, the oscillations in pressure is expected to become stronger. Preventing the flow from moving freely in in the system is expected to yield larger fluctuations in pressure during oscillations. Partly bypassing the pump opens an alternative path which allows for variable, even transit reversed flow, in the test section inlet. This configuration favors oscillations in flow rate known as a key characteristic of the DWO-mode.

5.4.2 Internal characteristics

DWO were produced at a constant flow rate G=300 kg/m^{2}s, power Q=1200 W, inlet pressure P=7 bar and degree of inlet subcooling ΔT_{sub}=10 K. The pump bypass valve was modified while the above mentioned parameters were kept constant. The pump motor drive speed had necessarily to be increased as more and more fluid was circulated back when opening the pump bypass valve. Zero turns indicates a closed bypass meaning that the flow is purely dictated by the pump characteristics.
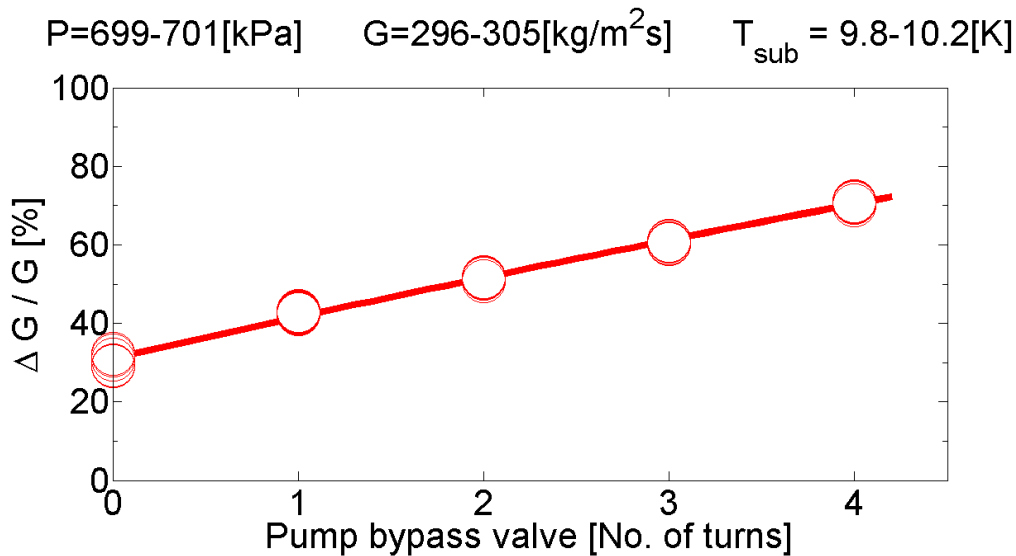
Figure 5.5 DWO normalized flow amplitude – pump bypass valve (internal characteristic)

Oscillations in mass flow rate measured at the test section inlet restriction increases when the pump bypass valve is opened. The result is in accordance with the previously stated hypothesis. This is a notable finding as it demonstrates that characteristics of the external system affect instabilities in the test section. Particular, since so many different configurations are described in the literature.
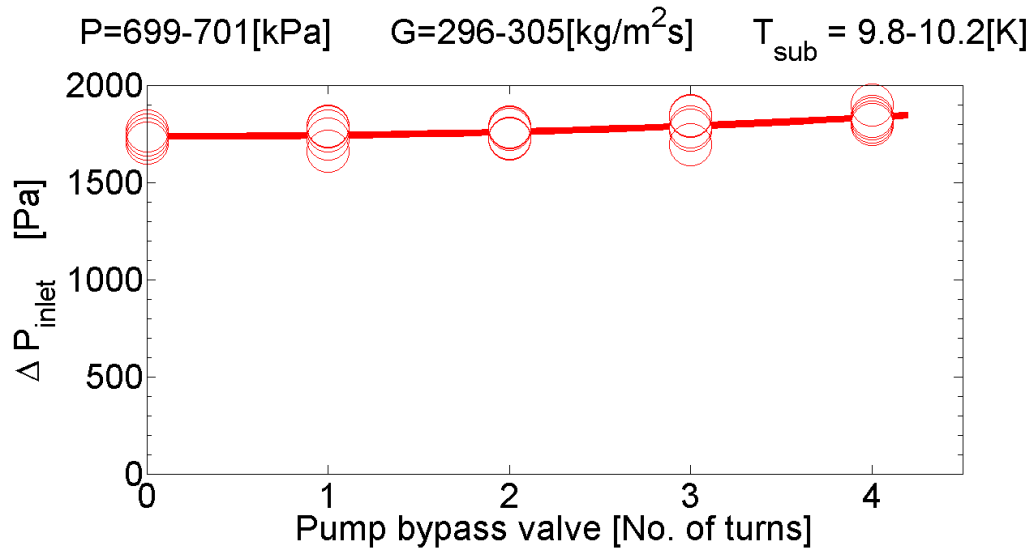
Figure 5.6 DWO Pressure amplitude – pump bypass valve (internal characteristic)

Modifying the pump bypass valve did not have very significant influence on the oscillations in inlet pressure.
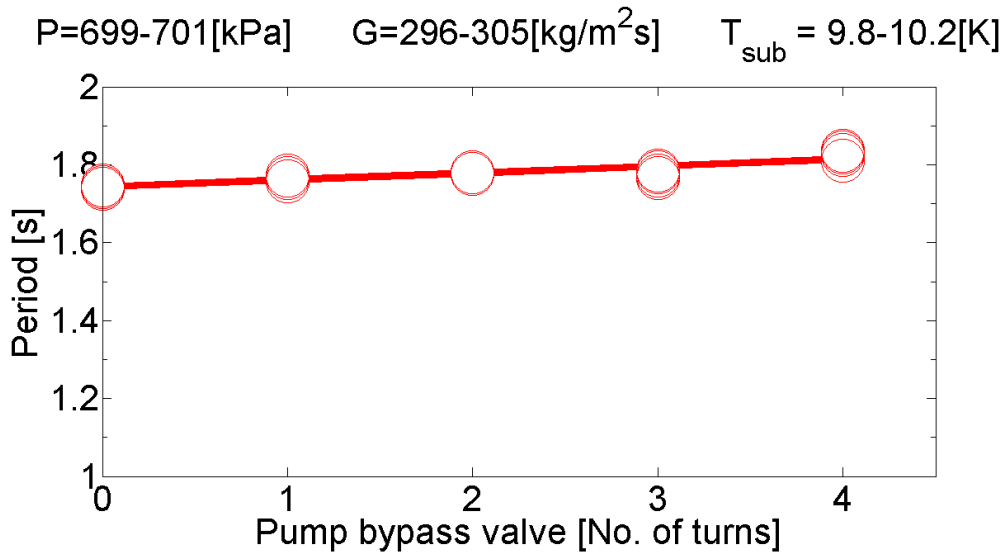
Figure 5.7 DWO period – pump bypass valve (internal characteristic)

The change in period is insignificant upon modification of the pump bypass valve. This is in agreement with the classical description of DWO stating that period is a function of transit time, which indeed is kept the same in the above experiments.

Closing the pump by-pass valve is found to dampen oscillations in flow rate. This will later become a useful measure to control the DWO-mode in preparation of experimental program. Pressure amplitude of oscillations was almost unaffected by the pump-bypass configuration suggesting that it is property of the test section internal geometry, restrictions and configuration, rather than the external pump characteristics. Characteristics of the pump subsystem have no influence on the period of oscillation, which is in good alignment with the classical DWO description.

5.4.3 External characteristics

The previous section established the fact that external system characteristics do influence DWO in the test section, even though the phenomenon is believed to be confined between the in- and outlet restrictions. This section aims to provide so insight to the external behavior of the system.

The results presented in this section are based on same experimental series as for the internal characteristics. Experiments with DWO was performed at G=300 kg/m^{2}s, P=7 bar, ΔT_{sub} = 10 K, Q=1200 W. The pump bypass valve was changed in incremental steps from closed to four turns open. The external part of the flow loop is not as well instrumented as the test section. It would have been convincing to quote restriction coefficients for the bypass valve, but there is no reliable way to compute it. Status of the bypass valve is therefore quoted in number of turns, though it is a somewhat unscientific measure.

A trace of the pressure head (ΔP_{pump}) is plotted against the flow rate for different pump bypass scenarios (Figure 5.8). Numbers of valve turns are indicated in the upper right corner, staring with a closed valve. The axes are of equal magnitude for mutual comparison between the four plots. The plots, drawn from 500 seconds of continuous logging, shows how DWO present in the test section cycles flow rate and pressure in the pump subsystem.
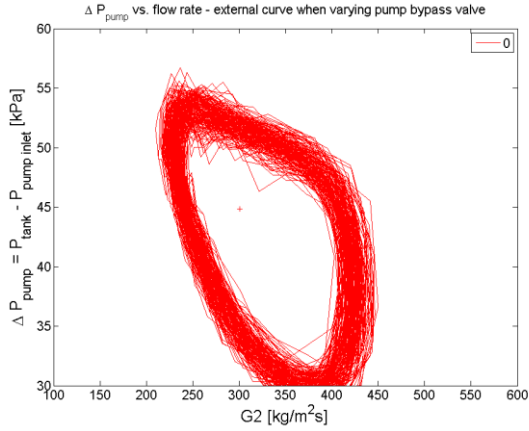
Closed pump bypass valve
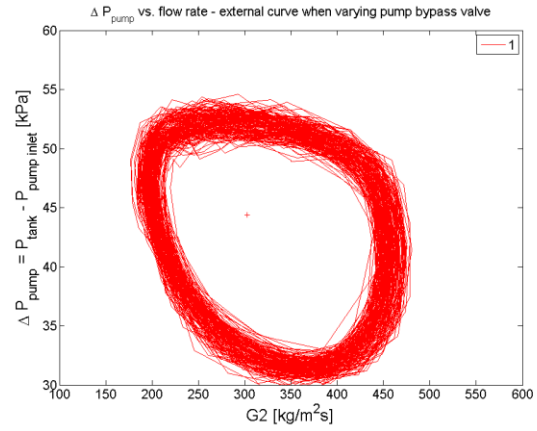
Bypass one turn open
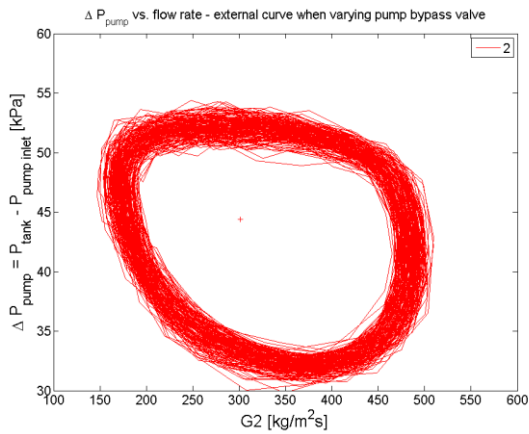
Bypass two turns open
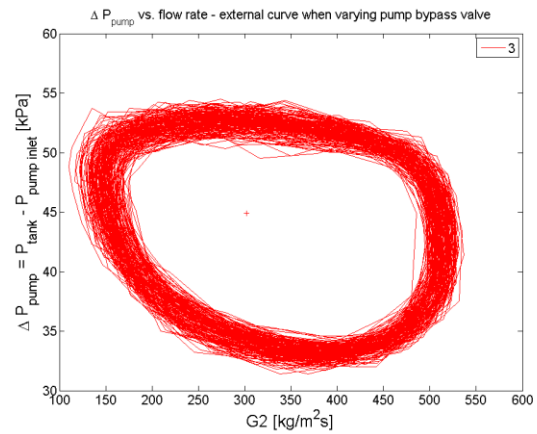
Bypass three turns open (default)
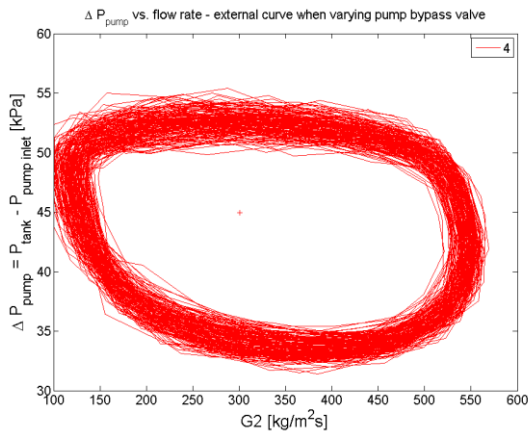
- Pump bypass valve four turns open

Figure 5.8 ΔPpump – flow rate. External curves for pump bypass setting from closed to 4 turns open

The external curve becomes wider when opening the pump bypass, which means larger fluctuations in flow rate per variation in pressure. This makes sense since allowance of a flow path parallel to the pump was expected to make the whole pump subsystem less stiff. It is now clear that the external loop behavior mirrors the result for internal characteristics; a pump with bypass yields a system with larger oscillations in flow rate.

5.5   The effect of an inlet restriction valve and exit orifice

Adding an inlet restriction is often quoted as main ingredient in reduction of the system stability. Developing stability maps for various inlet restrictions is not the purpose of this work, but a simple test was conducted by modifying the inlet restriction valve. The system was operated with constant uniform heat flux, mass flow rate, pressure and inlet subcooling. The outlet orifice was present and pump bypass partly open yielding DWO. The amplitude decreasing as the restriction is opened form it default position, suggesting that the system is moving towards a stable condition. Thus, opening the inlet valve will later be crucial to resume system stability in experiments.

A similar test was done with the exit orifice. The orifice can easily be removed but it is possible to direct flow thorough a parallel path. This also decreases the DWO amplitude, but omitting the exit orifice is not a sufficient measure to extinguish the oscillatory behavior of the system.

The findings so far indicates that a combination of omitting the exit orifice, opening the inlet restriction valve, and closing the pump bypass valve is required to bring the system to total stability.

5.6   The effect of DWO amplitude in heat transfer (constant period)

The experiments to be presented were conducted to assess how flow oscillation amplitude influences pressure loss and heat transfer characteristics of the system. Another objective is to see how imposed instabilities resemble the true DWO mode.

All experiments were performed with basis in equal conditions, that is a pressure of P=7 bars, flow rate G=300 kg/m^{2}s, 10 K inlet subcooling, and a total of 1200 W power. Three operating modes were tested, namely DWO, imposed instability and stable/steady.

The first case labelled with red circles is performed with test section inlet and exit restrictions yielding an unstable system with naturally occurring DWO as outcome. Amplitude of oscillation can be varied by changing the external system characteristics by modifying the pump bypass valve. Opening the pump bypass valve helps destabilizing the system and yields more significant flow oscillations. Opening the bypass valve by 2, 2.5 and 3 turns forms groups of points with different amplitude.

The second case labelled with black squares is supposed to resemble the first case, but this time with a mimicked instability. Test section inlet valve was opened; flow was allowed to exit the test section through both the adiabatic section; and the pump bypass valve was shut; effectively creating a stable system. Flow oscillation was then externally imposed by controlling the pump drive with a sine, which is supposed to resemble density wave oscillations. The period of oscillation was set equal to the period recorded from the natural DWO-mode. Amplitude of the externally imposed oscillations was varied by simply changing the amplitude of the sine signal in the pump drive controller.

The last case, labelled with blue diamonds, is configured similarly to the second case, except the pump drive being operated at constant speed. This gives a stable system behavior forming a reference case for pressure drop and heat transfer characteristics.
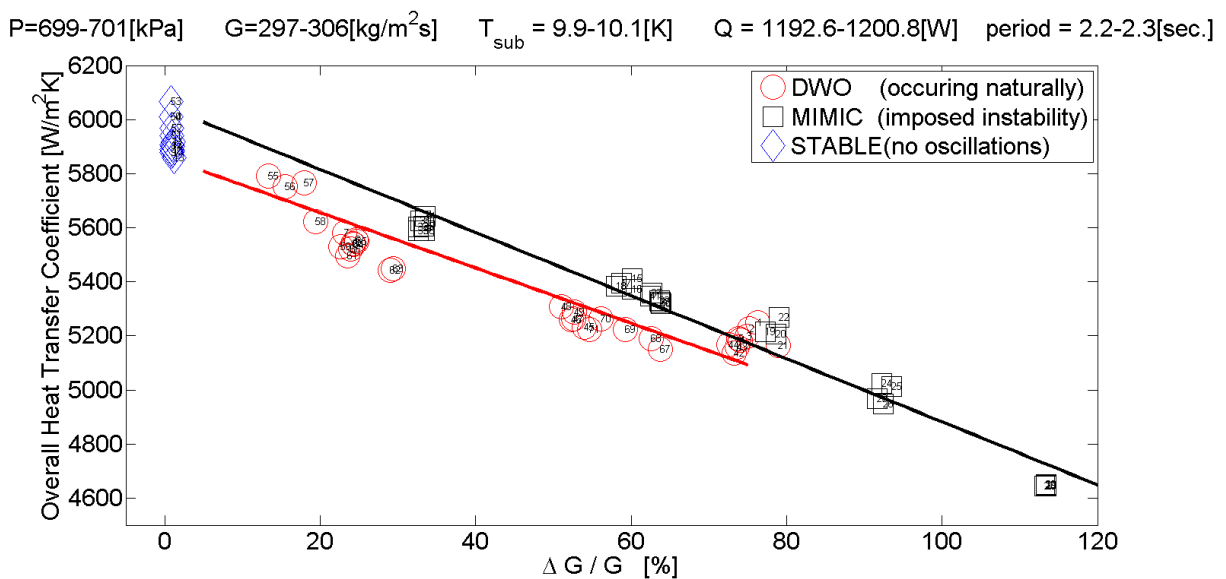
Figure 5.9 Overall HTC – Normalized flow amplitude. Comparing the effect of DWO and mimicked amplitude

It seems evident from the above plotted data that flow oscillations deteriorate overall heat transfer. The reduction in overall heat transfer is proportional to the flow amplitude. Extrapolation the points with oscillations (red and black line) to zero amplitude shows good agreement with the heat transfer achieved in the stable case (blue). Some disperse on the amplitude axis is seen in the DWO-mode (red). The amplitude of a naturally occurring DWO often shows a rather volatile behavior within every experiment, especially in the vicinity of its onset. Next to come is some considerations on the pressure drop.

An externally imposed flow variance mimicking DWO (Figure 5.9) has heat transfer characteristics similar to DWO occurring naturally in a system with inlet and outlet restrictions, given that the fluctuations in flow rate are of equal magnitude. In this case, flow oscillations of normalized flow amplitude of 100% show a 10% penalty in length averaged heat transfer performance.
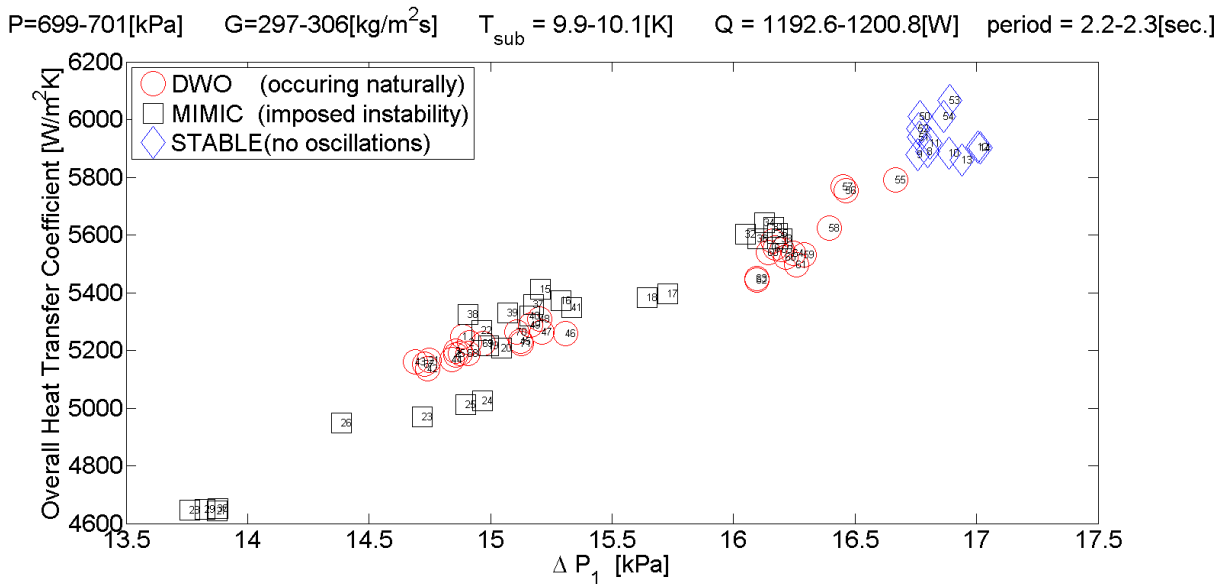
Figure 5.10 Overall HTC – Test section pressure drop. Comparing the effect of DWO and mimicked amplitude

Plotting the overall heat transfer coefficient versus the pressure loss in the heated section shows that the two are tightly coupled regardless of instability mode (i.e. naturally occurring or externally imposed). Also, the stable points lines up with the same trend.

The effect of amplitude on pressure drop and heat transfer characteristics of DWO was isolated from all other variables, among them the period. Overall heat transfer coefficient shows a linear

negative scaling from stable to increasing amplitude of oscillation. Mimicking is a viable solution for investigation pressure drop and heat transfer characteristics of true DWO, though one must mind the amplitude.

5.7 The effect of oscillation period in heat transfer (constant amplitude)

This section introduces the concept of shifting the oscillation period of imposed flow oscillations. The idea is to generate instabilities with oscillation period different from the natural DWO-mode, possibly isolating the effect of period from other variables to learn how it influences the pressure drop and heat transfer characteristics of the system.

The condition through this experimental series is fixed at 7 bars, 300 kg/m2s, 10 K subcooling and 1200 W heat input. Experiments are carried out by externally imposing instabilities to an otherwise stable restriction-less system. The period of the sine signal sent to the pump drive is varied, while the amplitude of the signal is modified keeping the relative flow amplitude approximately constant ($\Delta G/G \sim 66$ %). This is done to isolate the effect of period from the effect of flow oscillation amplitude.

Some additional experimental results with equal conditions are also plotted. The blue diamonds represents experiments with equal conditions though without varying the pump drive. An average is plotted as a horizontal blue line, providing a reference for the heat transfer performance of a stable system. The red circles are experiments with inlet and outlet restrictions having self-sustained DWO. The natural oscillation frequency of DWO is indicated by the vertical red line, see the next figure.
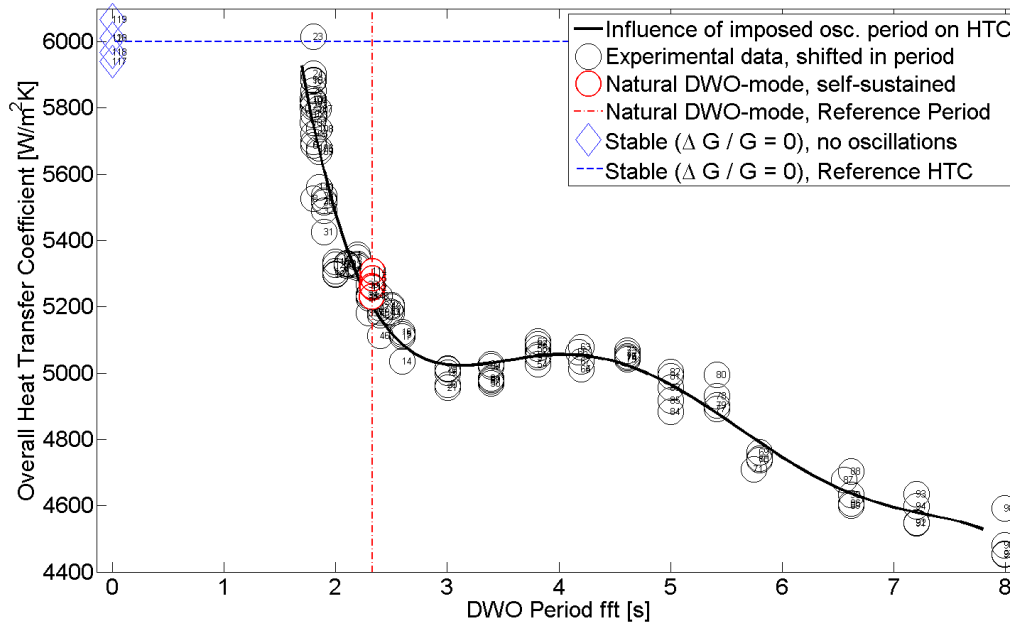
Figure 5.11 Overall HTC – Oscillation period. Period externally controlled by imposing instabilities with pump.

The overall heat transfer is steeply increased flow as oscillations are shifted towards higher frequencies. This Based on the plot above on might start believing that shifting oscillations towards lower periods brings the overall heat transfer to the skies. However, producing flow oscillations with period of less than 2 seconds was rendered impossible. The limitation is most likely due to insufficient responsiveness of the pump drive. This issue will be addressed in the subsequent section.

A small dip in is observed in the overall heat transfer coefficient when the period is shifted to longer time intervals than the natural mode. On further elongation of the imposed period, an unexpected change appears around 3.8 seconds. From this point, overall heat transfer drops further. It is in contradiction to this, still natural to believe that heat transfer will approach the stable level if oscillations were shifted towards infinite period, though it was not attempted to confirm this in the present experimental study.
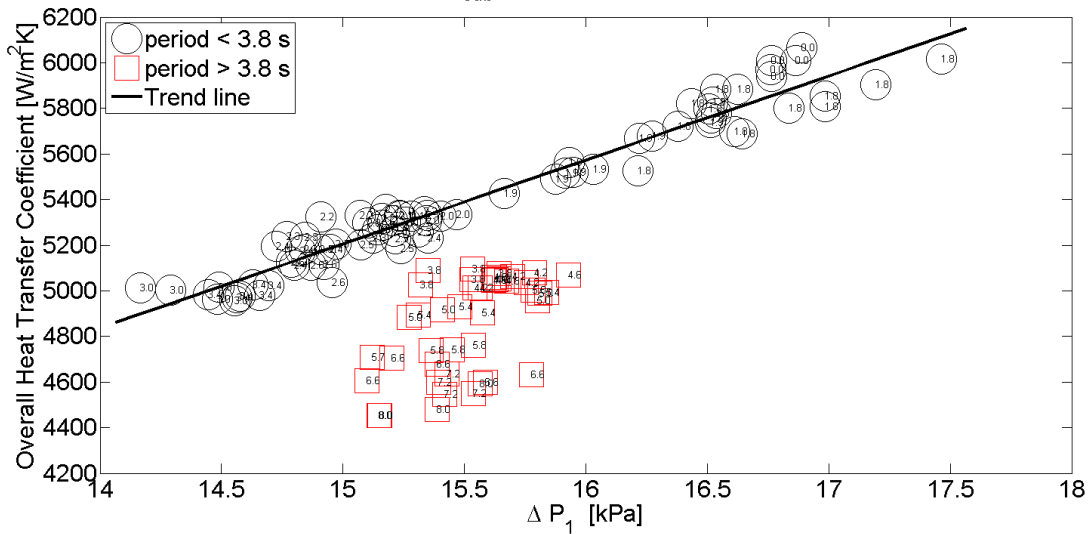
Figure 5.12 Overall HTC – Pressure drop. Period externally controlled by inducing instabilities with pump

Instead of experimental number, each point in the figure is labelled with its period of oscillation. For the experiments with period less than 3.8 seconds, heat transfer is strictly correlated to pressure loss. For oscillations with period significantly larger than the natural mode (red) is the heat transfer per pressure loss shows generally poorer. Thus, it is truly not a favorable regime of operation.

Heat transfer augmentation comes on the cost of higher pressure loss. Knowing the natural frequency (period) of the instability in the given system is crucial when mimicking the DWO instability.

It is useful to look at the problem form the point of view of turbulence. An attempted subjective explanation is that high frequency oscillation disturbs and leads to frequent breakdown of the viscous sublayer close to the tube walls, or that it boost the large turbulent eddies mixing the core flow, likely both. Disturbance of formation of a viscous sublayer augments heat transfer due to the existence of temperature gradients usually are present as it was laminar flow, even though the viscous sublayer tends to be incredible thin (law of the wall). The viscous sublayer [53] is sometimes referred to as the laminar sublayer but this is a bit misleading since the flow is not steady, but flow fluctuations do not contribute much because of the overwhelming effects of the viscosity. Oscillating the flow is also believed to feed more energy to the largest turbulent scales, the Eddies, thus enhances heat transport by turbulent mixing in the core region (also referred to as

the outer layer in open channels). This will increase the viscous dissipation of the turbulent kinetic energy explaining why the pressure drop increases proportionally with the induced oscillation period.

5.7.1 Accuracy of the method

It was found in the previous section that heat transfer characteristics of both mimicked and real DWO are indeed dependent upon the amplitude of flow oscillation. The idea of this particular experimental series was therefore to isolate oscillation period from amplitude by maintaining constant amplitude while shifting the period. Constant amplitude was maintained by choosing appropriate amplitude of the sine signal controlling the pump drive. Larger amplitude in the externally imposed flow was necessary to accommodate this as the shift in period was increased. Still, amplitude of flow rate in DWO is a very illusive quantity, susceptible to change thorough experiments. Also, the pump sine function in LabView has to be stopped to adjust mean pump speed. So, maintaining fixed amplitude is not a simple exercise.
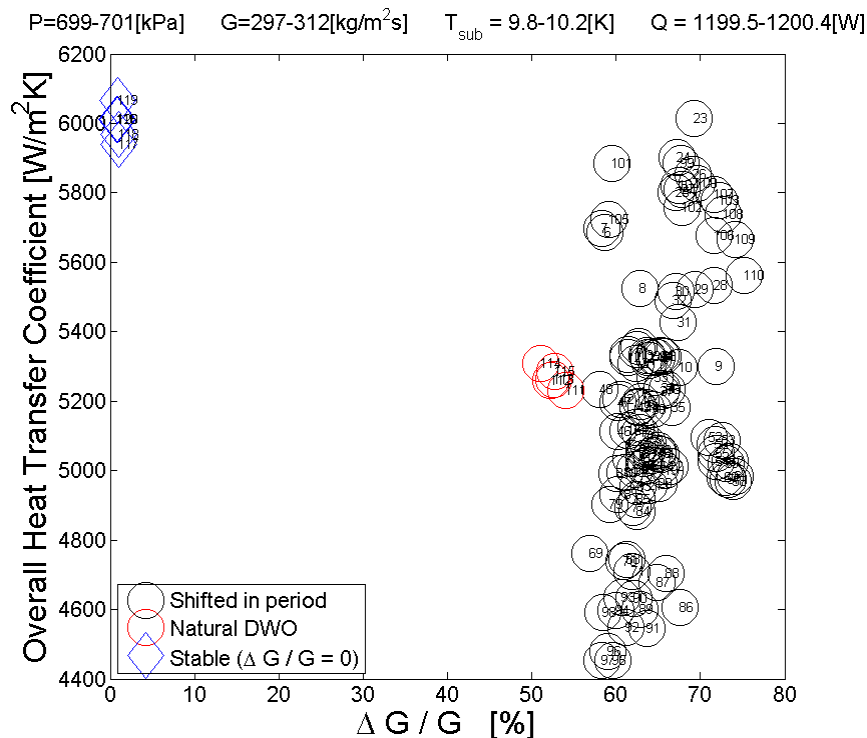
Figure 5.13 Overall HTC – ΔG/G. The effect of period is effectively isolated form amplitude.

The normalized amplitude in flow oscillation plot is included to provide a sense of the credibility of this experimental series. The aim was constant amplitude. Using Figure 5.9 as a guideline suggest that $\Delta G/G$: $\pm 10\%$ translates roughly into HTC: $\pm 100 W/m^2 K$ (4%)

The experimental series with constant period: Period ± 0.05 second offset in the vicinity of the natural DWO period translates $\pm 75 W/m^2 K$ (3%)

5.8 The effect of oscillation period: Part II (constant amplitude)

The previous section reviled a rather sensational boost in heat transfer when shortening the oscillation period, but a limited pump drive dynamic responsiveness disallowed proper experiments in the region of sub 2 seconds period.

In an attempt to address the issue of responsiveness of the pump drive limiting the minimum period, system conditions are now changed. The flow rate is halved (150 $kg/m^2 s$) and heat input reduced accordingly, which in turn helps reducing the overall velocity. Inlet subcooling was doubled (20 K) effectively increasing the length of the low velocity single phase region. Oscillation period of the DWO-mode is known to scale with heated section transit time. The combined effect of the mentioned adjustment in conditions is a DWO period of 4 seconds. Slower oscillations gives more headroom in the dynamic range of the pump when investigating the effect of imposing flow oscillations with shorter than natural period.
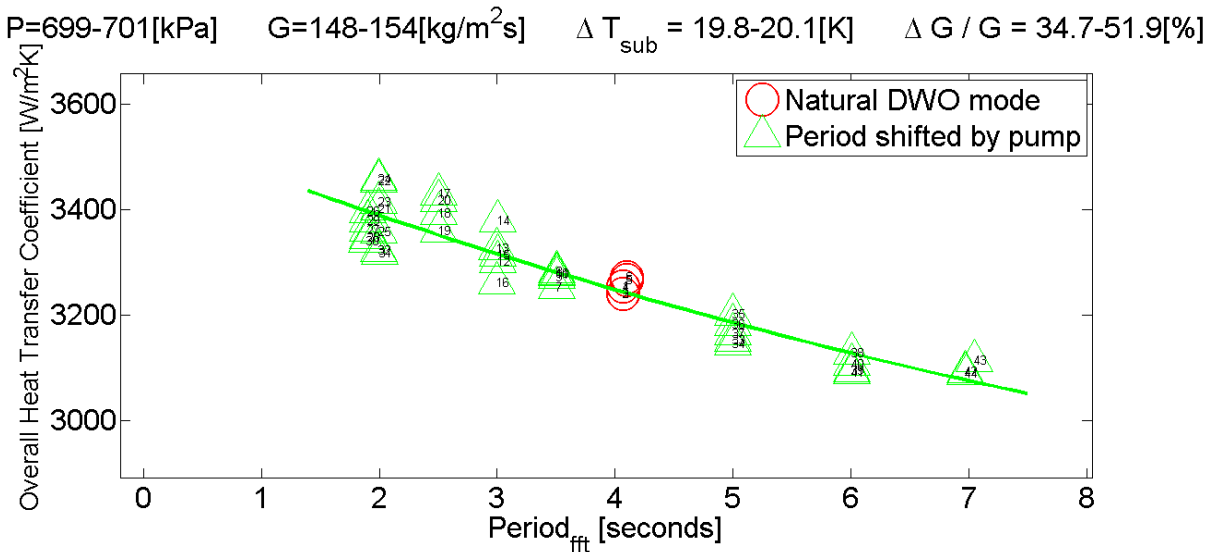
Figure 5.14 Overall HTC – oscillation period. The effect of shifting the period of externally imposed oscillations.

Shifting oscillations by external means towards shorter periods may benefit overall heat transfer, but the effect is in this case is diminutive. The y-axis of this plot is very fine, and the gain in heat transfer by shortening the period is just three percent. Implementing a pump with variable speed drive or similar device is not regarded a feasible way to boost heat transfer in a practical application.
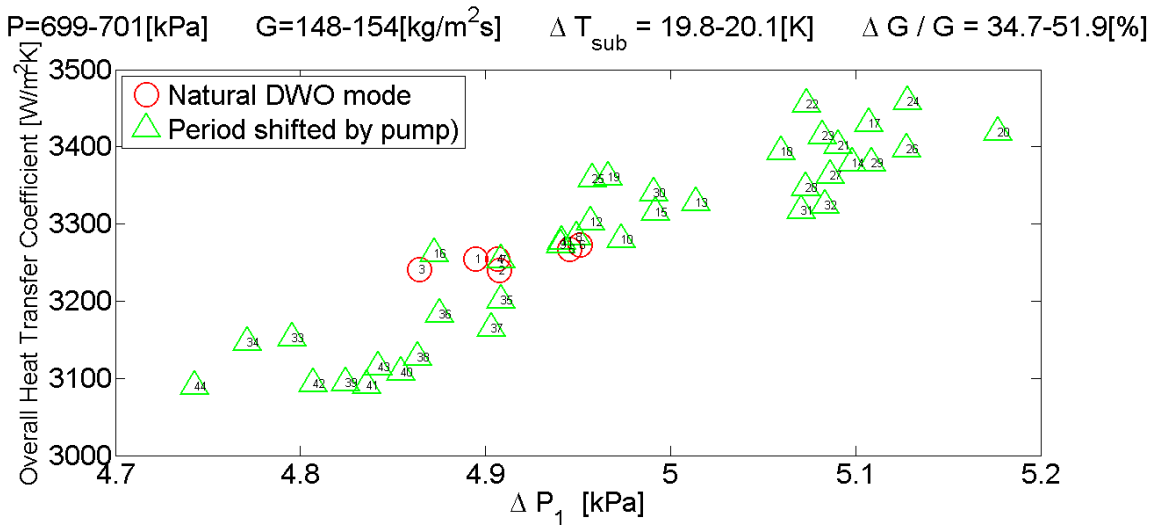
Figure 5.15 Overall HTC – Pressure drop. The effect of shifting the period of externally imposed oscillations.

It is once more seen that better heat transfer comes on the cost of higher pressure drop. If a higher pressure drop is affordable, several other methods in both design and operation can used to enhance heat transfer. For example, using smaller diameter pipes or simply increasing the flow rate will both increase overall heat transfer on the cost of pressure drop, are more viable solutions than shifting the oscillation period as demonstrated here.
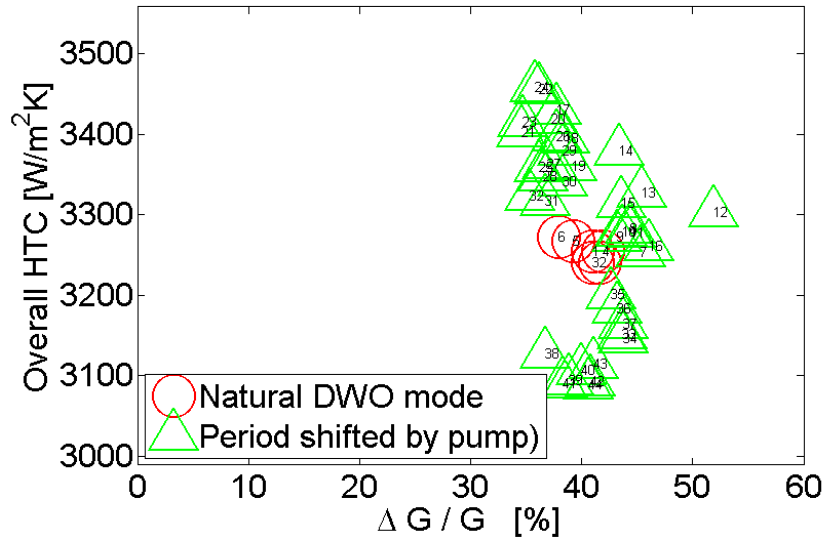
Figure 5.16 Overall HTC – ΔG/G. The effect of period is effectively isolated form amplitude.

Once again, the purpose was to maintain constant amplitude of about 40 % to so that the effect of period is isolated. The plot above is included to show that the amplitude of experimental data set is sound, though not perfect.

5.9   Closing words on the pre-work

This chapter has comprised evaluation of the effect of different parameters and how configuration of the experimental facility has influence in the DWO-mode. It may be regarded as extensive but the aim was to address a weak point in many research papers that mostly focus on presenting the results. This reflects the numerous considerations that must be taken when carrying out experimental work. This lays the fundament to prepare the main experiments which will be presented in the next chapter. Being able to set up and perform experiments showing the change in heat transfer upon occurrence of DWO may be regarded as a result in itself.

6 Results

This chapter provides an overview of the main experimental results. The experimental program will show that both flow rate and heat controlled experiments are viable solutions in investigation of the pressure loss and heat transfer characteristics of DWO.
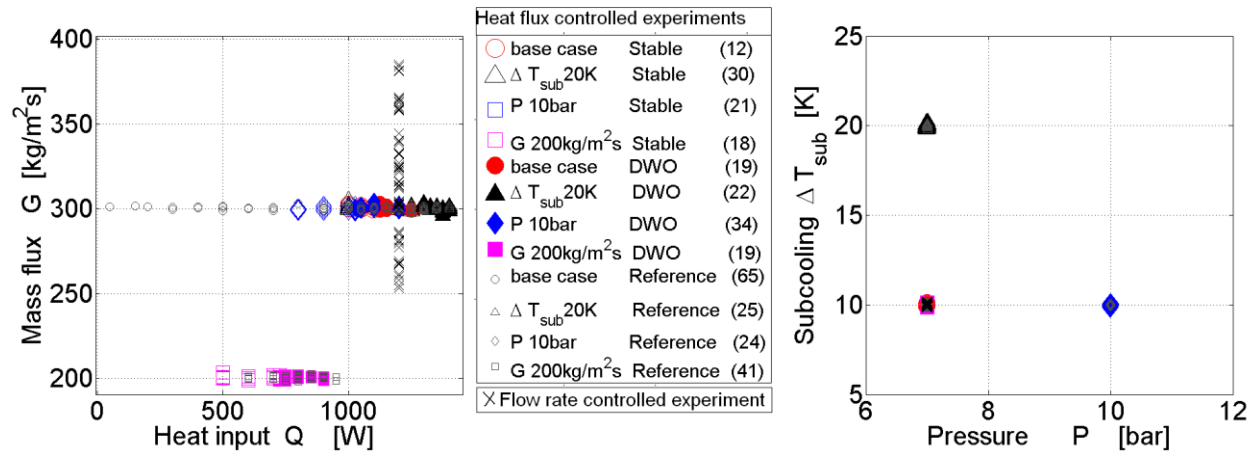
Figure 6.1 Experimental matrix

A figure briefly presenting the experimental matrix is included above. The purpose is to provide a rough overview over the main experimental program, not to spot out every single point. Numbers of experimental data points are quoted in parenthesis. In total 332 experiments (500 seconds each) were logged in the four cases of the heat flux controlled experimental series, while 106 data points where gathered for the flow rate controlled experimental series. Number of data points are indicated in parenthesis in the legend above. Good accuracy was obtained in fixing the inlet subcooling and pressure to their predetermined conditions.

Performing heat controlled experiments was the most successful. Thus, the heat controlled experimental series were repeated for an alternative flow rate, pressure and inlet subcooling to explore the effect of modifying those main system parameters.

6.1 Flow rate controlled experiment

The idea behind this experimental series is to plot the classic heat transfer coefficient versus Reynolds and pressure drop versus Reynolds (Moody equivalent). The flow rate controlled experiment resembles a heat exchanger having a constant heat duty while flow rate diminish until

reaching its thermal limit. An example could be a nuclear reactor experiencing low primary loop circulation in a loss of coolant accident.

Experiments were conducted with stepwise progression in system flow rate while maintaining a constant inlet pressure (P= 7 bars), inlet temperature (ΔT_{sub}= 10 K) and heat input (Q= 1200 W/ q"= 38.1kW/m^2).

Experiments were started at a modest flow rate with inlet restriction, exit orifice, and with pump bypass three turns open. This configuration is recognized by circular data points. Reduction in flow rate causes the flow to change from stable (black) to unstable DWO (red).

A second set of experiments was conducted in the same manner, but this time without restrictions and with almost closed pump bypass rendering the system stable at all practical flow rates. This stable reference case is identified by blue diamonds.

6.1.1 Heat transfer coefficient
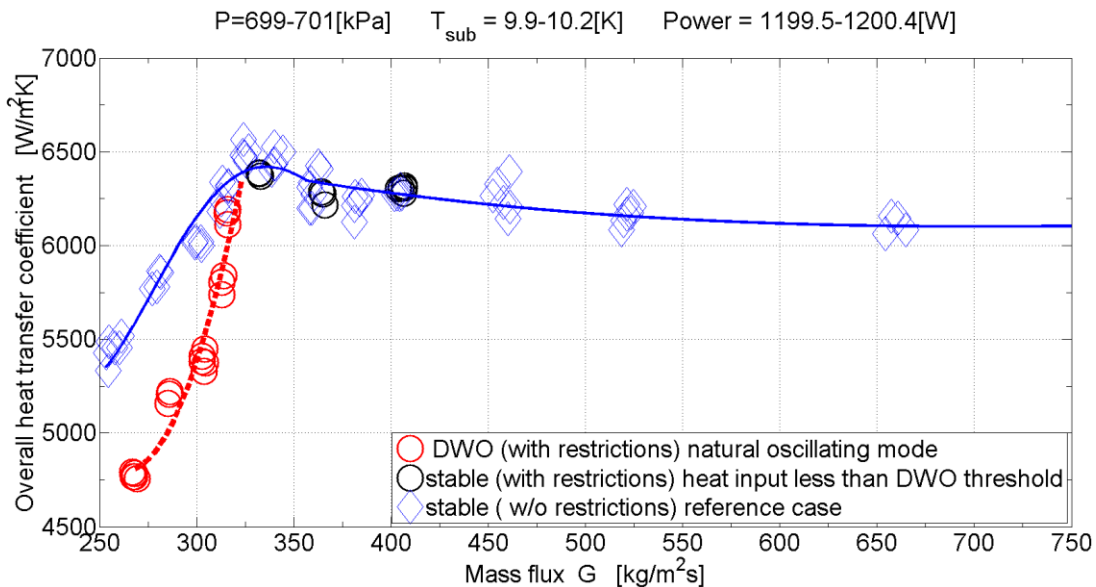
Figure 6.2 Overall HTC – Mass flux: Flow rate controlled experiment: P=7bar ΔT_{sub}=10K q"=38.1kW/m^2

The red line shows occurrence of an abrupt drop in heat transfer performance at the onset of DWO. The conditional stable (black dashed line extending the red) and stable (blue line) show similar heat transfer characteristics regardless of valve configuration. High flow rate cases, far out of the DWO, range was therefore only performed with the restriction-less (blue) configuration. Overall heat transfer is suddenly decreasing when moving into the region of lowest

flow rate. In this condition is exit vapor quality approaching unity, or even superheating. A minimum flow rate limit was encountered due to excessive temperatures close to the outlet of the heated section. Notice that overall heat transfer is almost independent of flow rate in the region of flow rate above 350 kg/m^{2}s. This confirms that nucleate boiling is the governing heat transfer mechanism, not forced convection in which the heat transfer coefficient is a function of flow rate.

A maximum flow rate limit was posed by the pump volumetric capacity at maximum allowable drive speed. For better visibility, the result can be plotted as a log-log plot of overall heat transfer coefficient and inlet Reynolds number.
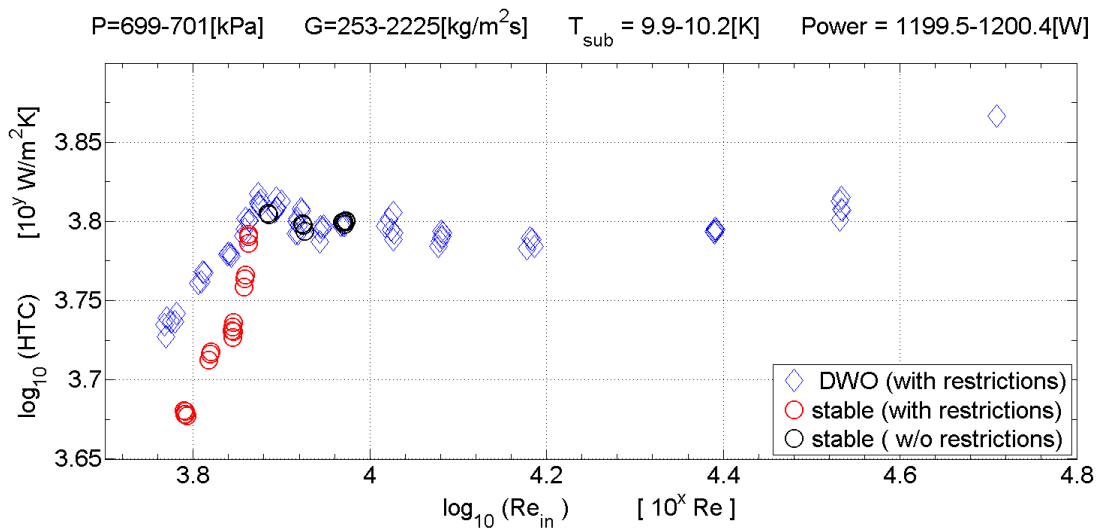
Figure 6.3 Overall HTC – Inlet Reynolds (log-log). Flow rate controlled experiment: P=7bar ΔT$_{sub}$=10K q"=38.1kW/m^2

Overall heat transfer coefficient is logarithmically plotted against the Reynold number. Experiments with the reference case were extended all the way to 2200 kg/m^{2}s (upper right data point). This is not a condition relevant to the DWO phenomenon; it was rather done to provide a broader perspective on heat transfer performance.

It is well worth noticing that triggering of DWO not necessarily is the only cause of heat transfer deterioration. The stable case does also suffer from reduced heat transfer when flow rates drop below a certain value.

6.1.2 Pressure loss
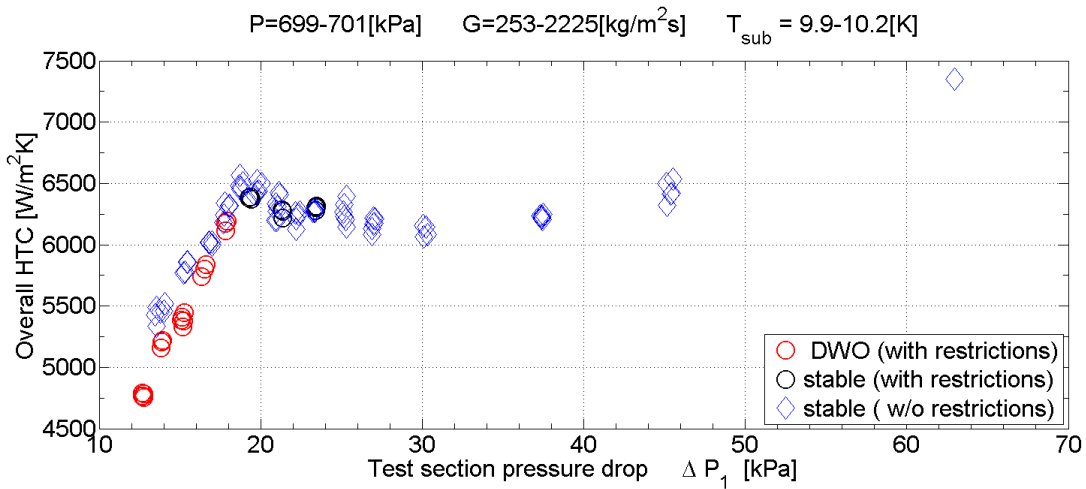
Figure 6.4 Overall HTC – Pressure drop. Flow rate controlled experiment: P=7bar ΔTsub=10K q"=38.1kW/m²

Figure 6.4 shows the relation between heat transfer and pressure loss over the length of the heated section. Optimum heat transfer performance per pressure loss is achieved close to the inception of DWO. An interesting feature, but designing an application for operation in this region might be risky. Occurrence of DWO seems to be undesirable as the heat transfer shows poorer characteristics than the stable reference case.
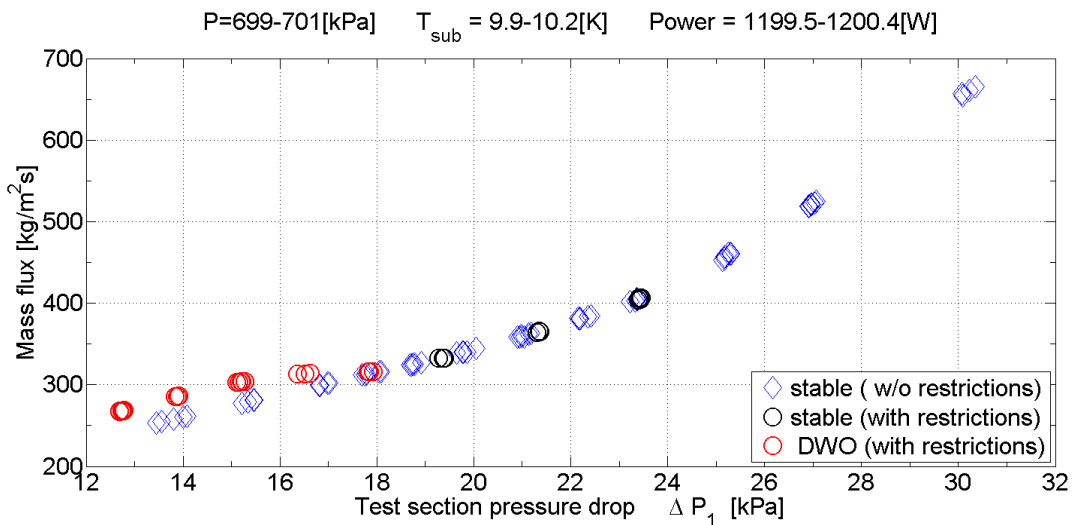
Figure 6.5 Mass flux – Pressure drop. Flow rate controlled experiment: P=7bar ΔT$_{sub}$=10K q"=38.1kW/m²

Flow rate is plotted against pressure drop shows a characteristic curve of the heated section. The two stable modes are precisely matching each other regardless of the difference in valve configuration. This is as expected as the pressure drop is measured in between, not over, inlet and

85

exit restrictions. It confirms that the internal characteristics of a stable system are independent of configuration. An interesting and vital finding is the fact that experiments featuring density wave oscillations have lower pressure losses than the stable equal flow rate counterpart.

6.1.3 Closing words

Doing flow rate controlled experiments is a viable solution for exploring the influence of DWO in pressure drop and heat transfer characteristics. However, disperse in flow rate makes the plots look a bit messy.

Another scenario, likely to happen in real applications, and suitable in an experimental study, is a heat exchanger transferring an increasing amount of heat until reaching its critical heat transfer limit. Giving origin to the heat controlled experiment.

6.2 Heat controlled experiment

The heat controlled approach for investigating transitions in boiling heat transfer characteristics is inspired by the classical experiment of Nukiyama [2] exploring film boiling. It is also a way to clarify the maximum tolerable heat load of a cooling system or heat exchanger with given specifications in terms of geometry and fluid condition.

In total 332 experiments of 500 second each were measured. The experimental matrix consists of four cases and results will be arranged in the following order:

1) *Base case* ($300\text{kg/m}^2\text{s}$, 7 bar, 10 K)
2) increased *subcooling* ($\Delta T_{sub} = 20$ K)
3) increased *pressure* (P = 10 bar)
4) reduced *flow rate* (G = 200 $\text{kg/m}^2\text{s}$)

Experiments were conducted in three different modes giving four distinctive types of results, in which two are stable while the other two includes oscillations.

   a) Experiments were first performed with inlet restriction, exit orifice, and with partially bypassed pump to allocate the DWO and its point of inception. Experiments in this mode were labelled with circles, colored black for a stable system, and red when DWO are occurring.

b) The second mode is the stable reference case, labelled with blue diamonds. This was obtained by opening the inlet valve, allowing flow to freely exit past the exit orifice, and almost closing the pump bypass valve, rendering the system unconditionally stable.

c) In the third mode, labelled with green squares, the flow rate was oscillated by external means. That is, oscillations in flow were induced by the variable pump drive. The purpose is to mimic DWO.

A series of experiments was conducted at a higher degree of subcooling than the base case. The effect of subcooling on various oscillation features has been debated in the literature on DWO. Previous work by the author done in the NTNU experimental facility has indicated that increased degree of inlet subcooling yields, higher heat input of DWO inception. There is a caveat though, when oscillations do occur they tend to be more violent. Another feature of high inlet subcooling is a longer DWO period, this is commonly associated with the increase in boiling channel transit time caused by an elongated single phase region.

6.2.1 Overall heat transfer coefficient, base case introduction
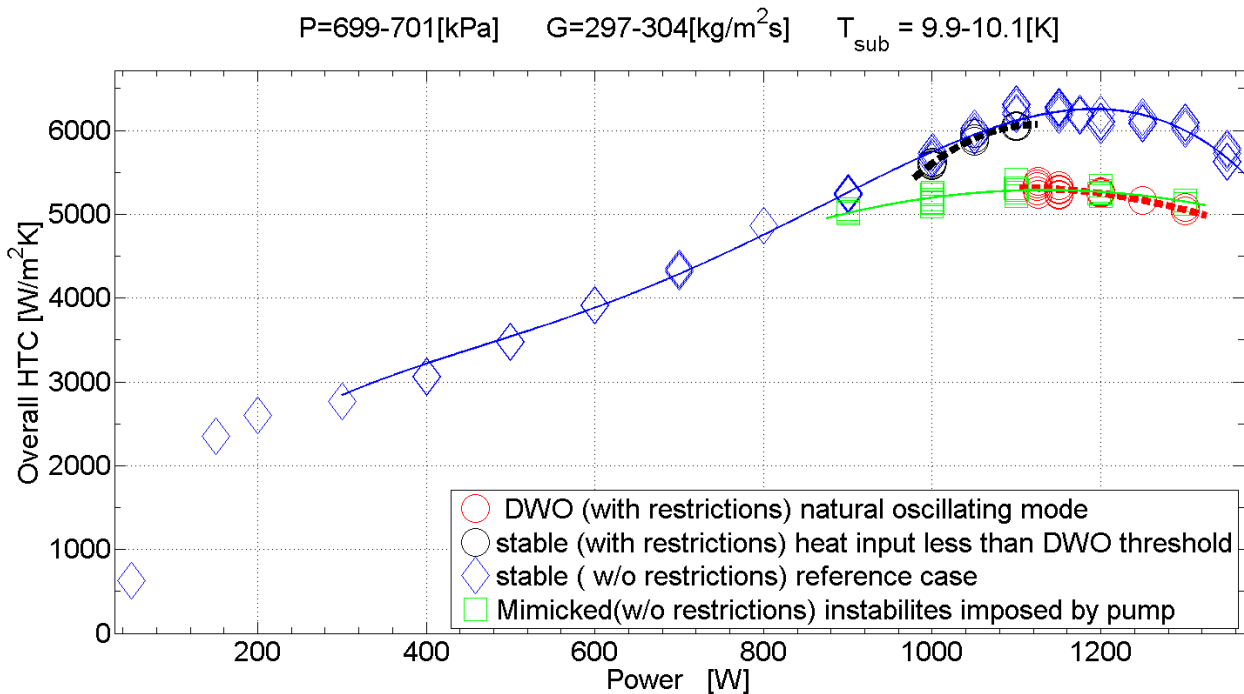
Figure 6.6 Overall HTC – Power (full range). Heat controlled experiment, base case.

Figure 6.6 shows how the overall heat transfer is changing on heat input for the different experimental modes. The big picture is that heat transfer increases with increasing heat flux. This is a well-known feature of nucleate boiling.

The overall heat transfer coefficient is greater for the stable cases (black and blue) than the cases with flow oscillations. If one increases the heat flux, following the black dashed line from left to right, heat transfer is increasing, until the inception of DWO. Heat transfer drops instantly a leap down when DWO starts, see the red dashed line. The stable system, configured without flow restrictions, reaches a maximum and loses heat transfer performance more graduate afterwards.

6.2.2 Overall heat transfer coefficient, all cases

The next four plots will provide a closer view of the overall heat transfer coefficient in proximity of inception of DWO in four different cases. The heat transfer coefficient is determined from the bottom row of thermocouples as described in the methods chapters. The four cases are; the base case, higher subcooling, higher pressure, and lower flow rate. Again, the maximum experimental power was upwards limited by test section temperature constraints.
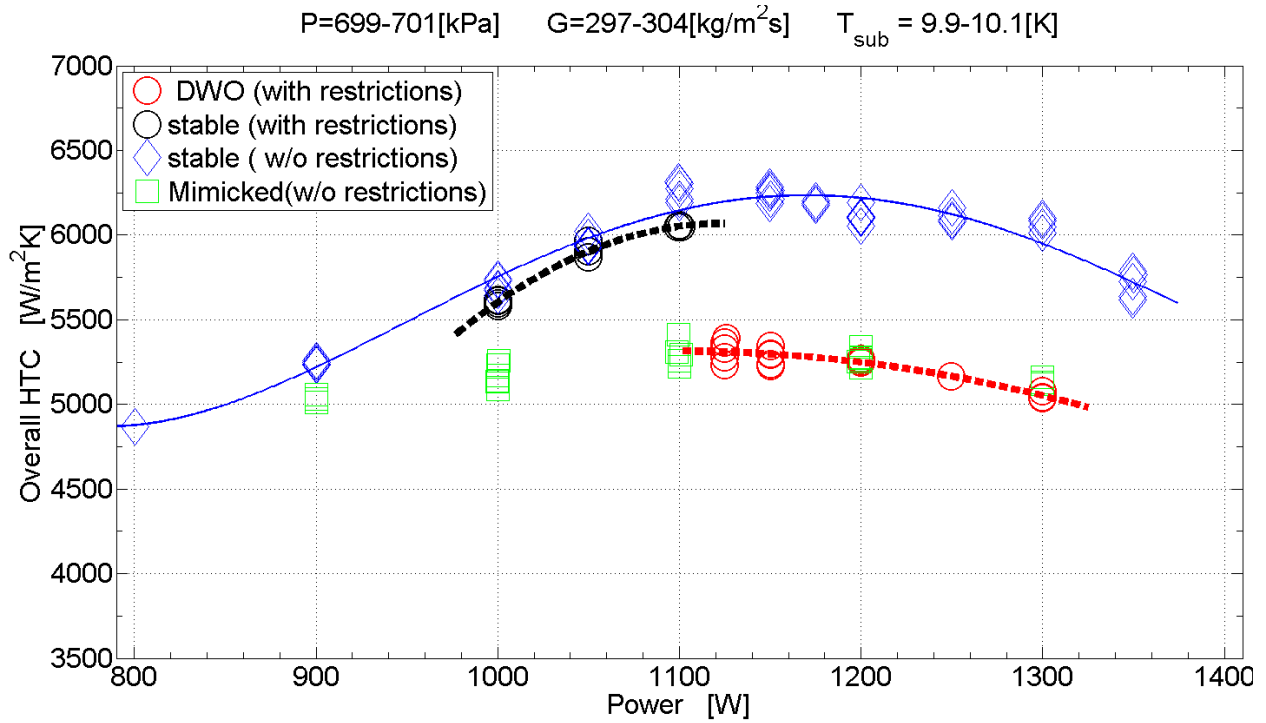
Figure 6.7 Overall HTC – Power. Heat controlled experiment, base case (G=300kg/m^{2}s P=7bar ΔT$_{sub}$=10K)
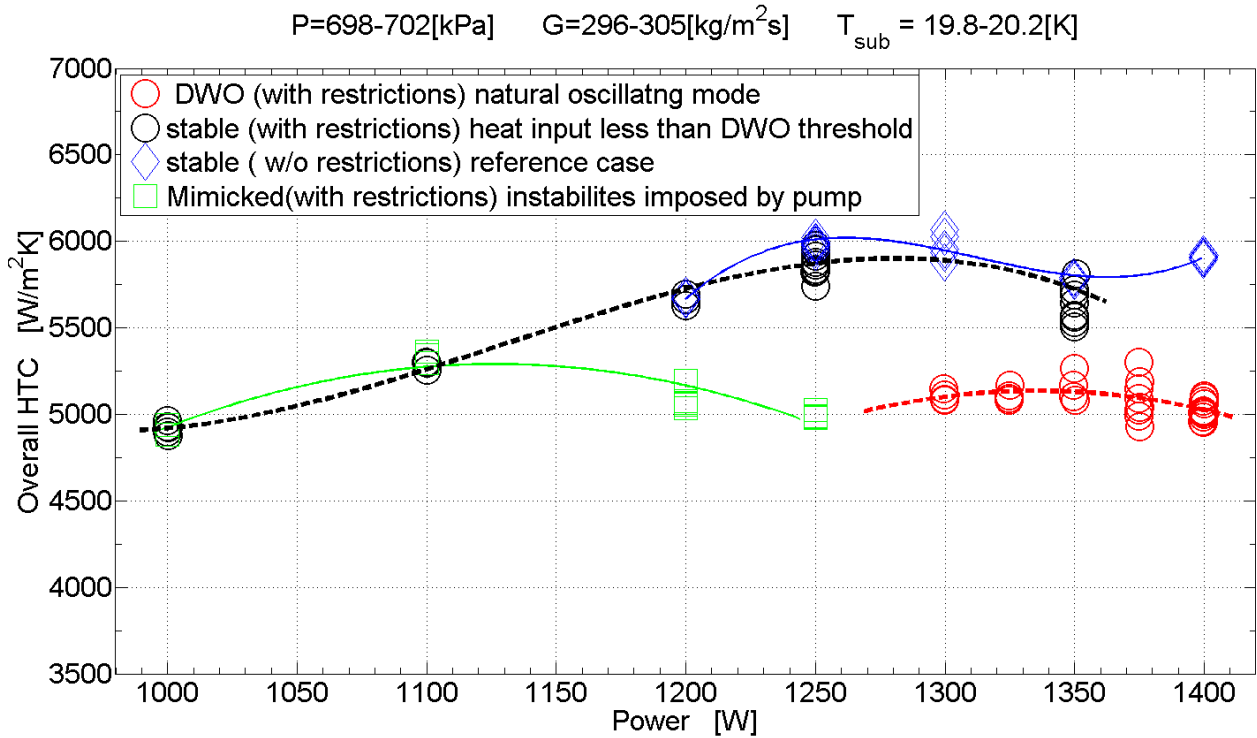
Figure 6.8 Overall HTC – Power. Heat controlled experiment, high subcooling (G=300kg/m^{2}s P=7bar ΔT$_{sub}$=20K)
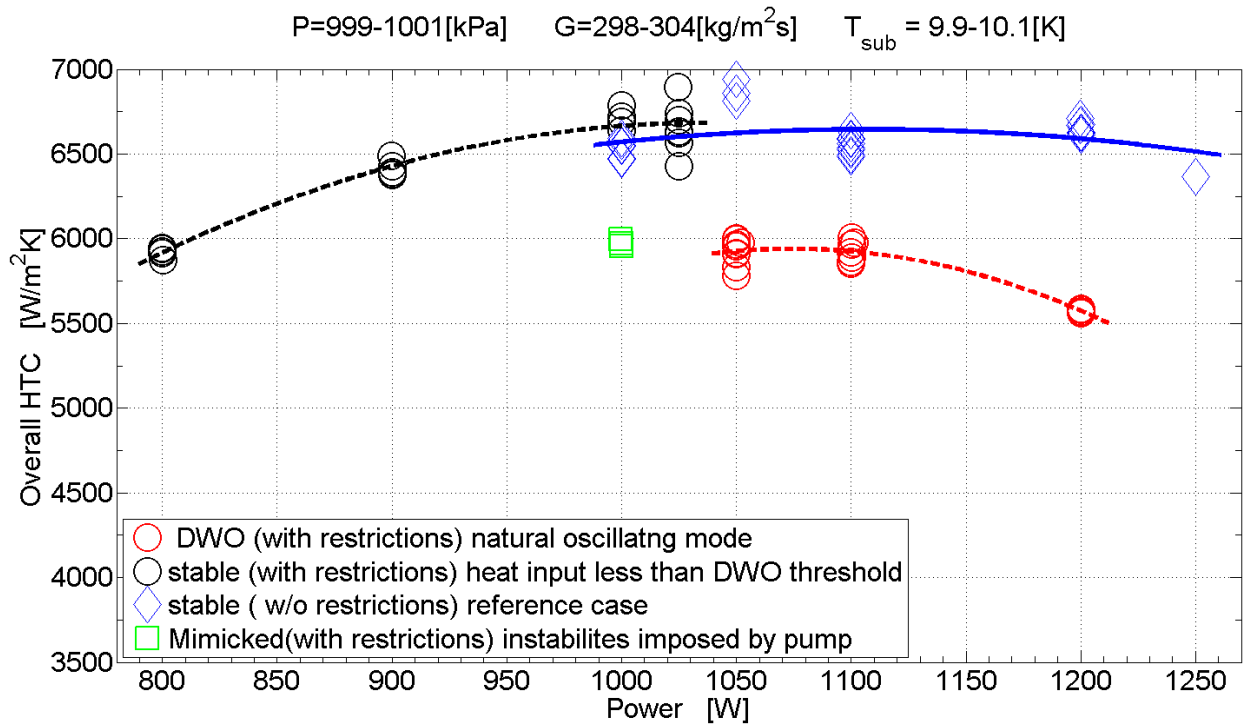
Figure 6.9 Overall HTC – Power. Heat controlled experiment, high pressure (G=300kg/m^{2}s P=10bar ΔT$_{sub}$=10K)

Figure 6.10 Overall HTC – Power. Heat controlled experiment, low flow rate (G=200kg/m^{2}s P=7bar ΔT$_{sub}$=10K)

The overall heat transfer coefficient in the stable system configured with restrictions (blue) is fairly consistent with the stable system without restrictions (black). In the configuration with restrictions, heat transfer drops instantly a leap down at the heat flux where DWO commences. This is seen as a discontinuity between the black and the red dashed lines, where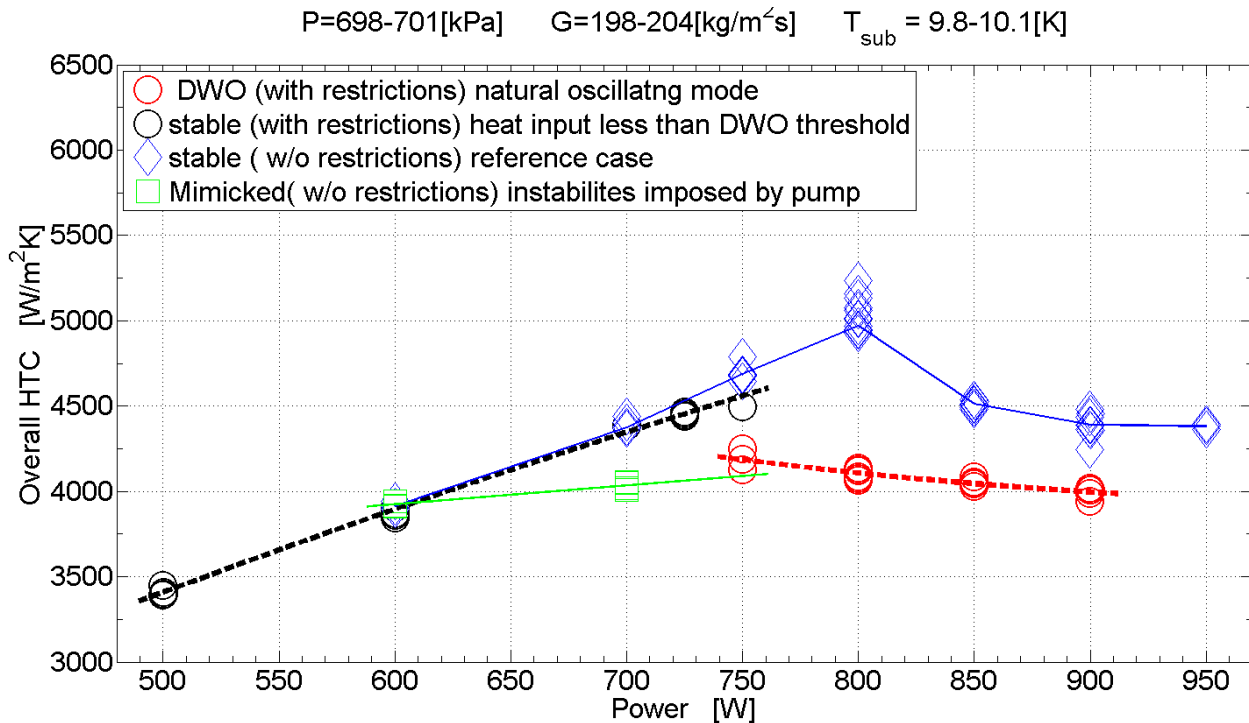 transition from black to red indicates the onset of DWO. The overall heat transfer is immediately dropping with roughly 10 % at the onset of DWO. The exit vapor fraction is high, or approaching one, in this region. High exit quality in a system with flow restrictions is commonly regarded as main criteria for the occurrence of DWO. This sudden depreciation in overall heat transfer is avoidable by opening the in- and outlet restrictions, as plotted with blue diamonds.

The stable system maintain its high overall heat transfer coefficient better, but it does also suffer from loss in heat transfer when exceeding the DWO threshold heat flux, although it stays stable as a matter of its restriction-less configuration. At this large heat fluxes, saturated or even superheated vapor, is exiting the heated section.

Experiments were also performed with flow oscillations induced by the pump by cycling its drive speed. For these mimicked flow instabilities (green squares), three observations are made:

1) High heat flux: Figure 6.7 shows that mimicked instabilities match the natural occurring DWO-mode in terms of heat transfer. This partly serves as a proof of concept.

2) Low heat flux: It is possible to show how flow oscillations can influence heat transfer though heat input too low for self-sustained DWO to persist. Making a comparison between the stable (black/blue) and mimicked (green squares) is indeed interesting since both has the same configuration (in and outlet restrictions) and same operational conditions (inlet pressure, inlet temperature, heat input and mean flow rate), but still different heat transfer characteristics. When instabilities are mimicked at heat flux a little below DWO threshold limit, heat transfer is significantly lower than the stable counterpart.

3) Lower heat flux: The difference in overall heat transfer between stable and mimicked is diminishing as heat flux is further reduced. A system operating under these conditions will likely not be prone to boiling instabilities anyway.

Some disperse is seen in the experimental data, in particular in the circular red points representing naturally occurring flow oscillations (DWO). This is common, even though logging is done for a full 500 seconds for each and every point in the figure.

6.2.3 Amplitude of oscillation

Two plots in Figure 6.11 shows the interrelationship between overall heat transfer and amplitude are plotted below. Results are somewhat inconclusive, but the experimental data was not gathered for this particular plot either.
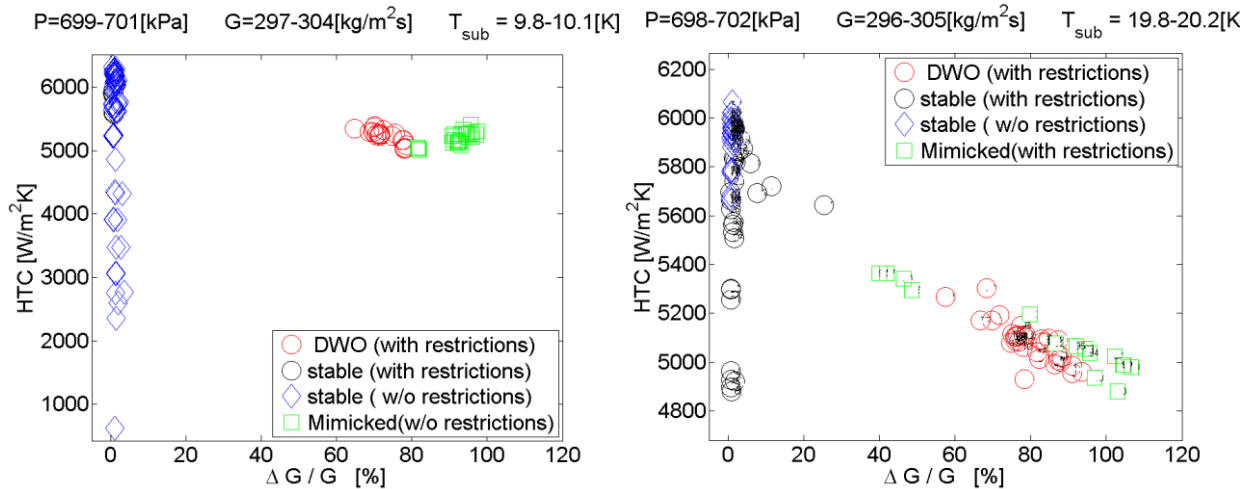
Figure 6.11 Overall HTC – Normalized flow amplitude (base case and high subcooling)

Two different trends are obseved. In the left base case figure, overall heat transfer do not show dependency on the amplitude. This is in contrast to the right high subcooling figure where the overall heat trabsfer coeffient is decreasing on increasing oscillation amplutude. The heat flux defecy on amplitude is well aligned for both real DWO and mimicked oscillations, and corresponds pefectly with the findings in the pre-work.

6.2.4 HTC in-depth analysis (base case)

Data in the two plots to come is the average of several experiments with same configuration and resemble typically an average of 2500-4000 seconds of logging. Inlet conditions and valve configuration are equal. A local heat transfer is plotted against test section length for various heat input values. The heat transfer coefficient is based on the bottom row of thermocouples for inner wall temperature and equilibrium mixed flow model for fluid temperature.
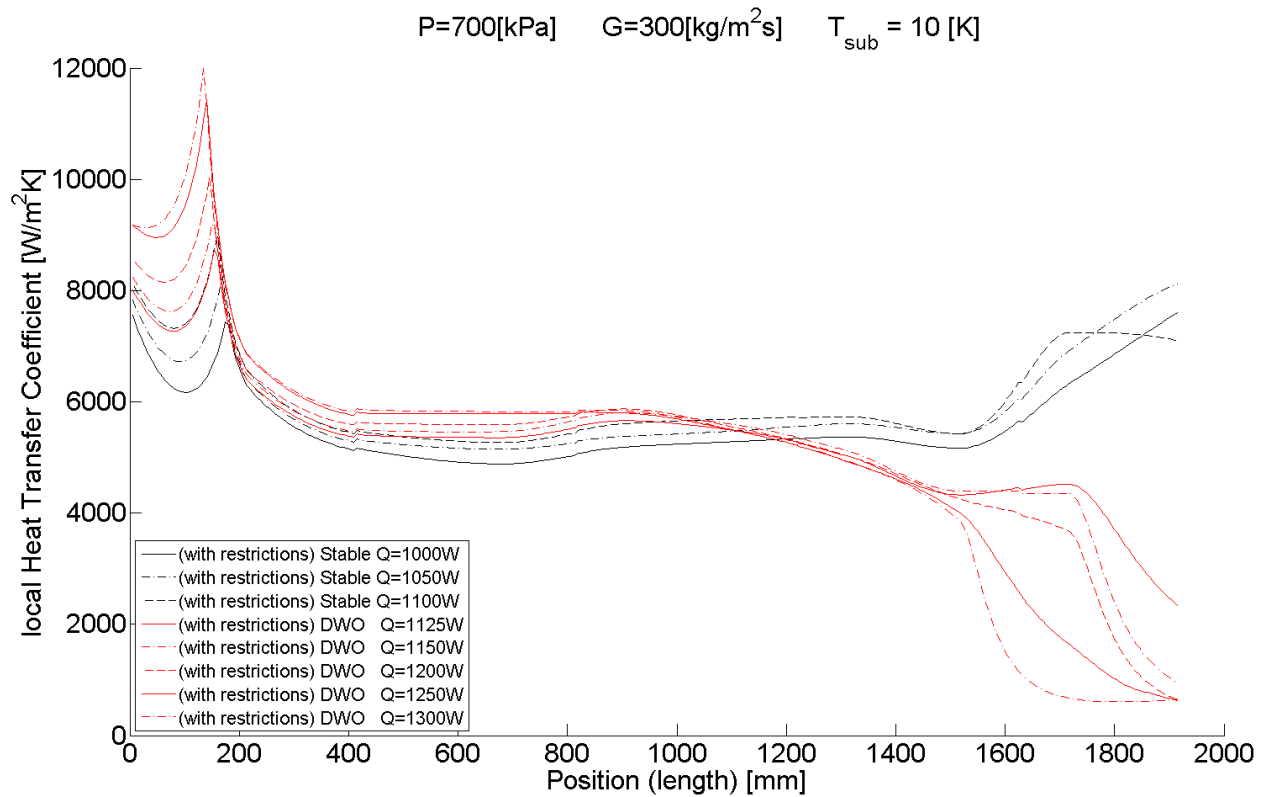
Figure 6.12 local heat transfer coefficient (DWO/stable) - test section length. (G=300kg/m²s P=7bar ΔT$_{sub}$=10K)

The lengthwise heat transfer coefficient plot (Figure 6.13) shows how increasing the heat flux influences heat transfer. In the first half (left) of the tube is the heat transfer coefficient improving on increased heat flux. This is a characteristic of local surface boiling. In the later half (right) shows somewhat different trend. A sudden drop in heat transfer is seen when the heat flux is increased past the DWO threshold limit. The stable (black) and oscillating (red) lines can clearly be distinguished by this fact. The cause is dry out of the tube wall in the last 10-20 cm of tube wall. The dryout seems to be triggered by DWO, since the stable cases below the DWO threshold heat flux shows a distinctive different trend from the higher heat flux DWO-cases. A dryout of heat transfer surfaces explains why the DWO experiments were achieving lower overall heat transfer in the previous section. The next plot shows tube wall temperature making the dryout becoming more evident. Three extra experiments of restriction less stable configuration were added as a benchmark.
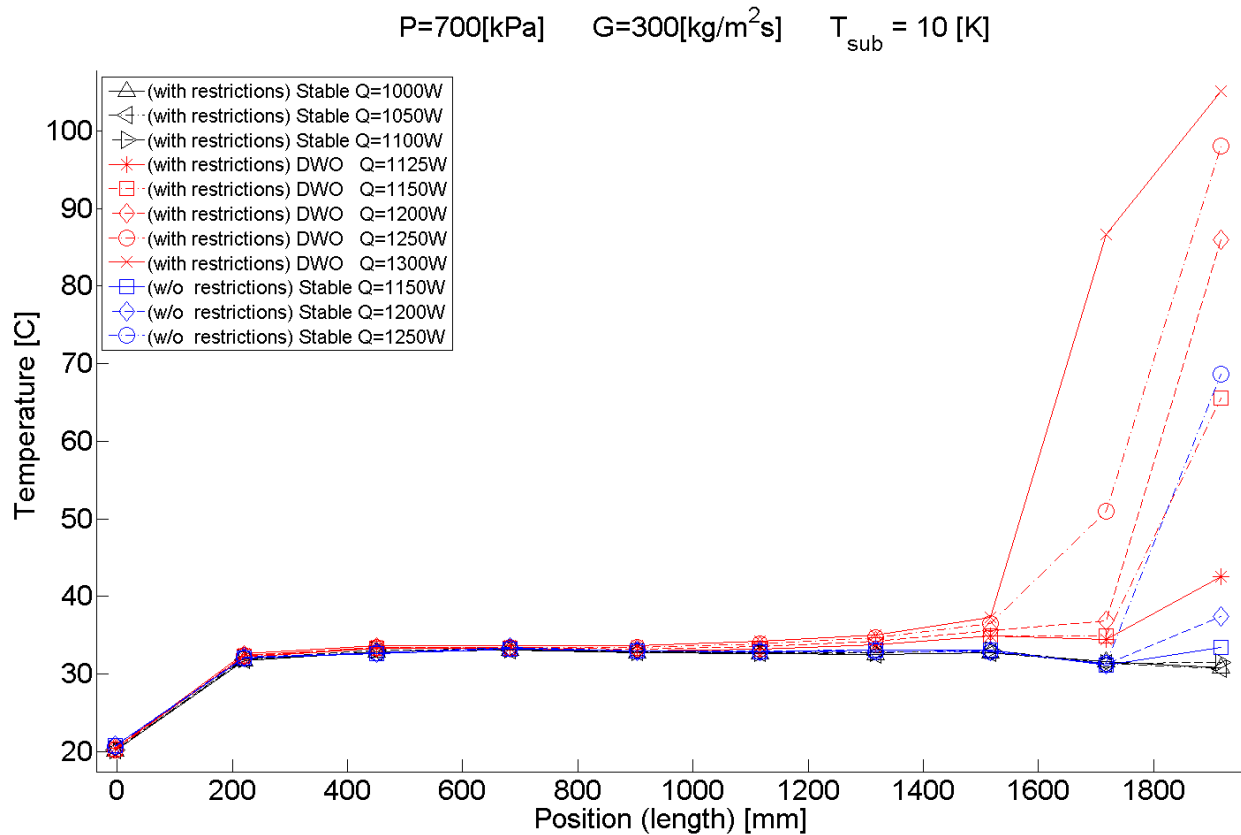
Figure 6.13 Inner wall temperature (DWO/stable) - test section length. (G=300kg/m²s P=7bar ΔT_sub=10K)

Plotting the temperature profile shows excessive wall temperatures caused by surface dryout close to the test section outlet. Examine the legend of Figure 6.13 to see that experiments of same heat input have same labels (square, diamond and circle for 1150 W, 1200 W and 1250 W respectively). Dryout close to the test section outlet is not seen in the stable (black) cases, but when heat input exceeds 1100 W and oscillations commences (red), the exit temperature starts to rise rapidly on further increase in heat input. The restriction-less case (blue) is plotted as a reference to see how the temperature profile develops in corresponding, but stable, case. It is observed from the blue lines and the legend that a dry out situation is encountered at 1250 W approximately. In other words, the stable configuration can handle roughly 10 % higher heat flux than the configuration susceptible for DWO, if the upper limit of operation is defined by the CHF.

6.2.5 HTC detailed analysis (DWO vs Stable in depth)

During the course of experiments unexpected but interesting data was gathered in the high subcooling case at 1350W (Figure 6.8). DWO was expected to be present at this power level in a

94

system with restrictions; still, several stable points were in fact logged. Experiments with the same conditions was repeated another day to confirm this abnormal result.

The experimental data achieved at Q=1350 W, P=7 bar, G=300kg/m^{2}s and ΔT_{sub}=20 K will now be further examined to see the difference between the heat transfer in a stable (non-oscillating) and unstable (DWO) flows. Notice that all four conditions (power, pressure, mass flux and inlet temperature) are fixed.
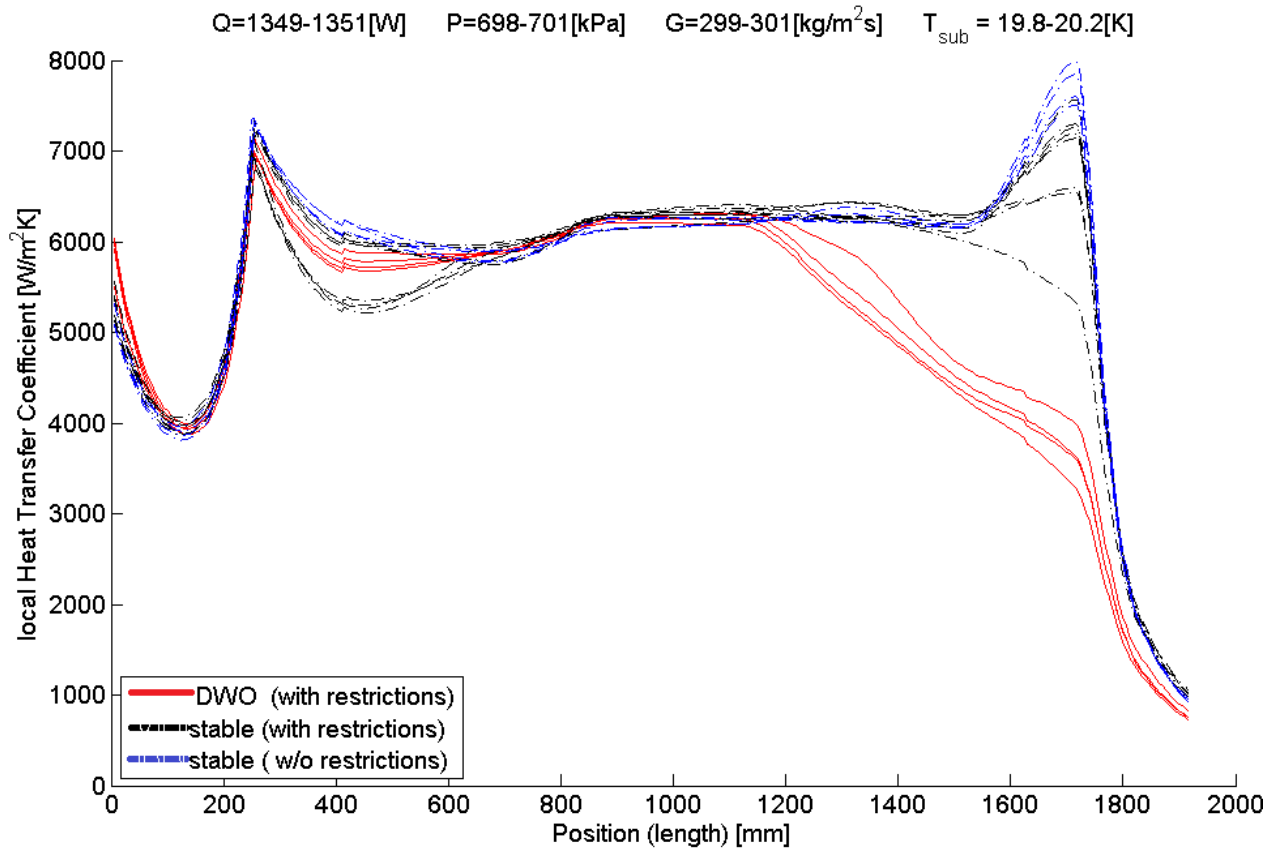
Figure 6.14 local HTC (DWO/Stable) - test section length. (G=300kg/m^{2}s P=7bar ΔT_{sub}=20K, q''=42.2kW/m^2)

Figure 6.14 shows the local heat transfer coefficient plotted over the length of the test section. The heat transfer coefficient is based on bottom side row thermocouples and fluid bulk temperature estimated by equilibrium model as described in section 4.6.2. One can immediately notice that the difference in heat transfer between the unstable (DWO, red) and stable flow (blue and black). A clear deficit is found around the boundary at which evaporation is overtaken by the bulk superheating. To better understand what lies behind this, another showing the actual temperatures is later plotted (Figure 6.16).

The reason why some of the black lines differ somewhat from the blue is that the experiments had some short oscillating transits in the flow.
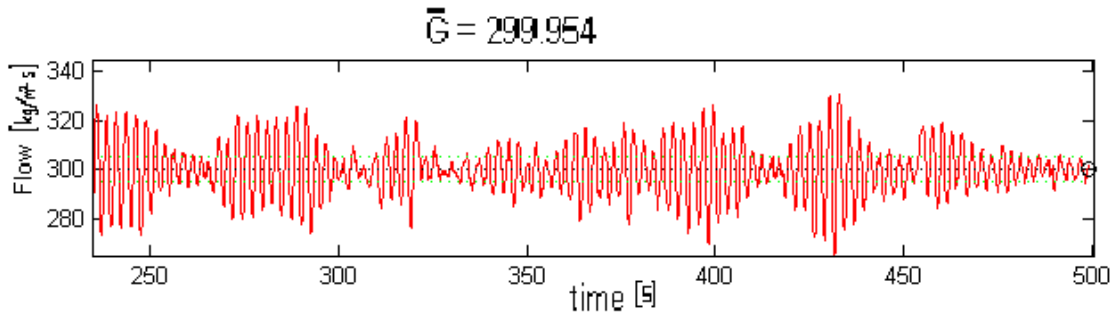
Figure 6.15 flow trace – time (example of weak unsteady oscillations)

Example of weak oscillations, notice the resolution of the y-axis. These oscillations are so weak that the might be called ripples, though they have a propensity for fixed period.
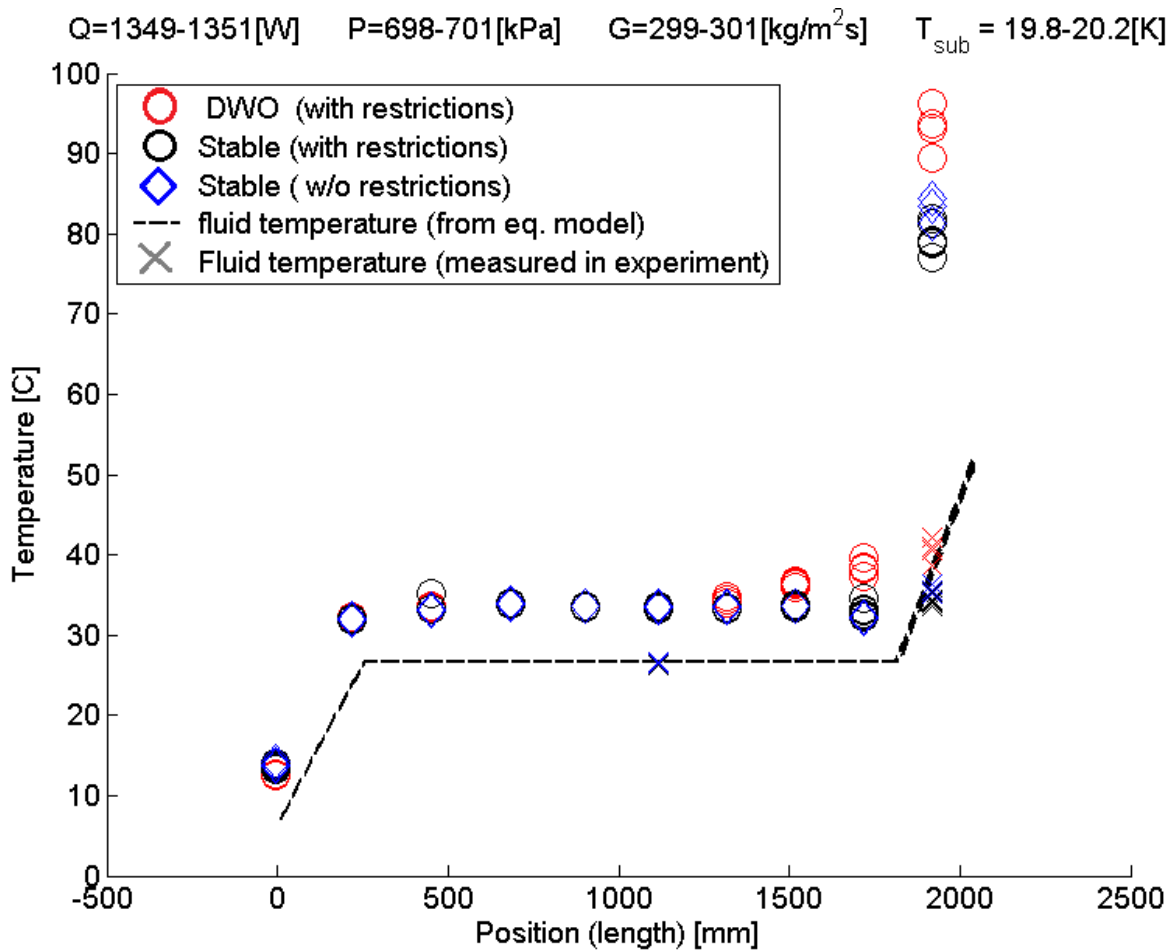
Figure 6.16 Inner wall temperature (DWO/Stable)- test section length. (G=300kg/m²s P=7bar ΔT$_{sub}$=20K q"=42.2kW/m²)

The previous figure shows the inner wall temperature, computed fluid temperature and measured fluid temperature. Heat input, pressure, flow rate and inlet subcooling are fixed in this plot.

It is observed that DWO co-occurs with movement of the dryout boundary upstream the test section. This is contributing to lower overall heat transfer performance previously observed.

The computed fluid temperature is fairly consistent with the measured, verifying the equilibrium mixed flow model introduced in the methods chapter (section 4.6.2). As a side note; the fluid temperature measured with the in-tube thermocouple at position 10 indicates that the measured fluid temperature also is higher when operating with DWO. An explanation could be stronger radiant heat transfer from hot tube walls influencing the result.

6.2.6 HTC detailed analysis (Mimicked vs Stable in depth)

This section will compare experiments of equal conditions (Q=1250 W, P=7.00 bar, 300 kg/m^{2}s and ΔT_{sub}=20 K) with different configurations. These are stable with and without restrictions and instabilities superimposed on stable flow by the pump variable drive. The two former as comparable average heat transfer while the mimicked has somewhat lower length averaged heat transfer coefficient. The conditions are in the stable region in terms of DWO, thus instabilities had to be imposed.
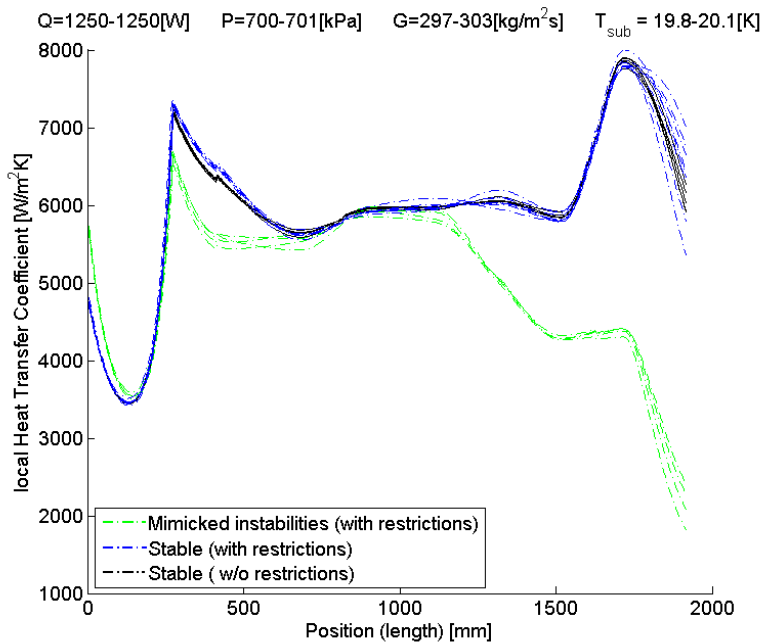
Figure 6.17 local HTC (Mimicked/Stable) - length. (G=300kg/m^{2}s P=7bar ΔT_{sub}=20K q"=39.1kW/m^2)

It can be seen from Figure 6.17 that the deficit in heat transfer in mimicked instabilities is mostly downstream part of the heated channel, similar to the situation of real DWO oscillations. Figure 6.17 also serves the purpose of visualize the overall heat transfer as computed prior to length averaging.
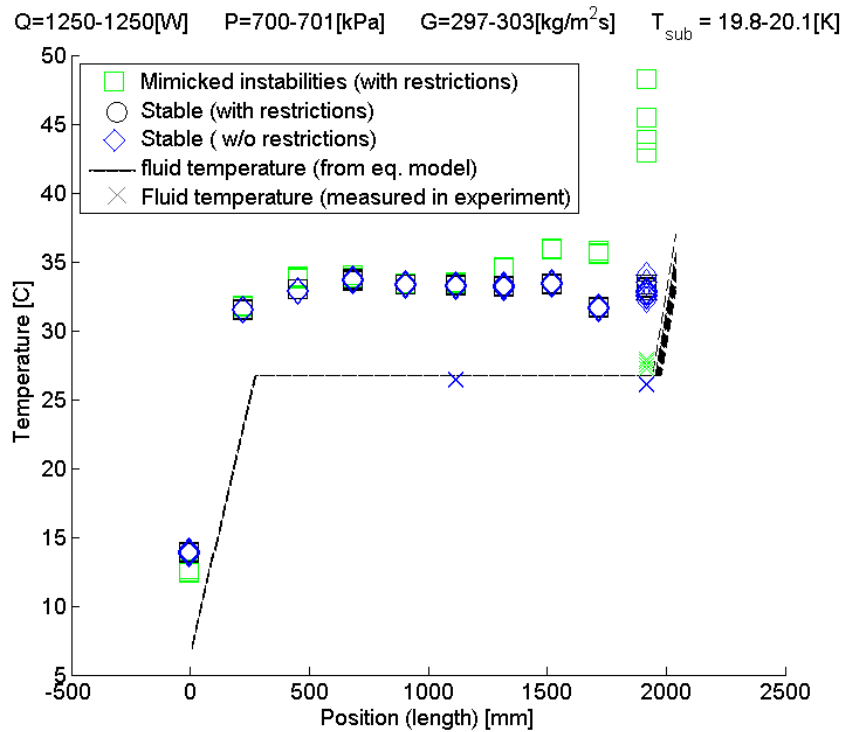
Figure 6.18 Inner wall temperature (Mimicked/Stable) – length. (G=300kg/m²s P=7bar ΔT$_{sub}$=20K q"=39.1kW/m²)

The figure above shows how flow instabilities triggers a dryout of the hot tube walls close to the heated section exit. The consequence is collapse of the heat transfer performance in this particular region. So far, it seems like both artificial induced oscillations and natural density wave oscillations have adverse effects on the critical heat flux limit of the system.

6.2.7 HTC detailed analysis (Top versus bottom temperatures)

Large differences in wall temperature between bottom and top of the heated tube are reported in previous experimental studies. This is likely caused by vapor voids gathering in the upper parts of the horizontal channel. Experiments with lowest flow rate are believed to be most exposed to such flow stratifications. A clarification is needed since the overall heat transfer coefficient quoted in this thesis solely relies on bottom wall temperature.

98
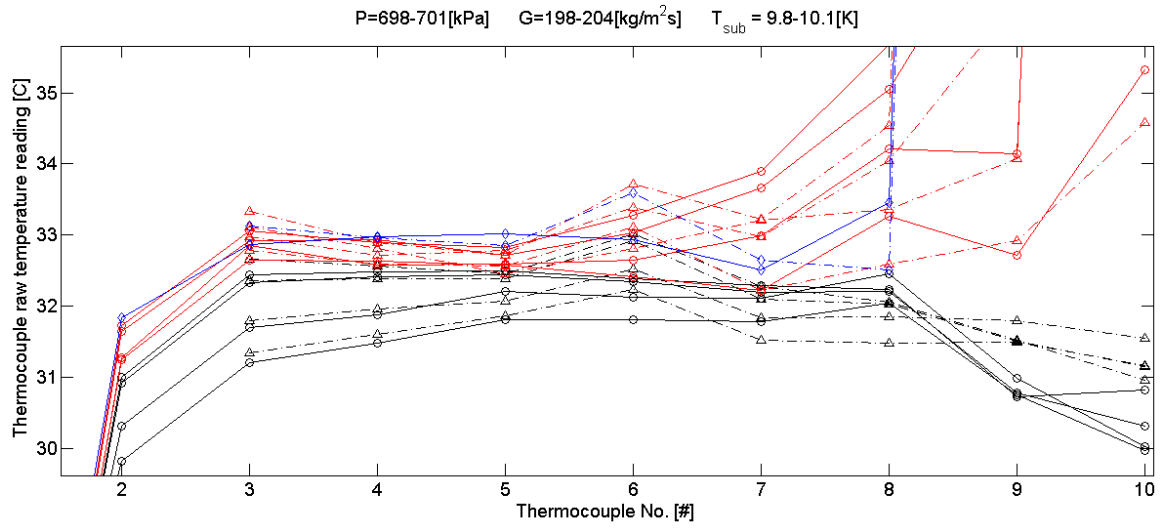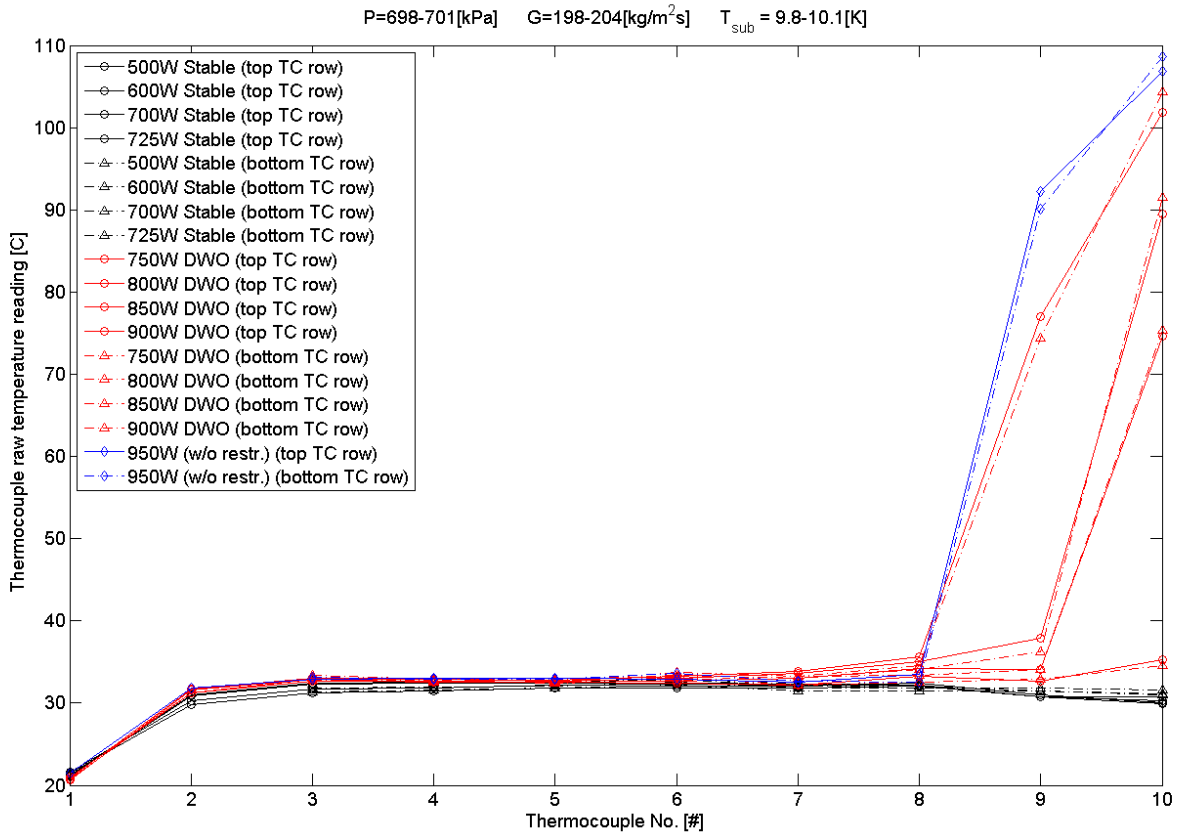
Figure 6.19 Top and bottom temperature compared (G=200kg/m^{2}s P=7bar ΔT$_{sub}$=10K)

Top and bottom wall temperature is fairly consistent along the length of the tube. No real signs of flow stratifications are seen in the experimental data. The second figure shows a zoom in on the

evaporation region. The wall temperature is usually very close to the temperature of the fluid under evaporation, so the heat transfer coefficient is very sensitive to variations in temperature measurement. Position 1 and 2 on the heated section are only equipped with thermocouples on bottom, therefore was the bottom row of thermocouples chosen for measurement of the overall heat transfer.

6.3 Local heat transfer coefficient

The local heat transfer coefficient is determined from heat flux, the wall temperature, and the measured fluid temperature. This is in contrast to the previous presented results where fluid temperature was calculated form a model and evaluated over the full length of the heated section. Internal thermocouples for in-fluid direct temperature measurement are only available on two locations, namely position 6 (1117 mm) and 10 (1917mm) (See Figure 3.2). The wall temperature is determined from an average of the four thermocouples surrounding stainless steel tube at the two mentioned locations.

The four cases will again be consecutively presented in the following order; base case, high subcooling, high pressure and reduced flow rate.

6.3.1 Local heat transfer coefficient, saturated region

The local heat transfer coefficient is measured 1117 mm from the test section inlet. For the range of parameters in the present experimental study is this location within the evaporation region. The region is characterized by two phase flow where the fluid is boiling at a nearly uniform temperature.
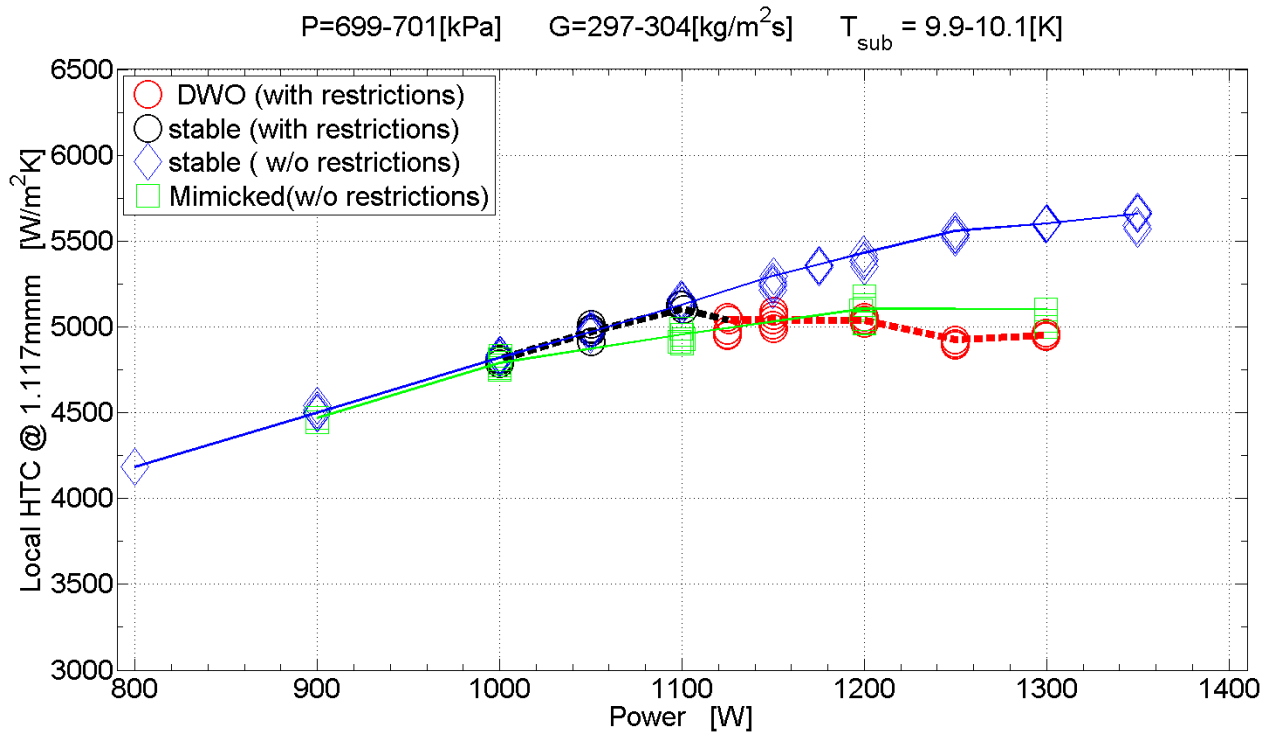
Figure 6.20 Local HTC (z = 1.117mm) – Power controlled, base case (G=300kg/m^{2}s P=7bar ΔT$_{sub}$=10K)
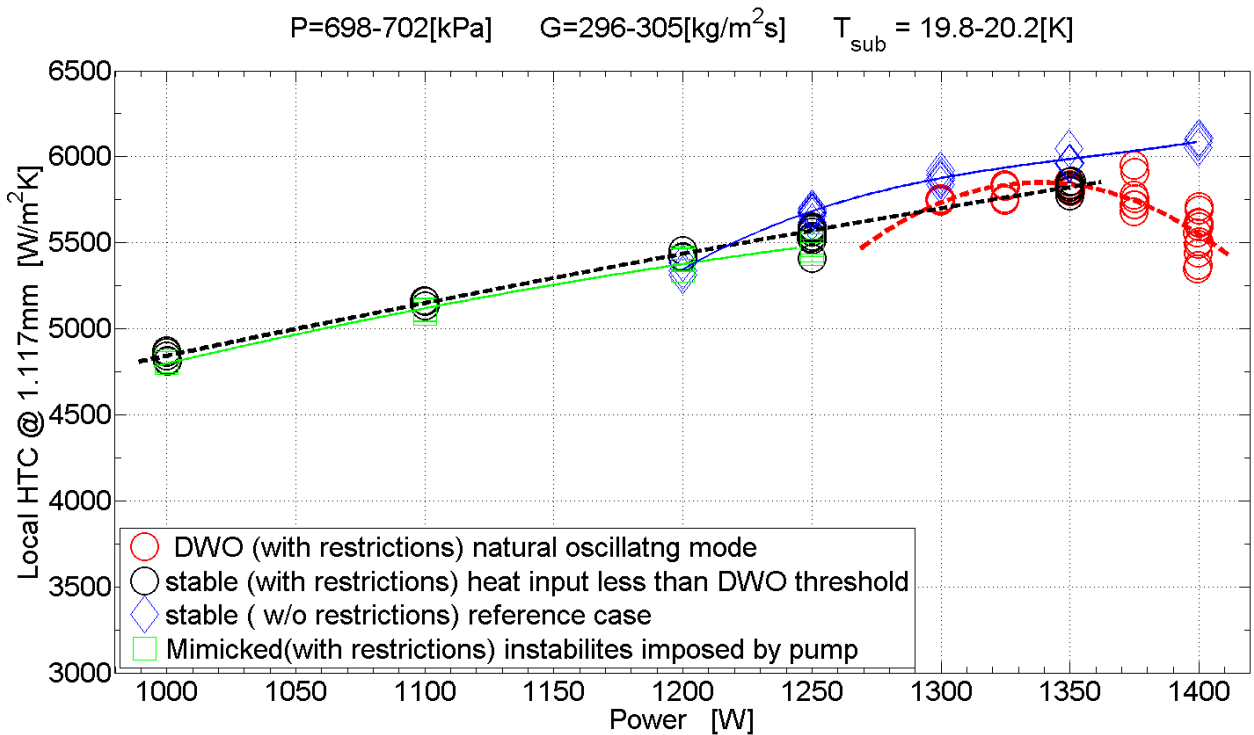
Figure 6.21 Local HTC (z = 1.117mm) – Power controlled, high subcooling (G=300kg/m^{2}s P=7bar ΔT$_{sub}$=20K)
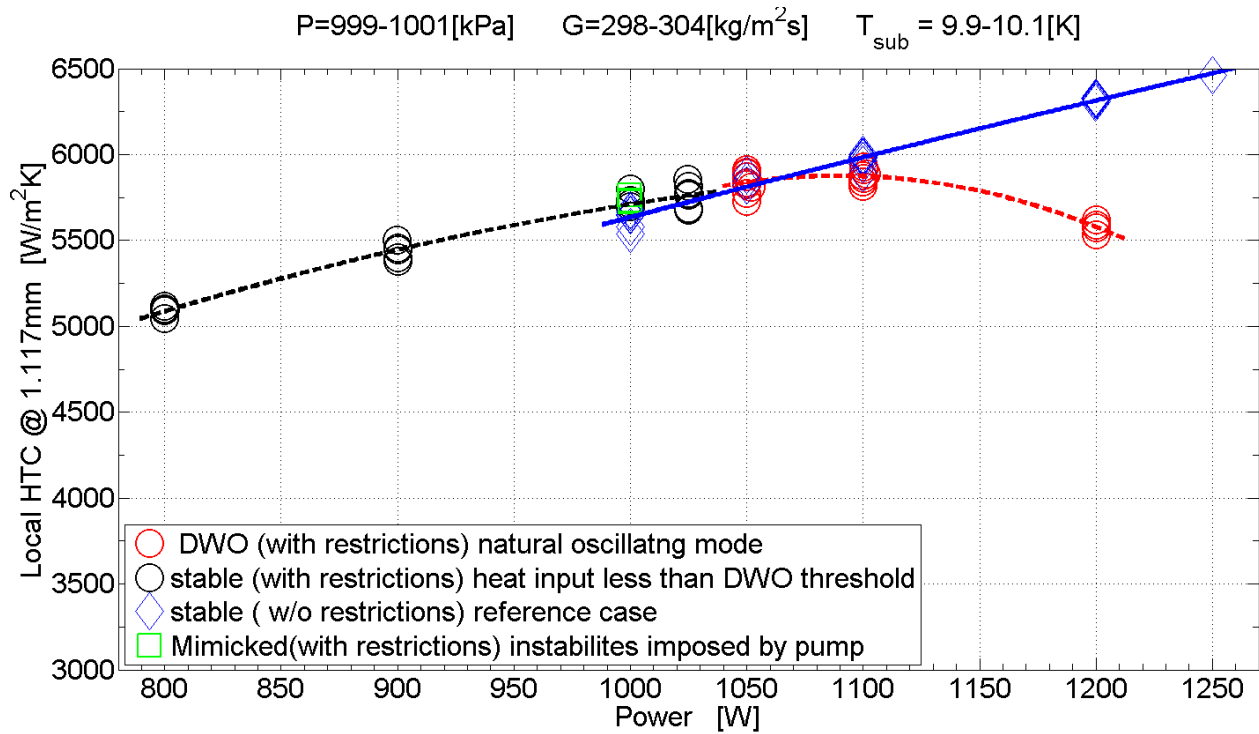
Figure 6.22 Local HTC (z = 1.117mm) – Power controlled, high pressure (G=300kg/m²s P=10bar ΔT$_{sub}$=10K)
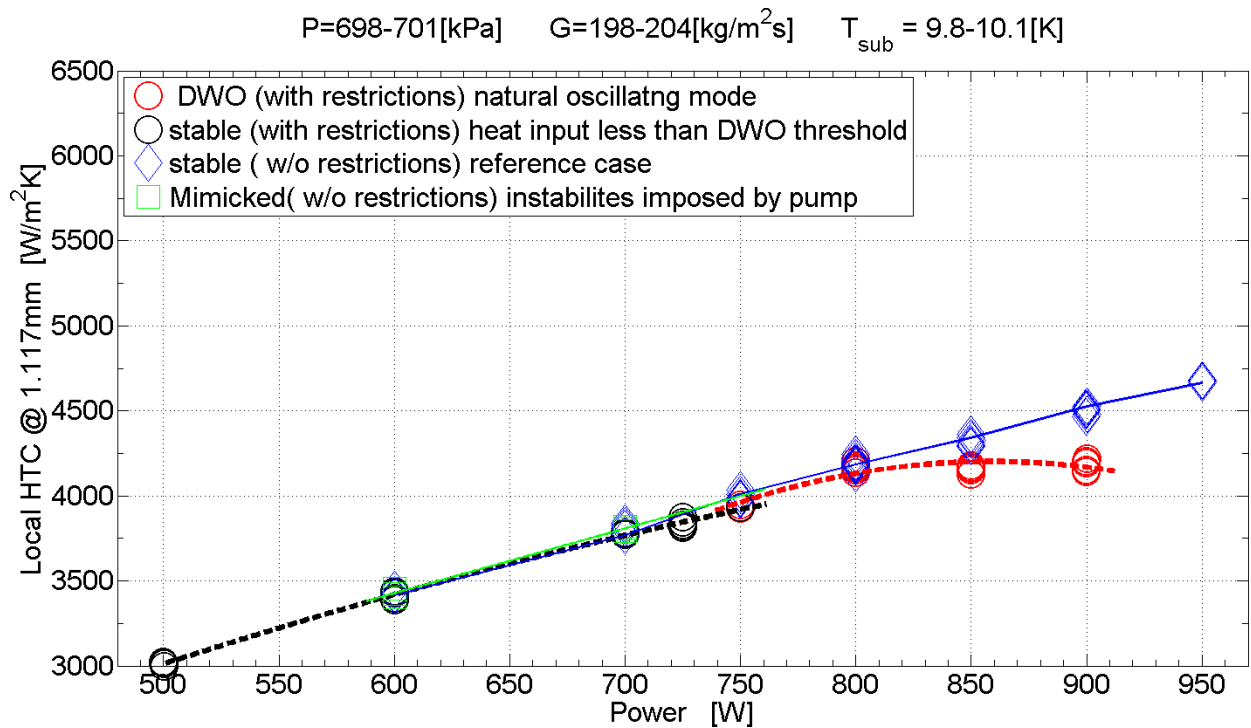
Figure 6 Local HTC (z = 1.117mm) – Power controlled, low flow rate (G=200kg/m²s P=7bar ΔT$_{sub}$=10K)

102

Heat transfer performance of the three configurations aligns well. The exception is the experiments with restrictions where heat transfer splits from the trend for the worse. One can say that heat transfer performance scales perfectly with heat flux, except for cases with DWO where heat transfer shows declining performance in comparison to the stable case. A notable observation is that heat transfer does not undergo a sudden change upon inception of DWO. Thus, DWO instabilities cannot be said to directly trigger heat transfer deterioration in the evaporation region of the heated channel. Still, presence of DWO has unfavorable influence on heat transfer on further increase in the heat input to the system.

It is interesting to observe that the imposed oscillations intended to momick DWO show little to no influence on the heat transfer in the evaporating region. This result hint that flow oscillations only disturb heat transfer in high heat flux situations, or that flow oscillations only disturb heat transfer when the vapor quality is high. The later statement comes from the fact that for a given set of inlet conditions vapor quality will increase with increased heat fluxes at a specific location downstream the heated section.

The next section brings attention towards the heated section outlet where heat transfer is known to change most severely.

6.3.2 Local heat transfer coefficient, outlet region

The local heat transfer coefficient is measured 1917 mm downstream the 2023 mm heated section. Close to the outlet is the fluid typically of either high quality vapor or superheated vapor. The thermocouples placed here are also the ones that record the most notable transition in heat transfer.
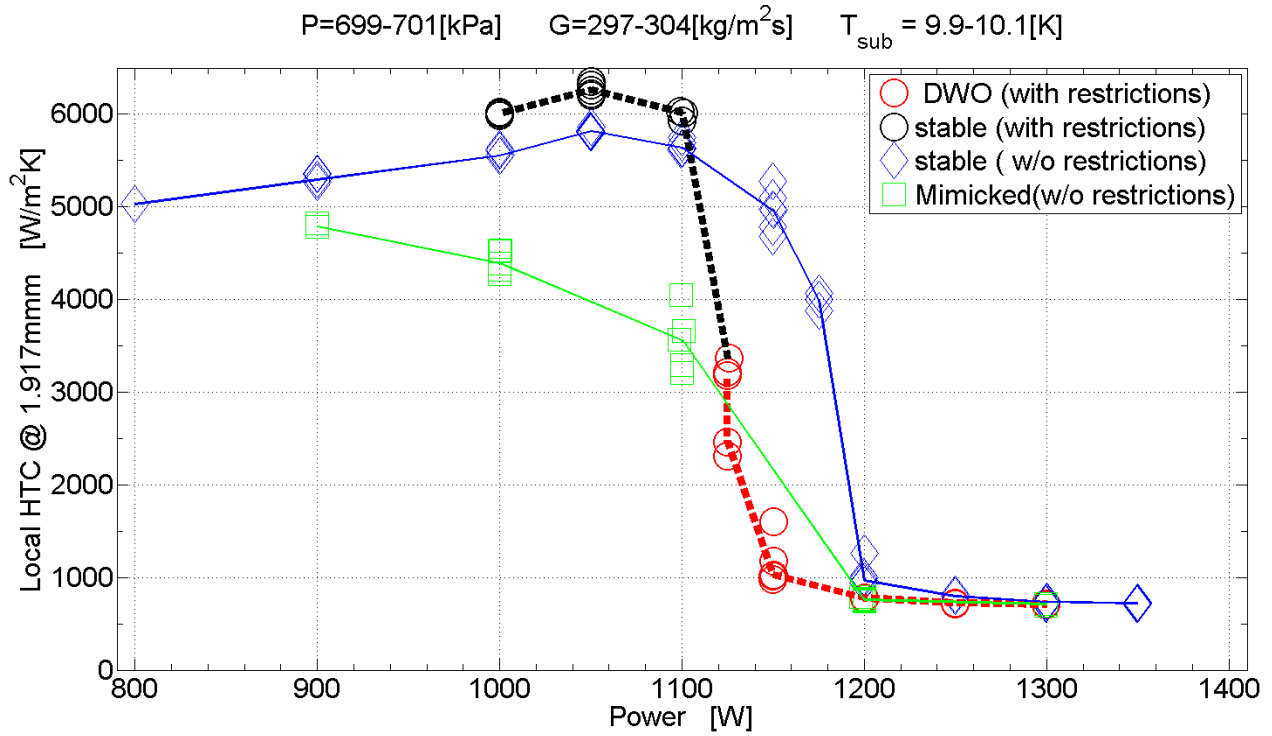
Figure 6.23 Local HTC (z = 1.917mm) – Power controlled, base case (G=300kg/m²s P=7bar ΔT_sub=10K)
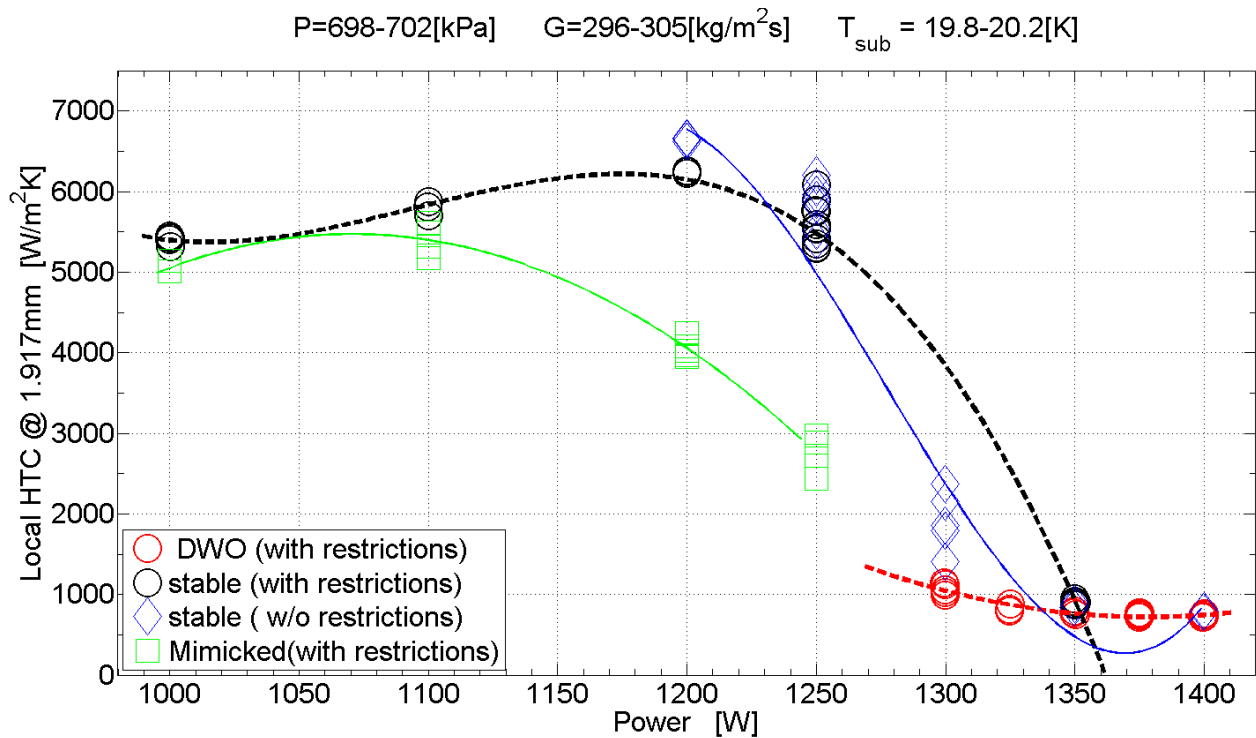
Figure 6.24 Local HTC (z = 1.917mm) – Power controlled, high subcooling (G=300kg/m²s P=7bar ΔT_sub=20K)
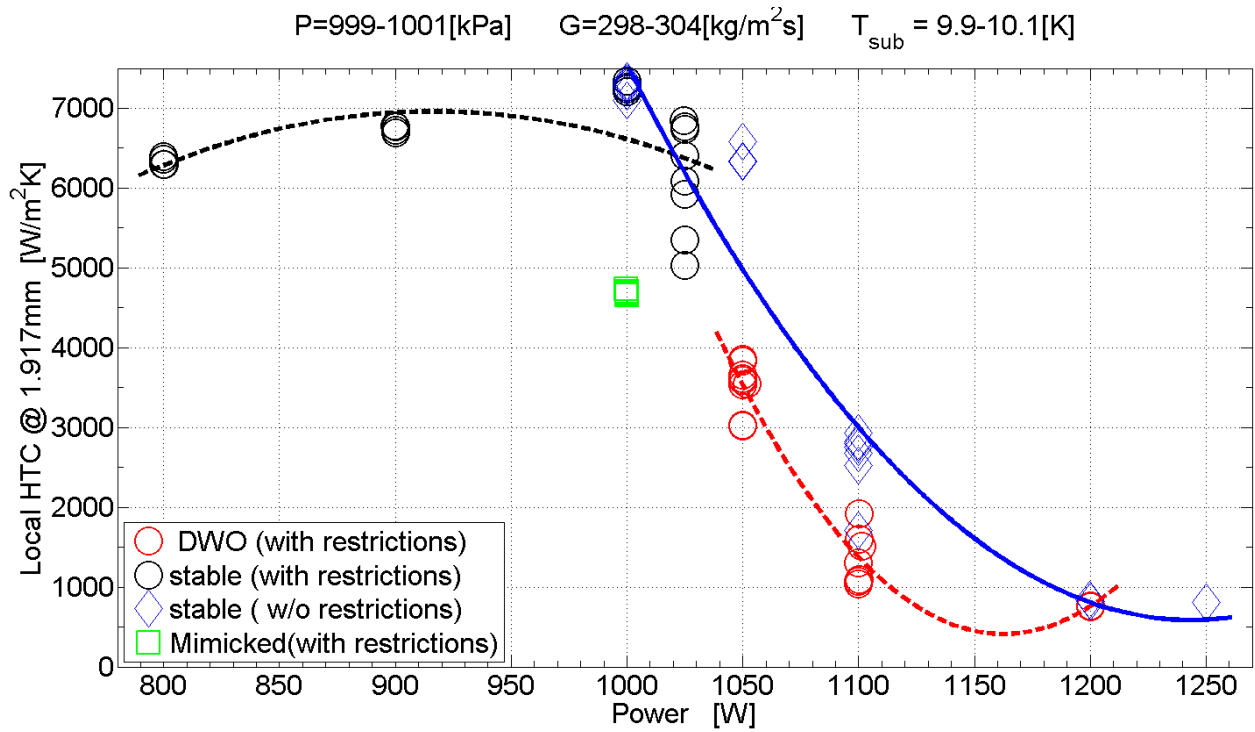
Figure 6.25 Local HTC (z = 1.917mm) – Power controlled, high pressure (G=300kg/m²s P=10bar ΔT$_{sub}$=10K)
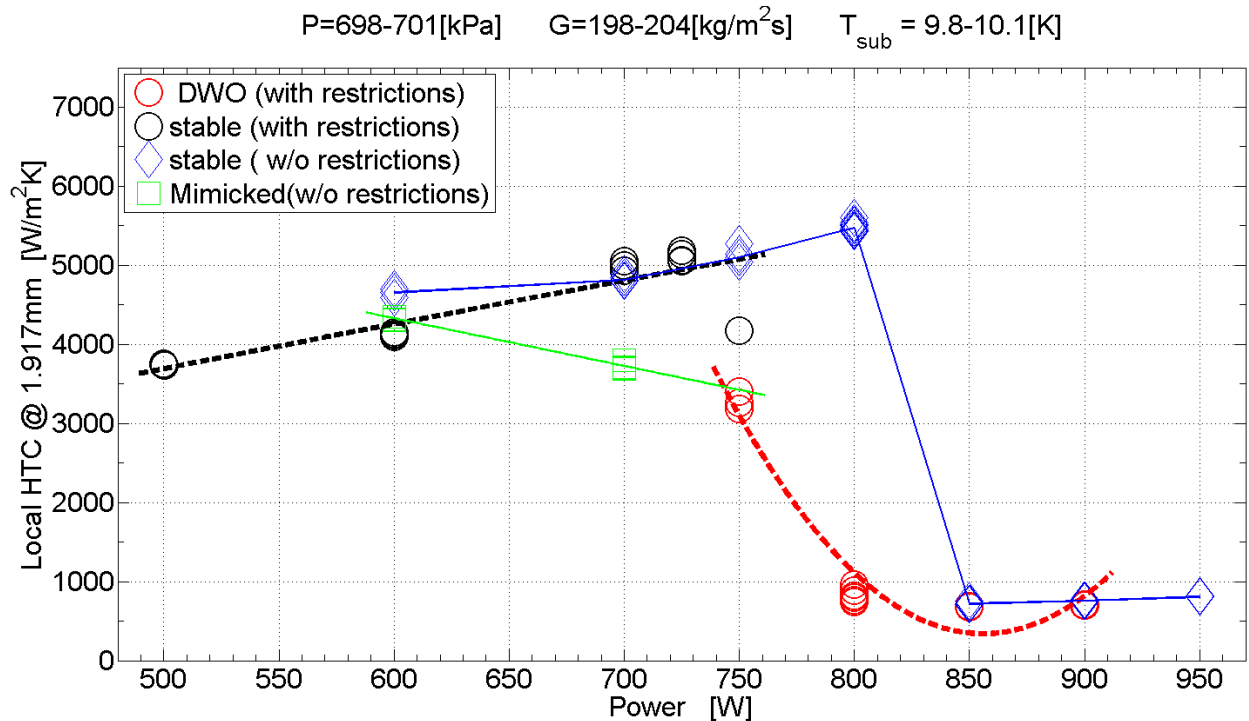
Figure 6.26 Local HTC (z = 1.917mm) – Power controlled, low flow rate (G=200kg/m²s P=7bar ΔT$_{sub}$=10K)

The local heat transfer coefficient is increasing with heat input until it suddenly drops to only a fraction of its maximum value. This boiling crisis is characteristic sign of reaching the critical heat flux. It can be said that the boiling crisis is triggered by DWO since heat transfer drops instantly when DWO commences. However, the restriction-less stable configuration does also suffer from a boiling crisis, at somewhat higher heat flux though. The local vapor quality is close to one when the critical heat flux is encountered in either configuration. Almost absence of liquid in the flow well explains dry-out of the heated surface.

Instabilities induced at heat fluxes too low for DWO to occur bridges the stable and DWO case. These oscillations of external origin has heat transfer similar to the stable case at the beginning, but losses heat transfer ability gradually as heat input is increased, finally showing heat transfer performance comparable to DWO as the heat input surpasses the DWO threshold value.

A system with inlet and outlet restrictions will experience a boiling crisis at lower heat flux than a stable system. The DWO triggered CHF is in present experiments reached at about 5-10% less heat flux than the stable case. The stable configuration does only perform marginally better than the unstable DWO configuration. Other systems more suspicious to DWO than the current could possibly have more benefit from a more stable restriction-less configuration. A more unstable system would, as one can imagine, correspond to the green points which in this study was mimicked oscillations.

When boiling is performed at vapor qualities approaching superheating, dry-out is likely to occur regardless of flow stability. The finding is interesting since the region closest to the outlet might be regarded as the most critical point in practical applications considering uniform heat flux because it will be the hottest spot inside the heat exchanger.

6.4 Pressure drop

This section shows an evaluation of heat transfer against pressure drop. Overall heat transfer is the quantity that is physically most meaningful comparison to the pressure drop, since pressure drop also is measured across the full length of the heated section. This shows the usefulness of the somewhat cumbersome computational process involved in deriving an overall heat transfer coefficient.
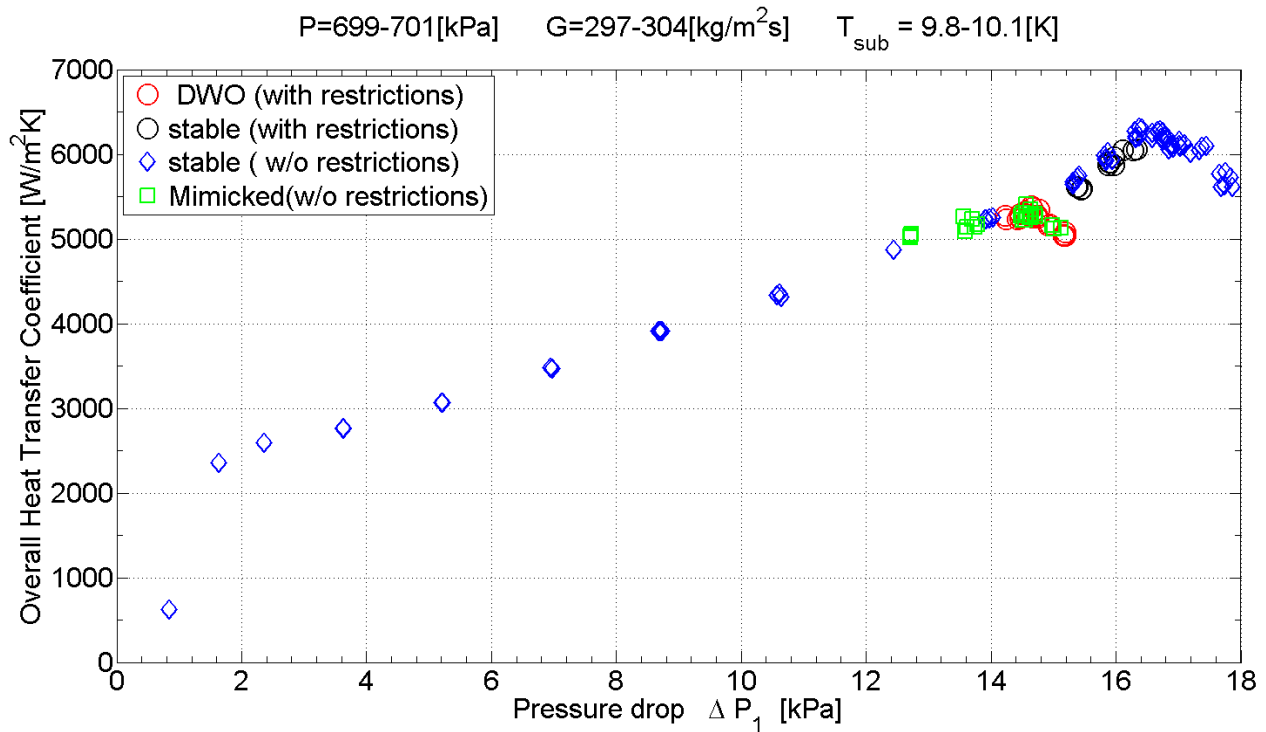
Figure 6.27 Overall HTC – Pressure drop. Power controlled, base case (G=300kg/m²s P=7bar ΔT_sub=10K)

Overall heat transfer is linked to pressure drop. Enhanched heat transfer comes on the cost of increased pressure drop, this is once again confrmed. Flow instabilities, both mimicked (green) and the natural DWO-mode (red), yields poorer heat transfer for a given pressure drop than the stable cases (blue and black).

For the mimicked instabilities it is a bit unclear. But results indicates that the pressure drop characterisitcs, has similarities to a stable situation at heat flux below the DWO threshold, and similarities to a DWO situation at heat flux inside the ustable region.
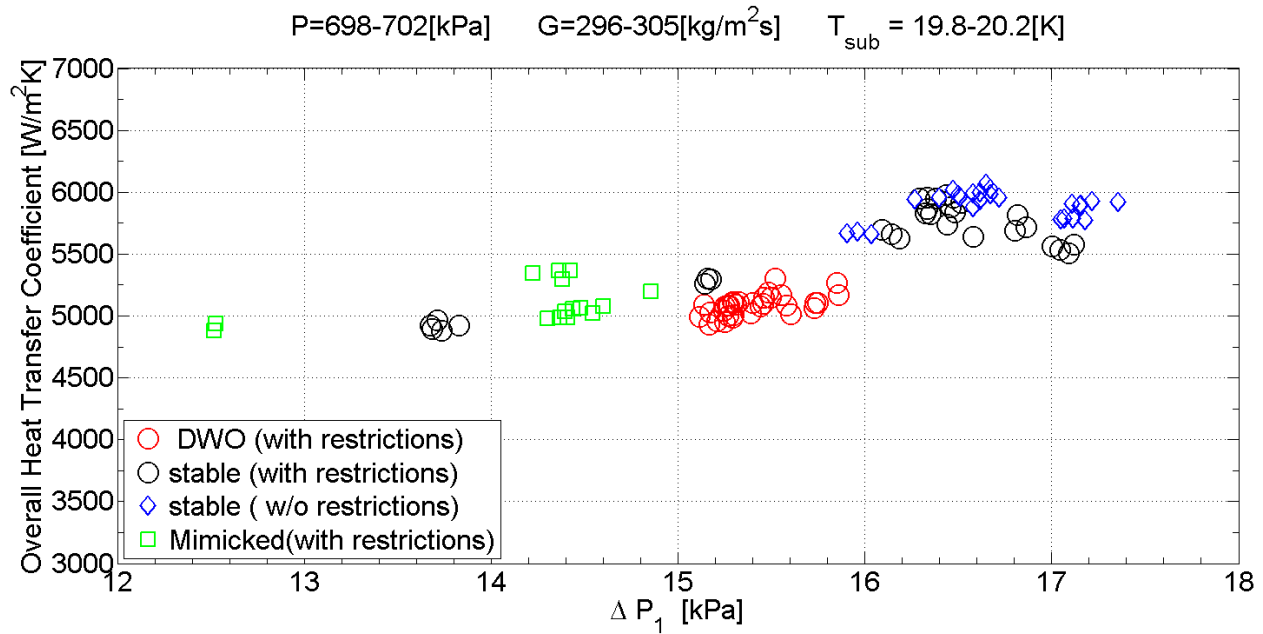
Figure 6.28 Overall HTC – Pressure drop. Power controlled, high subcooling (G=300kg/m²s P=7bar ΔT_sub=20K)
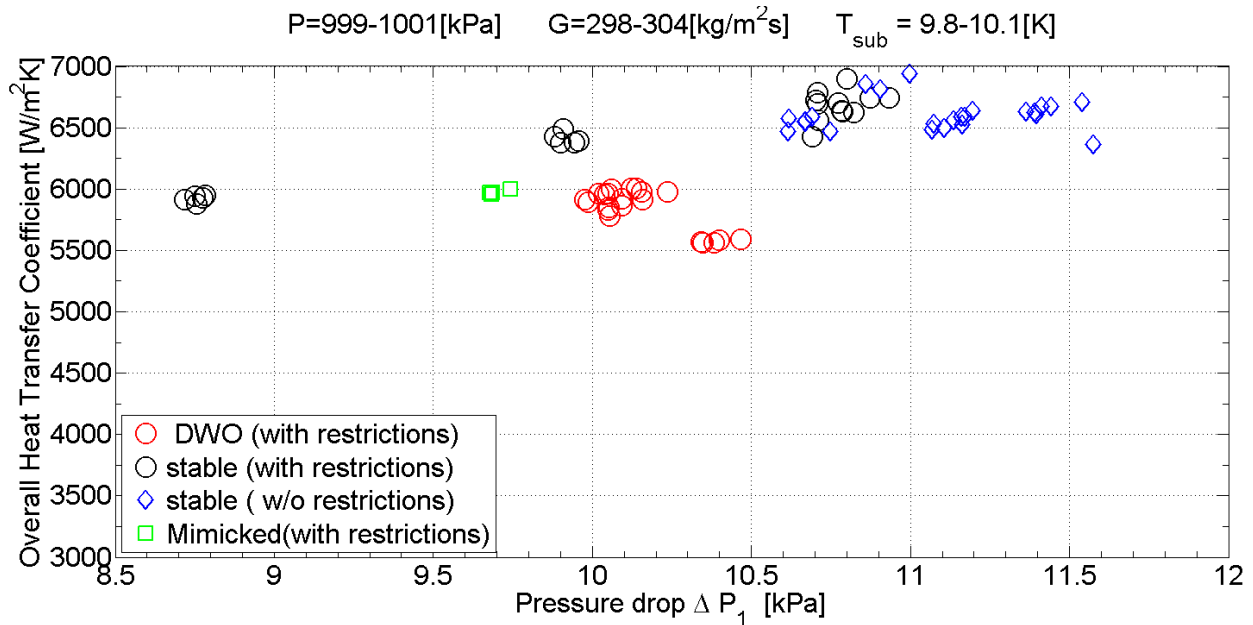
Figure 6.29 Overall HTC – Pressure drop. Power controlled, high pressure (G=300kg/m²s P=10bar ΔT_sub=10K)

The previous stated observations are supported by the experimental series with high subcooling (Figure 6.28) and high pressure (Figure 6.29). Though, the trends are a little less clear since the experimental material is less comprehensive.

The instabilities which were imposed at heat flux too low for DWO to naturally occur shows poorer overall heat transfer and less pressure drop than its stable counterpart.

108
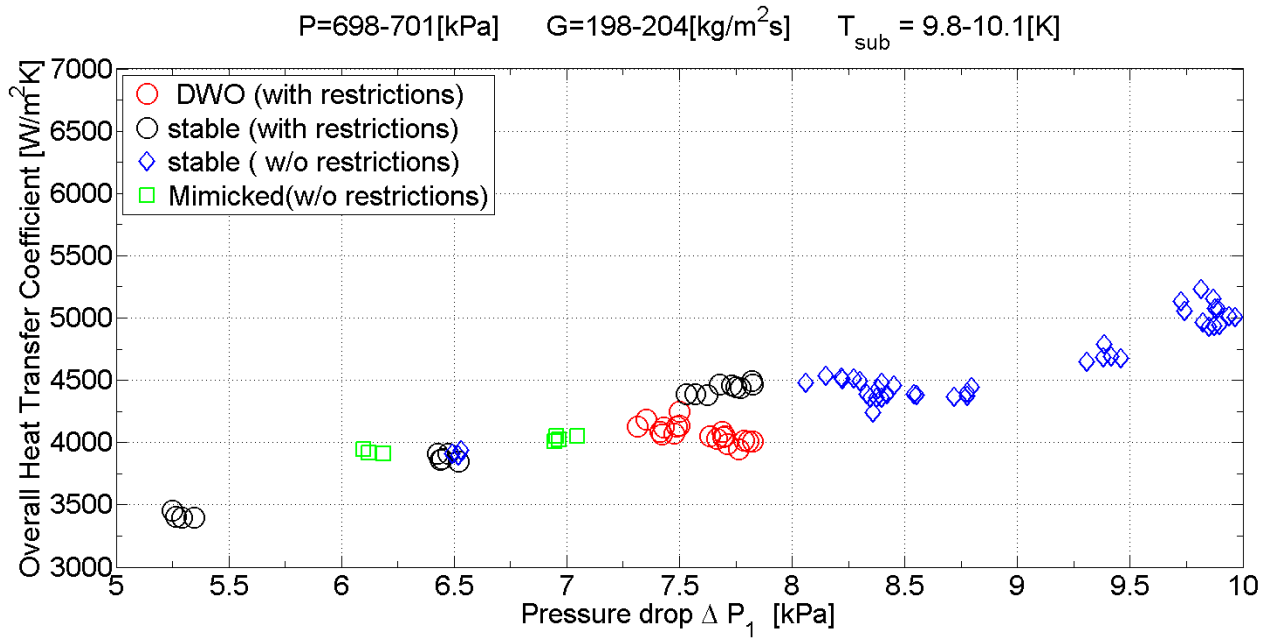
Figure 6.30 Overall HTC – Pressure drop. Power controlled, low flow rate (G=200kg/m²s P=7bar ΔT$_{sub}$=10K)

Finally the low flow rate case (Figure 6.30), where the same trends are confirmed.

Increasing the heat flux increases the pressure drop of this two-phase in tube boiling system. It is remraked that overall heat transfer shows good scaling with pressure drop. Experiments with DWO are a little out of trend, and shows slightly poorer heat transfer for a given system pressure drop. At the onset of DWO are both heat transfer and pressure drop simoltanesously reduced. This can be seen by the placement of the red DWO with restriction points to the low left to the black stable with restriction data points.

Flow oscillations, both self-sustained (DWO) and mimicked, tend to reduce the overall test section pressure drop.

7 Discussion

The primary difficulty in an investigation of boiling flow instabilities lies in the proper interpretation of results once they are obtained. The literature survey serves as a guide to pinpoint the most important parameters. The methods chapter gave an exhaustive description of the choice of analytical model obtaining a heat transfer coefficient and its implications. Experimental data is already presented in the previous results chapter. Main results will be presented again differently for further interpretation and discussion of its significance. The following section will provide in-depth discussion of these results, attempting to explain them, compare them to knowledge in the current up to date literature, and map out their practical significance. Considerable care must be exercised in the application of information obtained in the present experimental program on the design and operation of another system. This is due to the large number of mechanisms involved boiling heat transfer and boiling flow instabilities [1].

7.1 Mimicking DWO

A system with heat input less than the DWO threshold is in fact unconditional stable. For this reason, flow instabilities had to be mimicked. Using the variable pump drive to induce a cyclic flow rate aided instabilities to commence and persist though the heat input was too low. The period of oscillation was chosen to mimic DWO. Consequently, the required external flow amplitude to bring the system into unstable mode was usually rather small, especially close to the DWO threshold value. This is because the system is very prone to oscillations of a particular frequency in this region. Oscillating the pump drive speed with subtle amplitude was causing perturbations of the flow, thus aiding instabilities. Experimenting with mimicked instabilities is interesting. In particular if one reflects upon the fact that that DWO may onset under lower heat flux or higher mass flow in another system. Mimicked DWO allows for insight in such situation.

It should be noted that it is not possible to draw to sturdy conclusions from the data on mimicked instabilities. The main point of criticism is that the oscillation amplitude is under influence of the pump speed oscillations amplitude. It is already established that heat transfer depends on amplitude of flow oscillations. Another point that needs critical review is the period at which oscillations are mimicked. It was chosen according to the natural period of DWO, which is known to scale with the heated section transit time. This is not an issue when mimicking DWO in the range of conditions where DWO naturally occurs, since period is known. However, when

110

flow instabilities are imposed at heat fluxes less than the heat flux where DWO has been detected, it is unclear what kind of phenomenon one actually mimics. It is rather synthetic.

This criticism mainly applies to flow instabilities induced to a system not in a state prone to DWO (e.g. exit quality significantly less than one). Mimicking DWO within its operational envelope was in the pre-work shown to be a viable option given that the period and amplitude are set correctly.

7.2   Local heat transfer coefficient

Local heat transfer is plotted against the local vapor quality for the purpose of further discussion. This allows for mutual comparison among the four cases (base case, high subcooling, high pressure, low flow rate). The four cases can be distinguished by the color theme, which will be used throughout this chapter to simplify cross referencing. The configuration with inlet and outlet restrictions is highlighted by large colored markers, with filled markers indicating the presence of DWO. Connector lines are drawn between the data points. The stable restriction-less reference configurations is plotted with small grey markers.

Experiments with imposed instabilities, or artificially mimicked DWO, are omitted. Its absence will hopefully make the discussion more clear.

7.3 Local HTC: Two-phase evaporation region
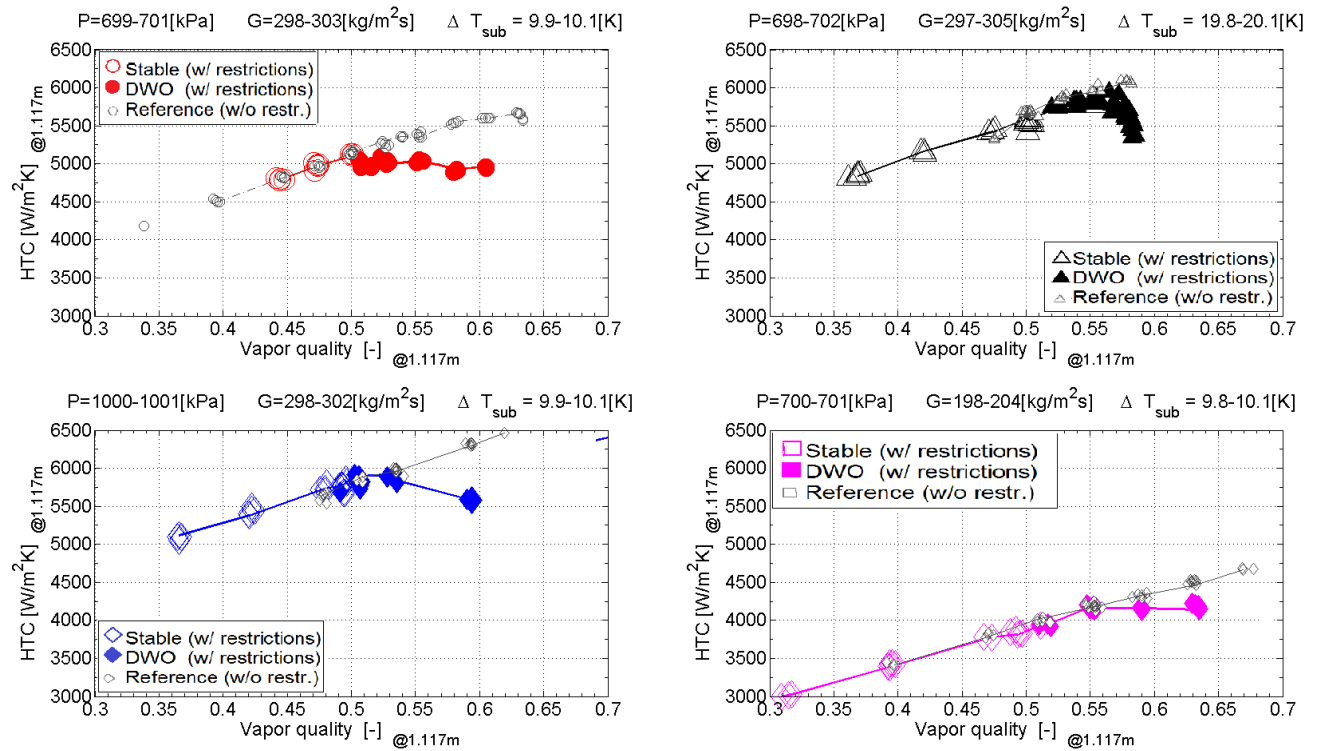
Figure 7.1 Local HTC – vapor quality. Saturated boiling in heat flux controlled experiments.

The heat transfer coefficient increases slowly but steadily with increasing vapor quality. For proper interpretation of the above results, it has to be stressed that the variation in vapor quality in these experiments is the sole result of varying the heat flux. This applies to all the four heat controlled experimental cases. Notice the scaling of the y-axis which is not extended to zero. Highest heat transfer in terms of vapor quality is achieved in the high pressure and degree of subcooling cases, while the case with lower flow rate shows significantly lower heat transfer coefficient.

7.3.1 The effect of quality, heat flux and flow rate

Lazarek and Black [33] found that heat transfer coefficient in both the subcooled ($x < 1$) and saturated ($0 < x < 1$) regimes were dependent on, and increasing with, the heat flux. The heat transfer coefficient was found to be independent of vapor quality in the saturated region. A consequence of the later is that local heat transfer coefficient in Figure 7.1 should equal the heat transfer coefficient in Figure 7.4, if vapor quality is equal. This seems to be true, albeit the vapor qualities are not completely overlapping in the two plots.

112

The results of an experimental investigation by Tran et al. 1996 [34] showed that heat transfer coefficient was independent of the local vapor quality and mass flux at $X > 0.2$. This is partly a contradiction to the present study where mass flux seems to matter. It was indicated that nucleate boiling was the dominant mechanism above this quality. Forced convective boiling was only associated with small heat fluxes, thus low qualities.

Saitoh et al. 2007 [35] found that the heat transfer coefficient increased with increasing mass flux or heat flux for a 3.1 mm tube. In the smaller 0.51 mm tube, the heat transfer coefficient increased with heat flux, but was not significantly affected by the mass flux. It was concluded that the contribution of forced convective evaporation to the boiling heat transfer decreases with decreasing diameter.

Copetti et al. [37] found similar dependencies; the heat transfer coefficient increased with increasing heat flux and mass flow rate, but the stronger heat flux dependency was mainly observed in the low quality region.

Comparing the results on heat transfer coefficient in the saturated region shows overall good agreement to the observations made by other researchers. The heat flux effect, which is relatively constant over the range of vapor qualities, indicates that the nucleate boiling mechanism is dominant. It is seen in the figure above that the low flow rate case has the lowest heat transfer coefficient. Notice, however, that the heat flux also is equivalent lower, a fact hidden by the choice of plotting heat transfer versus the quality.

Evaluating the flow rate controlled experiment in conjunction with the heat flux controlled is in this respect invaluable. The independency of flow rate in the saturated region becomes more evident by examine the results from the flow rate controlled experiment. Figure 7.2 shows local heat transfer coefficient in the saturated region against vapor quality. Variations in vapor quality do now origin from changes in experimental flow rate. The local heat transfer coefficient is observed to be almost constant. Only exception is the experiments where DWO occurs.

Pure convective boiling, were experimental heat transfer coefficient is independent of the heat flux, was not observed in out experiments for the range of parameters investigated. Behavior of the stable restriction-less configuration is all well described in the open literature.
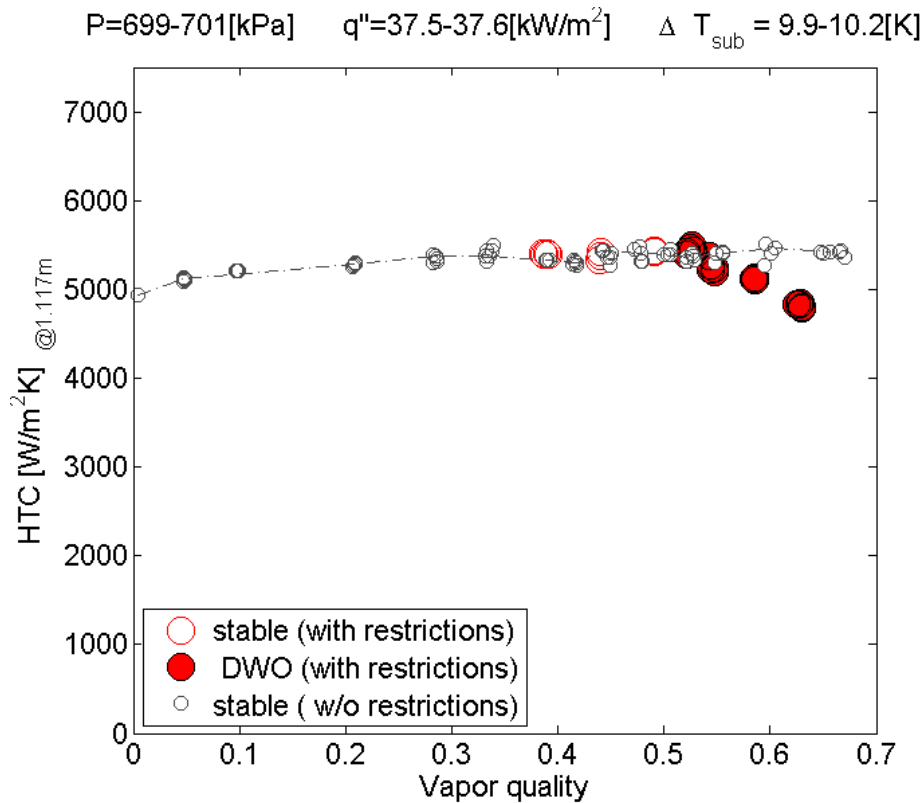
Figure 7.2 Local HTC – vapor quality. Saturated boiling in flow rate controlled experiment.

7.3.2 The effect of evaporating pressure

It is found that increasing the pressure from 7 to 10 bars increases heat transfer. This supports the findings of Saitoh et al. [35], but it should be noted that their experiment on pressure effects were carried out at much higher pressures ranging from 30 – 37 bar, which is rather close to the critical pressure of R134a (40.6 bar [54]). The thermo-physical properties of R134a are quite different at near critical condition to that at lower pressure condition, in particular for the liquid-vapor density ratio which approaches to unity. Lazarek and Black [33] also observed that the heat transfer coefficient is increased at increase in pressure. Their experiments were carried out in lower pressures ranging from 1.3 to 4.1 bars. Mind that this study was on R113.

Specifying ΔT_{sub} for each experimental case instead of the inlet temperature is advantageous when it comes to comparison between different inlet pressures. It seems evident that increasing the pressure causes the heat transfer coefficient to increase over a range of reduced pressures. An attempted explanation is that increasing the pressure reduces the surface tension. This reduction in surface tension corresponds to a decrease in superheat of liquid required for bubbles to nucleate and grow, and consequently nucleate boiling occurs at smaller superheating. In other

114

words, nucleate evaporative boiling occurs at slightly lower heated wall to fluid saturation temperature when pressure is increased, and reduction of the driving temperature difference is known to result in improved heat transfer.

Experiments with eleven upflow parallel rectangular mini-channels with refrigerant R134a did not show the same scaling with pressure. Agostini and Bontemps [38] did not find a sizable influence of pressure on the heat transfer coefficient, although it was quoted that nucleate boiling was the dominant heat transfer mechanism. This suggests that pressure only has influence on heat transfer in macro-channels.

7.3.3 The effect of inlet subcooling

A higher degree of inlet subcooling, or lower inlet temperature, elongates the subcooled region. This region is characterized by single-phase flow, although subcooled boiling does occur at high heat fluxes. The literature on two-phase boiling heat transfer is most concerned with the downstream saturated region, with the effect of subcooling consequently falling out of scope.

Increasing the degree of inlet subcooling by a factor of two does only give minor improvement in heat transfer. In view of this relationship, local heat transfer at a position inside the saturated region can be regarded almost insensitive to inlet subcooling. The most protruding effect of increased subcooling is that it lifts the threshold heat flux for onset of DWO and causes more violent oscillations.

7.3.4 The effect of flow instabilities in the saturated region

The discussion has up to this point only addressed observations made in stable systems. It is evident that experiments with DWO do not have the same gain in heat transfer on increasing vapor quality as its stable counterpart. Recap Figure 7.1. In the base case and low flow rate cases, local heat transfer does not continue its growth when DWO are experienced. In the high pressure and high subcooling cases, local heat transfer is actually depreciated. Saitoh et al. 2007 [35] also found that the experimental heat transfer coefficient decreased when flow oscillations was generated. These measurements were also taken in the saturated boiling region.

The difference in local heat transfer coefficient between the DWO and the stable configuration in the saturated region do not emerge immediately on the onset of DWO. Nor is it occurring suddenly. To be more specific: When the heat flux, and consequently vapor quality, are

increased; DWO first commences without influencing the local heat transfer coefficient, but the presence of DWO do become unfavorable as the heat flux is further increased. Further interpretation of this observation can indicate that DWO do not directly trigger the deterioration in heat transfer at a particular location in the saturated boiling region.

The absence of DWO is advantageous for the local heat transfer in the region of saturated boiling. Speculations on how DWO is negatively influencing the boiling heat transfer mechanisms follow this. An explanation may be that flow oscillations periodically trigger the CHF in a finite moment of time. This is most likely to occur in a part of the cycle with either low density and/or pressure. This temporary reduction in heat transfer may also appear in conjunction with periodically brief transition to a droplet field. Flow visualization inside the stainless steel heated tube is out of the question, but it is known from the test section outlet that DWO usually are accompanied by a spectrum of flow patterns varying throughout its cycle.

7.3.5 Other flow instabilities

A shortcoming of the present study is that only one type of flow instability is covered, namely DWO. A central question to address is the cause of reduction in saturated boiling heat transfer. And further, can flow instabilities with other time scale be more harmful? Flow oscillation phenomenon with longer periods, for instance PDO, may allow sufficient time for heat transfer performance to be more seriously reduced. The heat transfer transits during the short DWO cycle might be evened out by accumulation of heat due to the heat capacity of the tube wall. Experiments of the pre-work (section 5.7) dealing with the effect of shifting the mimicked DWO period strengthens this concern as they showed reduction in heat transfer as the period was increased.

7.4 Comparison of experimental data to correlations

The measured boiling heat transfer coefficient is compared to a selection of existing correlations found in the open literature. More elaborated descriptions and equations have been introduced in the literature survey (chapter 2.6). The original articles were more carefully examined to ensure proper implementation of the correlations. Evaluation is done at thermocouple positioned at $z = 1117$ mm since correlations are developed for purpose of saturated boiling, and do not apply to transition to a superheated vapor regime.

Figure 7.3 will show comparisons of flow boiling heat transfer coefficients between experimental data and existing correlations from the literature. Only data with inlet and outlet restrictions are plotted, which consists of 177 data points, whereas markers are filled to indicate occurrence of DWO.
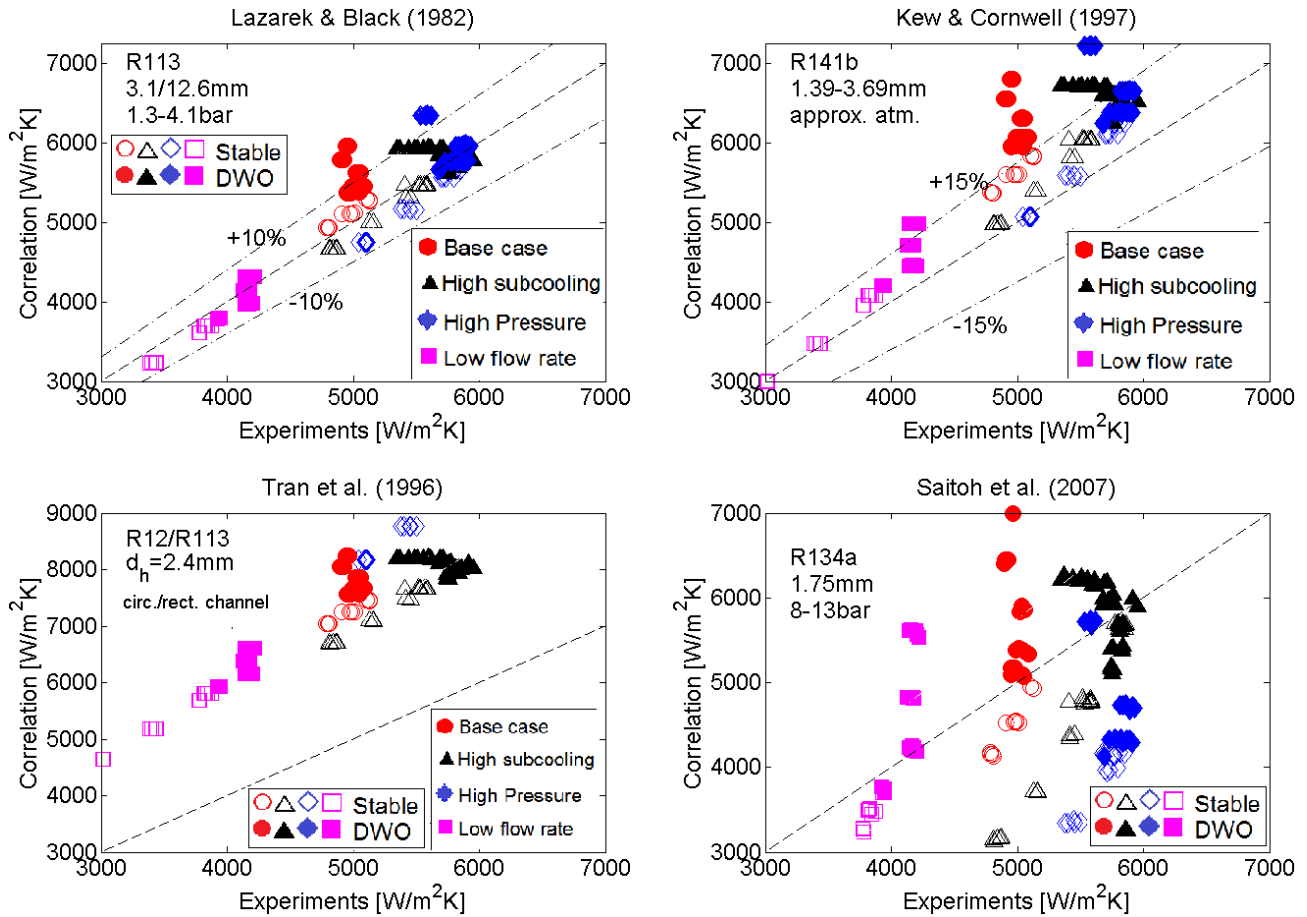
Figure 7.3 Comparison of experimental results to two-phase boiling correlations

The correlation proposed by Lazarek and Black in (1982) [33] yields an accurate prediction of the local heat transfer coefficient albeit having a relative simple form. The stable data falls inside a 10 % confidence interval. This matches the results of the single phase verifications and proves the value of using an average of the temperature measured at the four circumferential distributed thermocouples. Prediction of heat transfer falls mostly out of this tight band when DWO set, but stays within a decent 20 %.

A modified version of the Lazarek and Black correlation was proposed by Kew-Cornwell (1997) [39]. A term was added to compensate for the tendency of increase in heat transfer on increasing

heat flux observed in larger channels. This essentially resembles the trend in current experiments and should improve the accuracy of prediction. Owing that the original coefficient was spot on, adding the correction term causes predictions to become a bit higher than the experimental data. The Kew-Cornwell correlation does still perform relatively well. The stable data falls within a 15% error band, which is just as good as the fit of the authors had with their original data to the correlation thy developed. Heat transfer data with DWO are found within 30 % of the predicted value.

These correlations are developed for stable flows and, as it can be seen, they do not account for the depreciation in heat transfer triggered by DWO. The two fist correlations were based on the Boiling number and the Reynolds number.

The correlation of Tran et al. 1996 [34] overpredicts the local heat transfer coefficient by about one and a half time the experimental. In particular the high pressure (blue diamonds) case, even though the correlation indeed accounts for pressure by taking the liquid to vapor density ratio into consideration. This correlation do also differs from the two previous by relying on the non-dimensional Weber number instead of Reynolds. The Weber number describes the ration fluid's inertia to the surface tension, while the Reynolds number is a measure of the relative importance inertial forces compared to the viscous forces. The choice of emphasizing surface tension in the correlation shows that the correlation of Tran is worked out for mini-channels.

The channels of Tran et al. had a hydraulic diameter of 2.4 mm. This is not being much less than the < 3 mm tubes used by Lazarek & Black and Ken & Cornwell, but it may make a difference. Cheng and Wu (2006) [55] used the Bond number to distinguish macro- from mini- micro-scale. Channels with $Bo > 3$ classifies as a macro-channel since surface tension is small in comparison with gravitational force. Kandlikar and Grande (2002) [56] classified channels more trivially by hydraulic diameter. Channels larger than 3 mm were defined as conventional, or macro, channels. The channels of Tran et al. and Saitoh et al. are by this definition classified as mini-channels. Which fluid, hydraulic diameter and pressure range correlations were based on is indicated in each plot.

The correlation of Fan [42] (2013) is interesting as his work also took DWO in consideration. It was found to astronomically overpredict the heat transfer coefficient. The correlation of fan is on the same from that the one of Tran et al., but it is much more sensitive to Weber number. This

reflects the fact that the correlation was developed for an 889 µm micro-channel. The Weber number scales with diameter and will thus have another magnitude in macro scale. Properties of the 3M Electronic liquid FC-72 [57] are also different from common refrigerants by have a smaller heat of evaporation and larger liquid to vapor density ratio. Combining the difference channel-size and fluid properties helps explaining this unexpected result on implementation of the correlation by Fan.

Saitoh et al. uses a more advanced Chen-type correlation. It is pointed out that the surface tension becomes dominant over buoyancy effects as the diameter of the two-phase channel decreases. The slip is also reduced.

Mini-channel type correlation is found less suitable as they typically overpredicts the local heat transfer coefficient. Studies addressing heat transfer issues in conjunction with flow instabilities are usually considering micro-channels [45] [46] [40] [41]. Less work has been done on heat transfer issues caused by flow instabilities in macro channels than in smaller geometries. This italicizes the need of further research into the topic.

7.5 Local HTC: Outlet of the heated channel

Local heat transfer coefficient recorded close to the outlet of the heated section is plotted in Figure 7.4. Each case distinguished by inlet condition is plotted separately. Markers are filled to indicate the occurrence of DWO. The stable reference case is plotted in the background with grey markers and dashed connector lines.
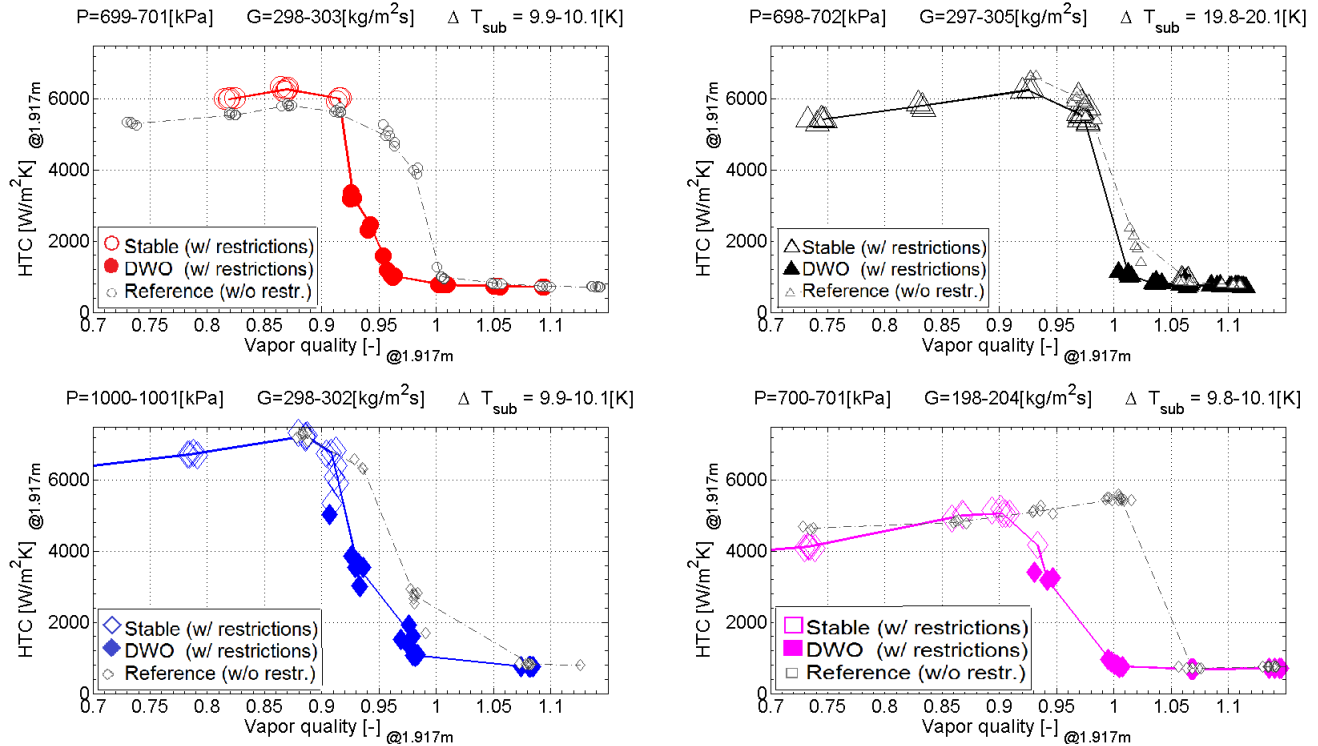
Figure 7.4 Local HTC – vapor quality. Heated section outlet in heat flux controlled experiments.

The figure above shows the effect of heat flux on local heat transfer close to the outlet of the heated section. As a continuation of the trend seen in the evaporating section (Figure 7.1), the local heat transfer increases on increasing heat flux, until it literarily collapses. This is the so called boiling crisis where the heated walls undergo a dry-out, and it appears to happen as the vapor fraction proceeds towards one. The same sudden deficit in heat transfer at qualities approaching one was also documented in the R134a horizontal tube experimental study by Saitoh et al. 2007 [35]. To be more specific, the heat transfer coefficient started to decrease when the vapor quality was 0.9 in the largest (3.1 mm) tube. This is in good agreement with the present results.

In the superheated region ($x > 1$) is the local heat transfer stabilizing at a much lower level. Under these conditions, bulk fluid boiling does no longer occur. The heat transfer mechanism consists of a combination of forced convection to the vapor and radiation; the later will gain dominance in situations where the heated surface temperatures become immense.

Encountering a dry-out when the vapor quality approaches one, or is in excess of one, is usually expected. However, it is noticed that the occurrence of a dry-out upon increase in heat flux is somewhat delayed when the flow is stabilized by removing the in- and outlet restrictions.

In practical applications, in particular those where a dry-out situation is fatal, avoiding flow instabilities will to some extent enlarge envelope of safe operation. However, the gain is modest or less. It can rather be said that operation in this high quality region is hazardous in either case. Heat transfer will at this point become seriously hampered regardless of DWO flow instabilities.

Practical applications, such as once thorough evaporators, build to generate saturated or even superheat vapor will encounter a dry-out situation by design. In this view, the main concerns regarding DWO are mechanical vibrations and thermal fatigue by cycling of wall temperature.

It has to be reminded that discussion of present results addresses observations in a macro channel. Kennedy et al. [40] demonstrated that the onset of flow instability was about 90% of the bulk exit saturation heat flux in an experimental investigation in horizontal micro channels under uniform heat flux. This DWO inception criterion aligns well with findings in the present study. When it comes to the heat transfer and eventually a dry out, smaller geometries seems to behave differently.

The literature on experiments in mini-channels, predicts that bubble confinement effects leads to, higher heat transfer coefficients than what is achieved in conventional tubes, but the fact that dry-out occurs at medium qualities (as soon as $x >\sim 0.4$) is dramatically decreasing the performance. [38]. Saitoh et al. [35] found the experimental heat transfer coefficient to start to decrease at significantly lower qualities in the smallest geometries. Heat transfer reached its maximum at x $<= 0.5$ in a 0.51 mm tube.
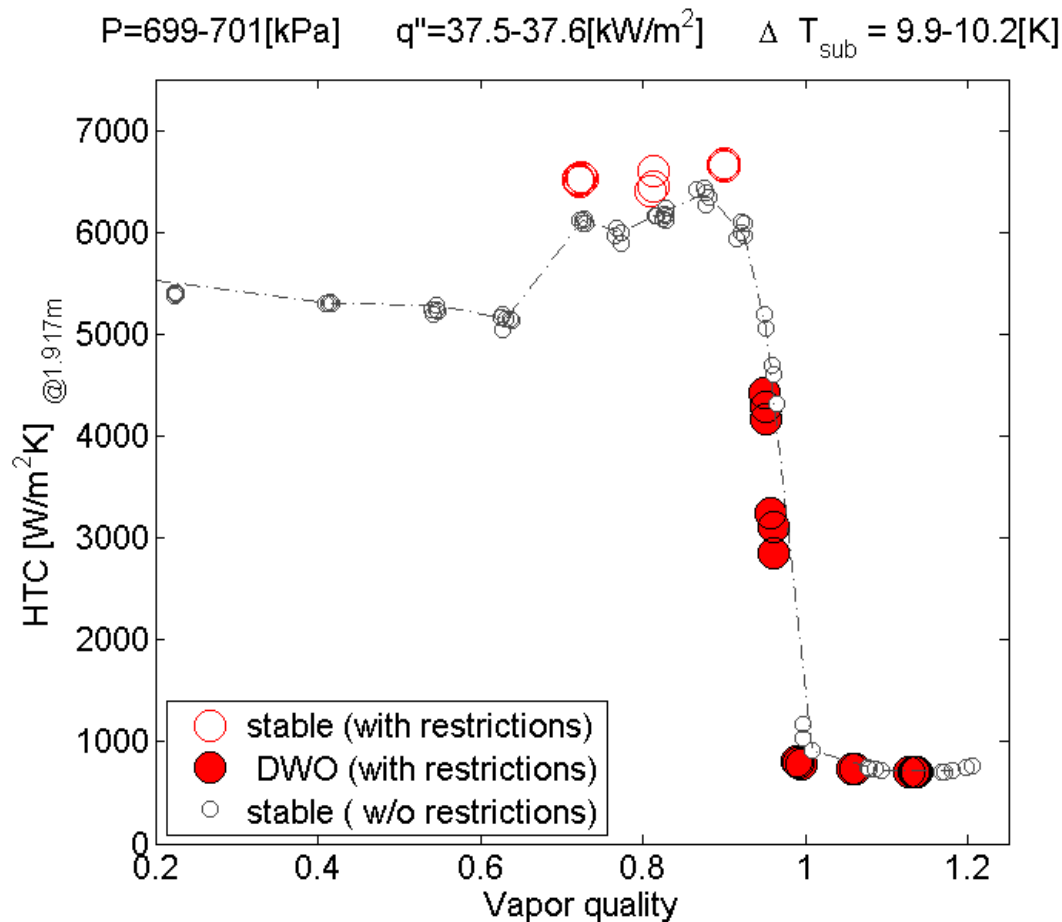
Figure 7.5 Local HTC – vapor quality. Heated section outlet in flow rate controlled experiment.

The previous discussion does also perfectly apply to application where flow rate is reduced until a dry-out and subsequent collapse in heat transfer coefficient occurs. In the above figure is the increase in vapor quality caused by decrease in flow rate in experiments with constant heat flux. Even though the saturated boiling heat transfer coefficient was previously stated to be independent of flow rate, a jerk appears at a quality of about 0.7. It is guessed that it is caused by a transition in flow regime as the flow controlled experimental series has a wide span in Reynolds number.

Onset of the critical heat flux is closer examined in the subchapter to come.

7.6   Critical heat flux

The critical heat flux is commonly identified by an abrupt increase in the temperature of the heated surface. This particularly applies to heat controlled boiling experiments. The next figure shows the driving temperature difference versus heat flux for the four cases.

122
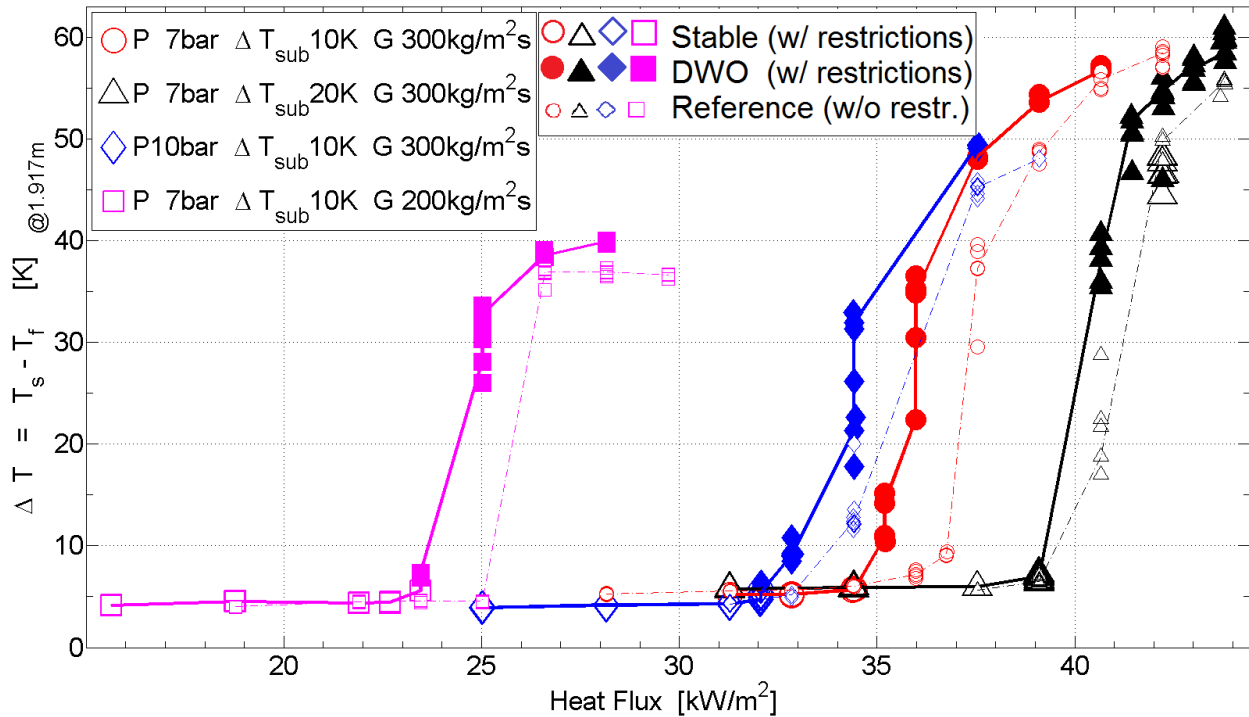
Figure 7.6 Temperature difference – heat flux. Normal CHF and premature CHF

Fan [42] classified the critical heat flux into normal CHF and premature CHF. Normal CHF is measured under stable flow operating condition while the premature CHF is accompanied with flow oscillations. The two are therefore distinguished by the flow behavior in experiments.

In the present research, flow instabilities and premature CHF are always coexisting. Tracing the thick connector lines from left to right, the driving temperature remains constant low for a while, until it suddenly starts to increases rapidly marking the CHF. Closer examination of the plot reveals that markers are becoming filled at the location of the premature CHF. This confirms that the premature CHF is triggered by DWO. The normal CHF can be examined by tracing the dashed lines connecting the small markers. The premature CHF is found to have lower value (5-10 %) than the normal CHF at a constant mass flux. This phenomenon was also observed by Fan. Experiments with FC-72 in mini-channels had more alarming trends, premature CHF could be initiated at heat fluxes at only half of the normal CHF.

If the purpose of an application is cooling, encountering the critical heat flux will have devastating consequences for its performance. There are three basically parameters of main interest when one designs a generic heat exchanger intended to operate utilizing boiling heat

transfer. These are ONB, the slope of the boiling curve whereas heat transfer is increasing, and eventually the CHF. Consider an R134a evaporator built in a similar manner as the present experimental configuration: If it is designed with a safety factor of, let say 0.80 x CHF or better, neither DWO nor premature CHF poses direct threats to its integrity. Such application is likely not vulnerable to DWO, and thus not premature CHF, at all due to its more moderate vapor quality nature. To know this has practical significance in itself.

It is important to be aware of the limitations in the present work, as it only represents the situation of R134 a boiling in a horizontal tube with given geometry and small range of conditions. Conclusions must be treated with great care if one attempts transfer them to other systems. A criterion for inception of DWO can predict the onset of premature CHF and vice versa.

7.7 Pressure drop

In the results chapter, overall heat transfer was found to scale quite well with pressure drop, except the experiments with DWO characterized by a combination of somewhat reduced heat transfer and pressure drop.

The establishment of an overall heat transfer coefficient described in the methods chapter was useful with regards to the pressure drop since it is an overall quantity. Figure 7.7 shows how pressure drop evolves as exit vapor fraction changes upon increase in the heat flux. The plot allows for comparison between the unstable and stable restriction-less reference system, the later having the smallest markers. Plotting against the vapor quality allows for a more mutual comparison between the four cases, the x-axis also aligns to the other plots in this chapter.
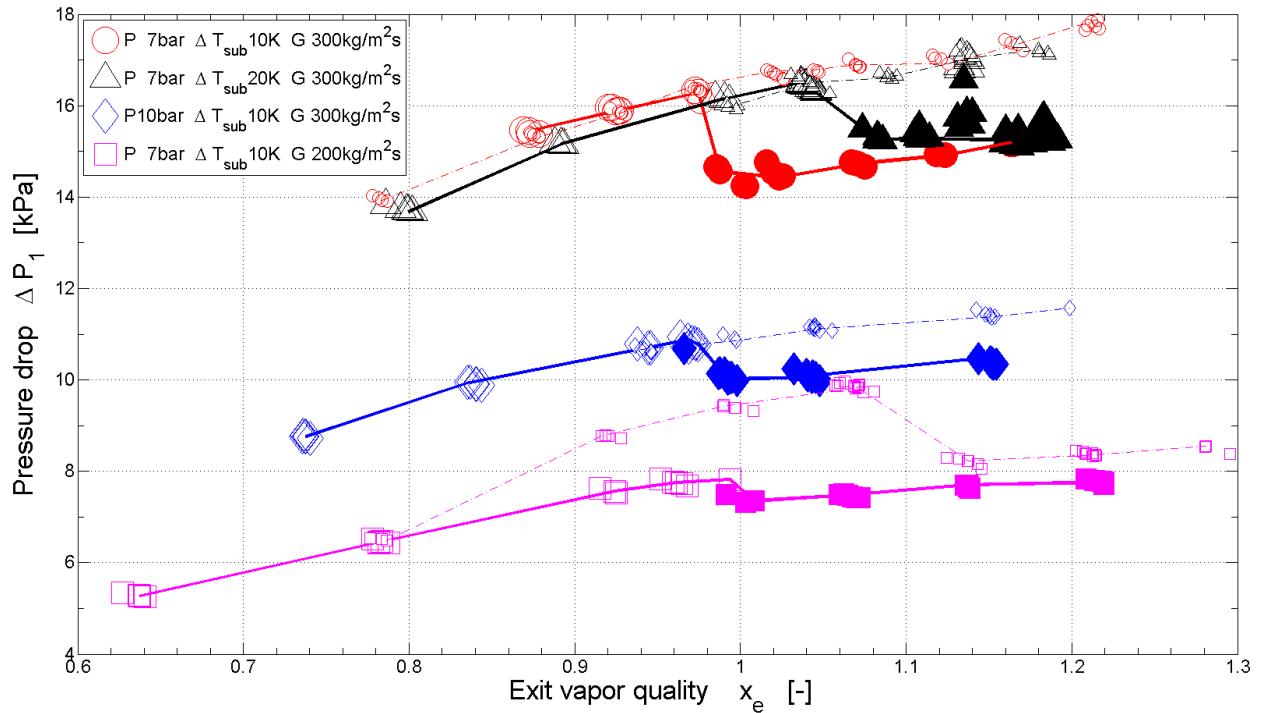
Figure 7.7 Pressure drop – exit quality. For four heat flux controlled experiments.

Increasing the heat flux and consequently the exit quality, yields an increasing two phase pressure drop. This is perfectly in agreement with two-phase theory and literature, since more vapor means larger volume, increasing both velocity (the frictional loss) and flow acceleration (due to expansion).

It is already pointed out that DWO is accompanied by reduced heat transfer, and it can be seen from the figure that pressure drop suddenly drops on the onset of DWO. Lower pressure drop implies a slightly higher outlet pressure since the inlet pressure is kept constant. This could lead to the conclusion that higher pressure gives higher boiling temperature which causes the superheated boundary to move a small distance downstream, but the opposite seems to be the case. Occurrence of DWO moves the dry-out boundary a small distance upstream the heated section. This is contra intuitive and accentuates the complex nature of the DWO phenomenon.

8 Conclusion

An experimental program has been developed and conducted to study the effects of flow instabilities of the heat transfer and pressure drop characteristics of a boiling system. Experiments were conducted in an in-tube horizontal boiling macro-channel with uniform heat flux using refrigerant R134-a as the working fluid. A mass flow rate controlled experiment was conducted for one case while heat controlled experiments were conducted with four inlet conditions in order to determine the effect of system pressure, flow rate, and inlet temperature. The mass flow rate controlled and heat flux controlled experiments showed similar trends. Varying the mass flow drastically changes the Reynolds number which in turn prompts a wide span of flow patterns.

A system configuration with inlet and outlet restriction with some degree of inlet subcooling was found to be unstable as long as the exit quality became sufficiently high. Only one mode of sustained well defined oscillations of significant amplitude could be detected, namely DWO, in contrast to many other studies reporting DWO superimposed on other instability modes. DWO is characterized by waves of alternating higher and lower densities traveling across the system. The classical description suggesting that the oscillation period is one to two times the boiling channel transit time is confirmed.

The onset and characteristics of DWO are mapped out for this particular system, which is not to be underestimated as the number of contradictions in the DWO literature shows that system configuration do matter. When increasing the heat input, the amplitude is found to increase very rapidly close to the threshold value, while growth ceases when the heat input become excessive, yielding mostly superheated vapor in the boiling channel exit. The magnitude of oscillation amplitude is inherently linked to the proximity to inception.

The implications of various system parameters such as inlet- and outlet restrictions and pump bypass valve were experimentally determined. It is found that system characteristics external to the heated section do influence the behavior of DWO. Thus, considerable care must be exercised in the application of information obtained on a particular system on the design and operation of another system. Numerous variations were also found in experimental apparatuses described in the literature.

Flow oscillations were successfully superimposed on a stable system by cyclic variations in the pump drive speed. Generation of flow instabilities were hence allowed at vapor fractions less than the threshold value of DWO inception. Oscillations of different amplitude were generated at fixed inlet conditions and period, effectively insulating its impact from all other parameters. Overall heat transfer was linearly decreasing with increase in oscillation amplitude. The same technique could also be applied to shift the period of oscillation away from its natural frequency. Elongation of period had negative influence on overall heat transfer coefficient. This stipulates that the impact of oscillations with longer time scale, such as PDO, can be expected to have more severe consequences on system heat transfer performance than indicated in the present work. A limitation of the present study is that its scope is bound to DWO as the only instability mode, while PDO was excluded by omitting an upstream compressible volume. Heat transfer enhancement by shifting oscillations towards higher frequencies seems to be possible, though the gains are subtle. Such approach comes on the cost of increased pressure drop. Correct choice of amplitude and period in mimicked instabilities is essential in order to resemble the heat transfer and pressure drop characteristics of the natural DWO mode.

Degree of inlet subcooling did not significantly influence local saturated boiling heat transfer, as it is a property related to the upstream subcooled region. However, the effect of subcooling has been disputed in the DWO literature. Findings in the present study can be summarized as follows. Increasing the subcooling is found to increase the threshold heat input value of inception, but oscillations becomes more violent at a given heat input in the unstable range. Subcooling has a stabilizing effect on the system since inception is delayed by increasing the threshold heat flux.

Omitting inlet and exit restrictions, and closing the pump bypass valve, rendered the system unconditional stable. This allowed for determination of the normal CHF and production of reference data for pressure drop and heat transfer coefficient. The saturated boiling local heat transfer, were dependent on, and increased with heat flux, indicating that nucleate boiling is the dominant heat transfer mechanism.

A sudden drop in overall heat transfer is observed as the vapor quality approaches one. The onset of DWO, defining the premature CHF, causes an abrupt deficiency in local heat transfer near the outlet of the heated section. This event is somewhat delayed in a stable system distinguishing it as the normal CHF. The premature CHF was triggered at heat fluxes about 90% of the normal CHF.

More severe examples can be expected in less stable systems that are more prone to DWO instability.

The boiling heat transfer coefficient in the saturated region is not directly affected by the onset of flow instability, but shows diminishing performance in comparison to the stable case on further increase in heat flux. It is suggested, but not confirmed, that DWO triggers short bursts of dry-out of the heated surface in the low density part of its cycle. In flow visualization in the outlet of the heated section a variety of flow patterns are observed within one DWO-cycle, in particular when it commences. Categorization of flow patterns is a good starting point for further work.

Existing correlations for boiling flow heat transfer in macro channels showed predictions within a narrow (10-15%) error band, but this error band is doubled in width (20-30%) when DWO sets. Effects of flow rate and heat flux are well embedded in the present correlations. Increasing the pressure was found to increase the local boiling heat transfer coefficient. Correlations developed for micro channels were found unsuitable as the surface tension effects are much less prominent. It is remarked that micro channels has received most attention in research focusing on the influence of flow instabilities in heat transfer characteristics. Consequently, the same effort in macro channels, and especially horizontal, are greeted Additional issues of flow distribution instabilities may occur in systems with parallel channels, well beyond the scope of this study.

Overall heat transfer coefficient shows generally good scaling with pressure drop. A sudden drop in pressure drop was also observed on the inception of DWO. Experiments with DWO are less favorable than the stable as they are characterized by a lower heat transfer coefficient to pressure drop ratio.

Applications built to generate saturated or even superheated vapor such as once thorough evaporators, will encounter a dry-out situation by design. Heat transfer will consequently drop at some point due to the CHF regardless of system stability. In this view, the main concerns regarding DWO are mechanical vibrations and thermal fatigue by cycling of wall temperature. In other applications where a dry-out situation is fatal, for instance a cooler, avoidance of flow instabilities will to some extent enlarge the envelop of safe operation. The combined consequences of saturated boiling heat transfer deterioration and premature CHF is what makes occurrence of DWO delicate.

128

9 Further directions

More work is needed to fully understand the complex mechanisms involved in two-phase boiling flow instabilities, heat transfer and pressure drop is only a little part of it. Since the present work only focused on DWO in a single tube the following work may be conducted:

- More work is needed in the classification of flow pattern and their impact to the heat transfer. A suggested starting point is to classify the various flow regimes occurring during one DWO cycle. By analyzing the video one can further find how long each regime occurs in time. Systematic data on flow patterns and their time fraction can finally be linked to the heat transfer coefficient.

- More measurements have to be taken in multi-channel configurations. Industrial applications such as heat exchangers consist usually of arrays of parallel tubes. A fact stressing this is sudden jerk in pressure drop at the moment DWO incepted in the present single tube experiment.

- In experiments where the period was shifted by the pump, slower oscillations were found to deteriorate heat transfer more than DWO in its natural frequency. This indicates that oscillations of larger time scale may be more harmful. An upstream compressible volume should be added to capture heat transfer measurements during PDO.

10 References

1. **S. Maulbetsch and P. Griffith.** A study of system-induced instabilities in forced-convection flows with subcooled boiling. *MIT engineering project lab report, Technical report No. 5382-35.* 1965.

2. **S. Nukiyama.** The maximum and minumum values of the heat Q transmitted from metal to boiling water under atmospheric pressure. *Journal Japan Soc. Mech. Engrs.* 37 (p. 367-374), 1934, (Reprinted: Int. J. Heat Mass Transfer, Vol. 9., pp. 1419-1433).

3. **Y. Ding, S. Kakaç and K. J. Chen.** Dynamic Instabilities of Boiling Two-Phase Flow in a Single Horizontal Channel. *Experimental Thermal and Fluid Science.* 11:327-342, 1995.

4. **P. Saha, M. Ishii and N. Zubber.** An experimental investigation of the Thermally induced flow oscillations in two-phase systems. *Transactions of the ASME, Journal of Heat Transfer.* 1:616-622, 1976.

5. **H. YÜNCÜ, O. T. YILDIRIM and S. Kakaç.** Two-phase flow instabilities in a horizontal single boiling channel. *Applied Scientific Research.* 48:83-104, 1991.

6. **A. H. Stenning and T. N. Veziroğlu.** Flow Oscillation Modes In Forced-Convection Boiling. *Proceedings of the 1965 Heat Transfer and Fluid Mechanics Institute.* STANFORD U. PRESS, CALIF., P.301-316, 1965.

7. **K. Fukuda and T. Kobori.** Classification of two-phase flow instability by density wave oscillation model. *Journal of Nuclear and Technology.* 16:95-108, 1979.

8. **L.C. Ruspini.** Experimental and numerical investigation on two-phase flow instabilities. *PhD Thesis at NTNU.* 2013:4.

9. **Q. Wang, X. J. Chen, S. Kakaç and Y. Ding.** An experimental investigation of density-wave-type oscillations in a convective boiling upflow system. *Int. J. Heat and Fluid Flow.* Vol. 15, No. 3:241-246, 1994.

10. **D. Strømsvåg.** Fundamental mechanisms of density wave oscillations and the effect of subcooling. *Master thesis.* 2011.

11. **S. Kakaç, and B. Bon.** A Review of two-phase flow dynamic instabilities in tube boiling systems. *International Journal of Heat and Mass Transfer.* 51:399-433, 2008.

12. **M. Ozawa, S. Nakanishi, S. Ishigai, Y. Mizuta, and H. Tarui.** Flow Instabilities in Boiling Channels: Part 1 Pressure Drop Oscillations. *Bulletin of the JSME.* Vol. 22, Vol. 170:1113-1118, 1979.

13. **A. J. Cornelius.** An investigation of instabilities encountered during heat transfer to a supercritical fluid. *Ph.D. Thesis, Reactor Engineering Division and Associated Midwest Universities.* 1965.

14. **K. Akagawa, T. Sakaguchi, M. Kono and M. Nishimura.** Study on Distribution of Flow Rates and Flow Stabilities in Parallel Long Evaporators. *The Japan Society of Mechanical Engineers.* Vol. 14, 1971, No. 74.

15. **M. Ishii.** *Thermally induced flow instabilities in two-phase mixtures in thermal equilibrium.* s.l. : PhD. Supervised by N. Zuber, Georgia Institute of Technology, 1971.

16. **Ö Çomaklı, S Karslıb and M Yılmaz.** Experimental investigation of two phase flow instabilities in a horizontal in-tube boiling system. *Energy Conversion and Management.* 43:249-268, 2002.

17. **H. Andoh.** Discharged flow oscillation in a long heated tube. *MIT, Master of Science, Thesis supervisor: Peter Griffith.* 1964.

18. **A. H Stenning and T. N.Veziroglu.** Flow oscillation modes in forced-convection boiling. *Proceedings of the 1965 Heat Transfer and Fluid Mechanincs Institute.* NASA Grant NsG-424, 1965.

19. **Rizwan-Uddin.** On density-wave oscillations in two-phase flows. *Int. J. Multiphase Flow.* Vol. 20, No. 4:721-737, 1994.

20. **H. YÜNCÜ.** An Experimental and Theoretical Study of Density Wave and Pressure Drop Oscillations. *Heat Transfer Engineering.* 11:45-56, 1990.

21. **M. Yılmaz, Ö. Çomaklı, S. Karslı.** The effect of inlet subcooling on two-phase flow instabilities in a horizontal pipe system with augmented surfaces. *International Journal of Energy Research.* 26:113-131, 2002, (DOI 10.1002/er.770).

22. **S. Kakaç and L. Cao.** Analysis of convective two-phase flow instabilities in vertical and horizontal in-tube boiling systems. *International Journal of Heat and Mass Transfer.* 52:3984-3993, 2009.

23. **N. Liang, S. Shuangquan, C. Tian and Y. Y. Yan.** Two-phase flow instabilities in horizontal straight tube evaporator. *Applied Thermal Engineering.* 31:181-187, 2011.

24. **E. M. Chiapero.** *Two-phase flow instabilities and flow mal-distribution in parallel channels.* s.l. : Doctoral thesis at NTNU, 2013.

25. **L. Ugueto.** *Experimental study of density wave oscillations.* s.l. : NTNU Master's Thesis, 2013.

26. **M. Colombo, D. Papini, A. Cammi, M. E. Ricotti.** Experimental investigation of thermal hydraulic instabilities in Steam Generator helical coil tubes. *ENEA.* Report RdS/2011/105, 2011.

27. **Y. I. Kim, W. Baek and S.H. Chang,.** Critical heat flux under flow oscillation of water at low-pressure, low-flow conditions. *Nuclear Engineering and Design.* 193 (p. 131-143), 1999.

28. **S. H. Chang, Y. I. Kim and W. Baek,.** Derivation of mechanistic critical heat flux model for water based on flow instabilities. *Int. Comm. Heat Mass Transfer.* Vol. 23 No.8 pp. 1109-1119, 1996.

29. **S. H. Chang and W. Baek.** Understanding, predictiong and enhancing critical heat flux. *The 10th international Topical Meeting on Nuclear Reactor Hydraulics, Seoul, Korea.* October 5-9, 2003.

30. **H. Ukekawa, et al.** Dryout in a Boiling Channel under Oscillatory Flow Condition. *JSME International Journal.* Series B, Vol. 39, No. 2, 1996.

31. **A. Mentes, O. T. Yildirim, H. Gürgenci, S. Kakaç, T. N. Veziro͞glu.** Effect of heat transfer augmentation on two-phase flow instabilities in a vertical boiling channel. *Wärme- und Stoffübertragung.* 17, 161-169, 1983.

32. **X. Fang, R. SHI, Z. Zhou,.** Correltaions of Flow Boiling HEat Trasfer of R-134a in Minichannels: Comparative Study. *Energy Science and Technology.* Vol. 1, No. 1, 2011 PP. 1-15, 2011.

33. **G. M. Lazarek and S. H. Black.** Evaporative heat transfer, pressure drop and critical heat flux in a small vertical tube with R-113. *Int. J. heat and Mass Transfer.* Vol. 25, No 7, pp. 945-960, 1982.

34. **T. N. Tran, M. W. Wambsganss and D. M. France,.** Small circular- and rectangular-channel boiling with two refrigerants. *Int. J. Multiphase flow Vol.22, No. 3, pp.485-498.* 1996.

35. **S. Saitoh, H. Daiguji, E. Hihara,.** Boiling heat transfer of R-134A flowing in horizontal small-diamater tubes. *Proceedings of HT2007-32888, ASME-JSME Thermal Engineering Summer Heat Transfer Conference, July 8-12,.* 2007.

36. **S. Saisorn, J. Kaew-On, S. Wongwises,.** Flow pattern and heat transfer characteristics of R134a refrigerant during flow boiling in horizontal circular mini-channel. *International Journal of Heat and Mass Transfer.* 53 pp. 4023-4038, 2010.

37. **J. B. Copetti, M. H. Macagnan, N. Knusler,.** Boiling of R-134a in Horizontal Mini Tube. *ABCM J. of the Braz. Soc. of Mech. Sci. & Eng.* Special Issue Vol. XXXIII, 2011.

38. **B. Agostini and A. Bontemps.** Vertical flow boiling of refrigerant R134a in small channels. *International Journal of Heat and Fluid Flow.* 26 (296-306), 2005.

39. **P.A. Kew and K. Cornwell.** Correlations for the prediction of boiling heat transfer in small-diameter channels. *Applied Thermal Engineering.* vol 17, no. 8-10, pp. 705-715., 1997.

40. **J. E Kennedy, et al.** The Onset of Flow Instability in Uniformly Heated Horizontal Microchannels. *Transactions of ASME.* Vol. 122 (p. 118-126), 2000.

41. **D. Brutin, F. Topin, L. Tadrist,.** Experimental study of unsteady convective boiling in heated minichannels. *International Journal of Heat and Mass Transfer.* 46 2957-2956, 2003.

42. **Fan, YF.** Experimental Investigation of Flow Boiling Heat Transfer and Flow Instability in a Horizontal Microtube with an Inlet Orifice. *Ph.D Thesis.* Concordia University. Montréal, Québec, Canada, 2013.

43. **D. Brutin and L. Tadrist.** Destabilization Mechanisms and Scaling Laws of Convective Boiling in a Minichannel. *Journal of Thermodynamics and Heat Transfer.* Vol. 20, No. 4, October-December, 2006.

44. —. Pressure Drop and Heat Transfer Analysis on Flow Boiling in a Minichannel: Influence of the Inlet Condition on Two-Phase Flow Stability. *International Journal of Heat and Mass Transfer.* Vol 47, 2004, 10-11 (p. 2356-2377).

45. **YF. Fan, I. Hassan,.** Effect of Inlet Restriction on Flow Boiling Heat Transfer in a Horizontal Microtube. *Journal of Heat Transfer ASME.* February Vol. 135, 2013.

46. **YF. Fan and I. Hassan.** Experimental Investigation of Flow Boiling Instability in a Single Horizontal Microtube With and Witout Inlet Restriction. *Journal of Heat Transfer ASME.* August Vol. 134, 2012.

47. **E. Manavela Chiapero, D. Dider, M. Fernandino, C. A. Dorao,.** Experimental parametric study of the pressure drop characteristic curve in a horizontal boiling channel. *Experimental Thermal and Fluid Science.* 52 (p. 318-327), 2014.

48. **E. Manavela Chiapero, M. Fernandino, C. A. Dorao,.** Parametric study of the pressure characteristic curve in a boiling channel. *Computatuonal Thermal Sciences.* 3, 2011, 2 (p. 157-168).

49. **E. Manavela Chiapero, M. Fernandino, C.A. Dorao,.** Experimental results on boiling heat transfer coefficient, frictional pressure drop and flow patterns for R134a at a saturation temperature of 34 C. *International Journal of Refrigeration.* doi: 10.1016/j.ijrefrig.2013.11.026., 2014.

50. **L. Ruspini and E. Langørgen.** Risk assessment report: Two-phase flow instabilities project. *. Technical report, NTNU, SINTEF.* 2011.

51. **L.A. Belblidia and C.Bratianu.** Density-wave oscillations. *Annals of Nuclear Energy.* Volume 6, Issues 7–8, 1979, Pages 425–444.

52. **E. Manavela Ciapero, M. Fernandino, C.A. Dorao,.** Study of the influence of axial conduction in a boiling heated pipe. *Chemical Engineering Research and Design.* 90 pp. 1141-1150, 2012.

53. **H. Tennekes and J. L. Lumley.** *A first course in turbulence.* Cambridge, Massachusetts, and London, England : Teh MIT Press, 1972. ISBN 0 262 20019 8 (hardcover).

54. **DuPont (TM) Technical Information / based on NIST datasheet.** Thermodynamical properties of HFC-134a (1,1,1,2-tetrafluoroethane). *T-134a-ENG.*

55. **P. Cheng and H. Y. Wu.** Mesoscale and microscale phase-change heat transfer. *Advances in heat transfer.* 39.

56. **Grande, S. G. Kandlikar and W. J.** Evolution of microchannel flow passages Thermodynamical performance and fabrication technology. *Proceedings of IMECE2002, ASME International Mechanical Engineering Congress & Exposition.* 17-22 November, New Orleans, Lousianna, 2002.

57. **3M.** Fluorinert Electronic Liquid FC-72. *Product Information.*